Neural Stem Cell Compartments in a Mouse Model of Globoid Cell Leukodystrophy: Implication for Therapeutic Strategies

Thesis

Sara Santambrogio

NEURAL STEM CELL COMPARTMENTS IN A MOUSE MODEL OF GLOBOID CELL LEUKODYSTROPHY: IMPLICATION FOR THERAPEUTIC STRATEGIES

PhD thesis in fulfillment of the requirements of the Open University for the degree of Doctor of Philosophy in Molecular and Cellular Biology

2011

Director of studies
Dr. Angela Gritti

External Supervisor
Prof. Timothy M Cox

Vita-Salute San Raffaele University
San Raffaele Telethon Institute for Gene Therapy (HSR-TIGET)
DIBIT, San Raffaele Scientific Institute, Milan, Italy
Open University

DATE OF SUBMISSION: 28 MARCH 2011
DATE OF AWARD: 13 MAY 2011

ABSTRACT

Globoid cell leukodystrophy (GLD) is a rare genetic lysosomal disorder due to deficiency in the β-galactocerebrosidase (GALC) enzyme. GLD affects mainly children; the prognosis is severe, leading to death few years after the diagnosis. Demyelination is believed to occur as a consequence of Psychosine accumulation and neuroinflammation. Clinical observations in GLD babies suggest that GALC deficiency might affect myelination before overt storage and inflammation, but this issue has been poorly addressed in pre-clinical studies. Similarly, little is known regarding the effect of GALC deficiency on neural stem cell (NSC) in the neurogenic niches during CNS development. The goal of this study was to extensively characterize the role of GALC in regulating the function of NSC niches during the disease progression in Twitcher (Twi) mice, a relevant GLD model. By morphological and functional analysis we showed altered cellular organization and loss of proliferating neuroblasts in the subventricular zone (SVZ) niche of Twi mice as a function of disease progression. These data were confirmed by *in vitro* experiments showing decreased numbers of primary neurospheres generated from Twi NSC/progenitors. Both defects were rescued to normal levels in symptomatic Twi mice chronically treated with anti-inflammatory drugs. These results, as well as the up-regulation of several inflammatory molecules observed in Twi brains starting from the early symptomatic stage, suggested a major contribution by neuroinflammation at the late stages of the disease. However, these data did not rule out a direct contribution of GALC deficiency nor do they exclude a role of GALC in maintaining a functional niche during CNS development. Indeed, our results indicate decreased proliferation and maturation of NSC/progenitors derived from asymptomatic Twi mice, suggesting that GALC deficiency might lead to neurogenic impairment independently from CNS inflammation. These results improve our understanding of the pathogenic mechanisms of GLD with important implications for therapy.

STUDENT DECLARATION

This thesis has been composed by myself and has not been previously submitted for a degree.

I generated the data presented in this thesis.

I was helped in the experiments shown in Fig. 9 (Claudio Maderna).

Electron microscopy pictures and counts were performed by prof. Luca Bonfanti.

MAP ELISA data were obtained by using the commercial service RodentMAP by Rules Based Medicine (RBM), Texas, US.

Lipid quantifications by mass-spectrometry were obtained by the commercial service by Zora Bioscience, Finland.

Thin layer chromatography and sphingosine kinase activity were performed by Dr. Massimo Aureli.

Part of the results that I have reported and discussed in this thesis are contained in the following manuscript:

Santambrogio S, Ieraci A, Maderna C, Bonfanti L and Gritti A. *Perturbation of the SVZ neurogenic niche in a murine model of Krabbe disease: implication for pathophysiology and therapy.* In preparation

ABBREVIATIONS

AAV	ADENO-ASSOCIATED VIRUS
AD	ADULT
ARSA	ARYLSULFATASE A
BBB	BLOOD BRAIN BARRIER
BM	BONE MARROW
CB	CORD BLOOD
CBT	CORD BLOOD TRANSPLANT
CCL5	CC MOTIF CHEMOKINE LIGAND 5 OR RANTES, REGULATED UPON ACTIVATION, NORMAL T-CELL EXPRESSED, AND SECRETED
CNS	CENTRAL NERVOUS SYSTEM
CST	CORTICOSPINAL TRACT
CXCL10	CXC MOTIF CHEMOKINE LIGAND 10 OR IP-10, INTERFERON GAMMA-INDUCED PROTEIN 10 KDA
CXCL12	CXC MOTIF CHEMOKINE LIGAND 12 OR SDF-1, STROMAL CELL-DERIVED FACTOR-1
DCX	DOUBLECORTIN
DTI	DIFFUSION TENSOR IMAGING
EET	ENHANCED ENZYME THERAPY
EI	EARLY INFANTILE
ERT	ENZYME REPLACEMENT THERAPY
GALC	GALACTOSYLCEREBROSIDASE
GAL-TI	LACCER SYNTHASE
GAL-TIII	GALCER SYNTHASE
GC	GLOBOID CELL
GFAP	GLIAL FIBRILLARY ACIDC PROTEIN
GLC	GLYCOSPHINGOLIPID
GLC-T	GLUCER SYNTHASE
GLD	GLOBOID CELL LEUKODYSTROPHY
HSC	HEMATOPOIETIC STEM CELL
HSCT	HEMATOPOIETIC STEM CELL TRANSPLANT
IL-1 α/β	INTERLEUKIN 1 α/β
J	JUVENILE
KD	KRABBE DISEASE

LI	LATE INFANTILE
LSD	LYSOSOMAL STORAGE DISORDER
MAP	MULTI ANALYTE PROFILE
MCP-1	MONOCYTE CHEMOATTRACTANT PROTEIN 1 OR CCL2, CC MOTIVE CHEMOKINE LIGAND 2
MIP-1α	MONOCYTE INDUCED PROTEIN 1α OR CCL3, CC MOTIVE CHEMOKINE LIGAND 3
M6P	MANNOSE-6-PHOSPHATEPND
NCFCA	NEURAL COLONY FORMING CELL ASSAY
NEU3	SIALIDASE
NSA	NEUROSPHERE FORMING ASSAY
NSC	NEURAL STEM CELL
NSCT	NEURAL STEM TRANSPLANT
PND	POST NATAL DAY
PNS	PERIPHERAL NERVOUS SYSTEM
PSY	PSYCHOSINE
SAT-1	GM3 SYNTHASE
SGZ	SUBGRANULAR ZONE
SPH	SPHINGOSINE
SPHK	SPHINGOSINE KINASE
SRT	SUBSTRATE REDUCTION THERAPY
SVZ	SUBVENTRICULAR ZONE
SVZ-LV	LATERAL VENTRICLE OF THE SVZ
SVZ-RE	ROSTRAL EXTENSION OF THE SVZ
S1P	SPHINGOSINE-1-PHOSPHATE
S1PR	SPHINGOSINE-1-PHOSPHATE RECEPTOR
TTNF-α	TUMOR NECROSIS FACTOR α

Table of Contents

1. INTRODUCTION

1.1 Globoid Cell Leukodystrophy

1.1.1 Introduction to Lysosomal Storage Disorders

Lysosomes are membrane-bound organelles that contain a range of acid hydrolases such as proteases, glycosidases, sulphatases, phosphatases and lipases. Lysosomal storage diseases (LSDs) are monogenic diseases caused by mutation in genes coding for lysosomal proteins. This leads to progressive accumulation of unmetabolised substrates, functional impairment, cell toxicity and, eventually, cell death. Although monogenic diseases are simple in terms of causative gene defect, the biochemical and cellular cascade of events that ensue is highly complex (Futerman and van Meer, 2004). LSDs are typically inherited as autosomal recessive traits and occur at a collectively frequency of ~ 1:8,000 live births. Over 50 LSDs are known; they can be caused by defects in soluble lysosomal enzymes, in non-enzymatic lysosomal proteins (soluble or membrane bound), or in non-lysosomal proteins that affect lysosomal function. The degree of residual function of the defective protein influences the age of symptom onset. Patients null or almost null for a given protein, present symptoms in utero or in early infancy, whereas milder mutations lead to juvenile or adult onset disease (Futerman and van Meer, 2004). About 75%, of LSDs involve storage in both the central nervous system (CNS) and visceral tissue. CNS pathology is a common hallmark of LSDs, and LSDs are the commonest cause of paediatric neurodegenerative diseases.

Despite the distinctive types of storage material in different LSDs they share many common biochemical, cellular and clinical features. Thus, advances in understanding one particular disease can provide insight into other specific LSDs or into LSDs in general.

1.1.2 Globoid Cell Leukodystrophy: clinical manifestation

Globoid Cell Leukodystrophy (GLD), or Krabbe disease, is an autosomal recessive LSD caused by deficiency of the lysosomal enzyme β-galactocerebrosidase (GALC) which catalyses several glycolipids, including galactosylceramide (GalCer) and galactosylshpingosine (psychosine). It is a rare LSD, with an incidence of 1 in 100,000 live births worldwide. GLD was firstly described by Knud Krabbe in 1916 in children as a syndrome that began during infancy and was characterized by tonic spasms, nystagmus, muscular rigidity, progressive quadriplegia and early death (Krabbe, 1916). It affects both the central nervous system (CNS) and the peripheral nervous system (PNS) and the typical neuropathological finding includes generalized brain atrophy with the central white matter being replaced by gliotic tissue. Post-mortem examination of affected individuals reveals loss of myelin, degeneration of long spinal tracts, gliosis and infiltration of characteristic globoid cells of macrophage-microglia origin. The prognosis is severe, leading to death a few years after diagnosis. Clinically, GLD is classified according to the patient's age at onset. Different forms of GLD exist: early infantile (EI), late infantile (LI), juvenile (J) and adult (AD). The most severe variant is the one with EI presentation, which accounts for over 90% of patients, becoming manifest within six months of age in most cases (Wenger et al., 1997) and developing in four stages (Hagberg et al., 1969). Symptoms and signs are confined to the nervous system. No visceromegaly is present. Head size may be large or small; hydrocephalus has been observed. One infant, diagnosed with Krabbe disease in utero, had normal psychomotor development for the first two months of life but lost deep tendon reflexes by age five weeks, had markedly reduced nerve conduction velocities at age seven weeks, and developed neck muscle weakness at age three months. These findings suggest that careful examination could reveal clinical manifestations of Krabbe disease in an affected infant earlier than the reported age of onset (Wenger, 2000). Indeed, Escolar and collaborators detected significant differences in the cortico spinal tract (CST) of asymptomatic neonates affected by early onset KD by diffusion tensor imaging (DTI) with quantitative tractography. CST is one of the earliest white matter pathways to undergo maturation, beginning prenatally and early abnormalities may explain the plateau in motor development seen

in Krabbe babies treated with umbilical cord blood transplant (UCBT), even in the presence of improved overall brain myelination (Escolar et al., 2009; Kamate and Hattiholi, 2010). The LI variant is much less common and begins between 19 months and four years of age (Loonen et al., 1985). These patients have only moderate mental retardation during the first years, but gradually develop ataxia and spasticity. Peripheral neuropathy is severe. Disease progression is slower than in EI manifestation, with visual loss, mental regression, seizures and deafness. The prognosis is severe, leading to death 5-7 years after diagnosis. The late-onset variants are the J (onset at 4 to 19 years) and the AD forms (>20 years). These individuals can be clinically normal until almost any age when symptoms of weakness, vision loss, and intellectual regression become evident. The clinical course of older individuals is variable. These patients are characterized by a slowly progressive tetraplegia, sensor-motor demyelinating neuropathy and preserved mental function; survival into the seventh decade is possible (Jardim et al., 1999; Kolodny et al., 1991).

1.1.3 Diagnosis

1.1.3.1 LSDs

The LSDs are clinically highly diverse and can affect most organs, either in isolation or as part of a multisystem disorder. Ganglioside expression is particularly high in the nervous system and the gangliosidoses are neurodegenerative diseases. Keratan and dermatan sulphate are expressed at high levels in skeletal tissue and the mucopolysaccharidoses, which involve defects of their degradation pathways, are characterized by dysostosis multiplex (severe abnormalities in development of skeletal cartilage and bone). There is also considerable variation within each disorder, ranging from severe, infantile-onset forms to attenuated adult-onset disease, sometimes with distinct clinical features (Winchester et al., 2000). In some cases it is possible to have genotype–phenotype correlation, and there are some 'severe' genotypes which, in homozygotes or compound heterozygotes, are inevitably associated with neuronopathic disease (Cox, 2001). However, genotype/phenotype relationships are much less defined for the majority of mutations

which give rise to attenuated disease, and it is common for sibling pairs and even twins to demonstrate highly divergent clinical features as regards age of onset and degree of skeletal involvement (Lachmann et al., 2004). Similar inconsistencies exist for other LSDs and the difficulties in predicting phenotype from genotype have major implications in diseases where newborn screening is currently being considered.

Recently great relevance has been given to newborn manifestation. Indeed early diagnosis and intervention is essential to maximizing the potential benefit from some therapy and may prevent irreversible organ damage. Thus physician's awareness of these early presentations has important clinical implications. The interval between birth and the onset of the clinical symptoms can range from hours to month. Symptoms range to neurologic to respiratory, endocrine and cardiovascular manifestation; moreover dysmorphology (of different type: head, limbs, oral, gastrointestinal, bones and joints, skin etc.) could also be present (Staretz-Chacham et al., 2009).

Because usually there is an overlap of clinical features in many of LSDs, it is difficult to establish a diagnosis sorely on the basis of clinical presentation (Fig. 1). Urine screens that test for elevated levels of secreted substrate material are used routinely to examine the pattern of glycosaminoglycans and oligosaccharides in patients suspected of MPS or disorders that present with oligosaccharidurìa. When there is a strong index of suspicion, urine analysis is followed by enzyme activity assay, usually performed on leukocytes and plasma; in case of deficiency of secondary proteins it followed also the rate of radiolabelled substrate turnover in cultured cells. Molecular analysis is usually performed in a second step of screening, however is crucial for prenatal screening or population screening for high-risk ethnic group (Staretz-Chacham et al., 2009).

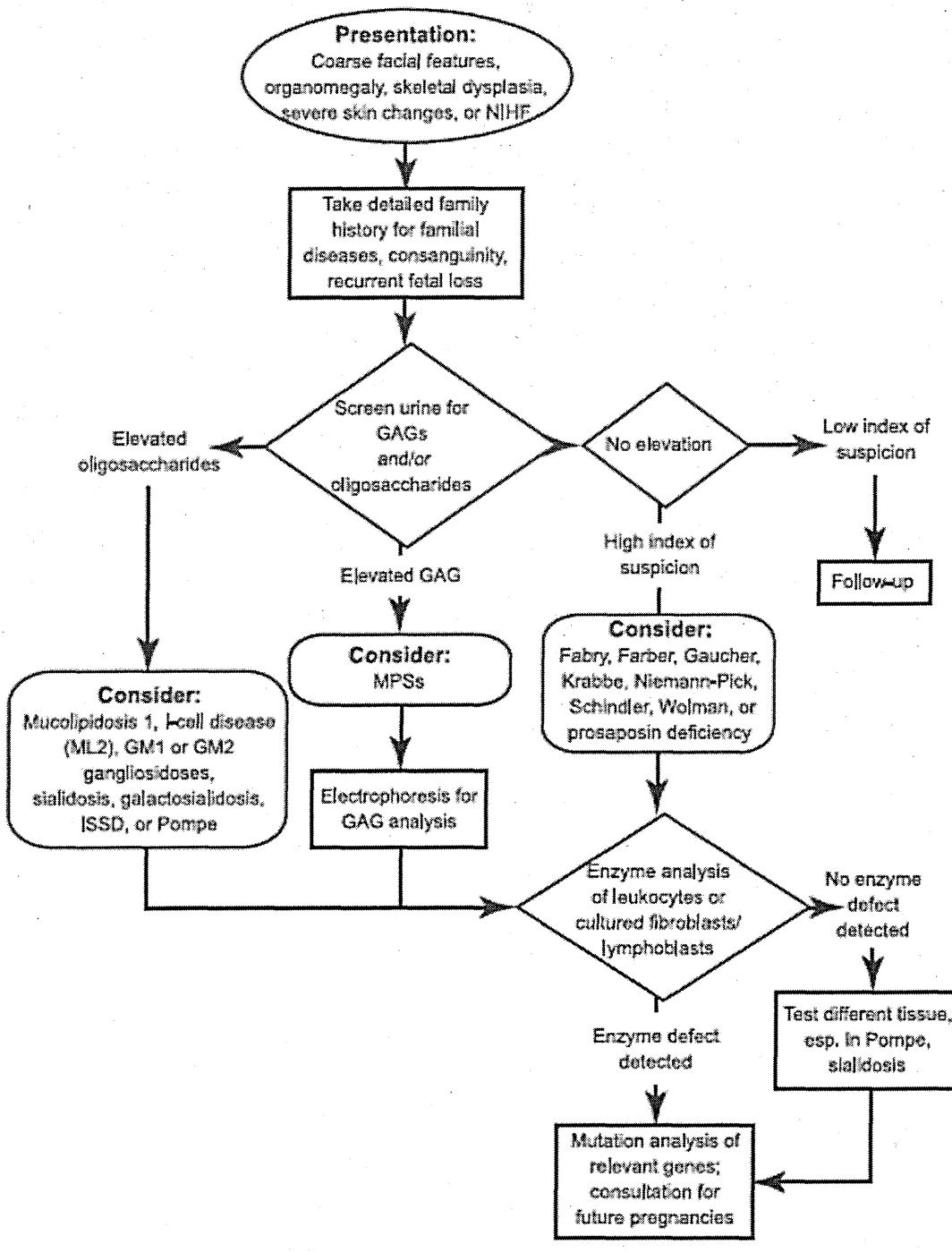

Figure 1. Algorithm of the clinical evaluation recommended for an infant with a suspected LSD (Starez-Chacaman, 2009).

1.1.3.2 GLD

Most cases of Krabbe Disease are diagnosed in infants; however a minority of patients are diagnosed in childhood and as adults. Currently the enzymatic test is performed to confirm the

diagnosis. GALC activity is measured in serum, leukocytes or fibroblasts, using a radiolabelled substrate (3H-GalCer). While normal values range between 0,9-4,4 nmol/h/mg (Callahan and Skomorowski, 2006), in GLD patients the average of measured GALC activity is 0,07 nmol/h/mg (Farina et al., 2000). The reduction of GALC activity can be further confirmed by repeating the same test on cerebrospinal fluid.

Magnetic resonance imaging (MRI) can also be useful to evaluate the white matter: infants with EI and LI GLD have abnormal T1 and T2 intensity, indicating a loss of myelin in the posterior limb of the internal capsule. During KD progression, grey matter atrophy and abnormality of cerebellar white matter and pyramidal tracts develop (Farley et al., 1992; Loes et al., 1999). Finally all white matter structures become abnormal. These regions show an abundant infiltration of GCs and macrophages and severe demyelination post-mortem. JU and AD GLD can present with relatively mild changes in the posterior corpus callosum and parietooccipital white matter (Sabatelli et al., 2002; Satoh et al., 1997). Electrophysiological studies and electroencephalograms (EEG) are helpful in evaluating nerve conduction and monitoring disease progression. The severity of the abnormalities detected by electrophysiological testing (slow nerve conduction) usually correlates with the severity of the abnormalities on MRI scans. EEG is typically normal at the early stages of the disease, but generalized slowing and multifocal epileptic spikes are observed in the later stages (Husain et al., 2004).

Molecular analysis is the unique way to assess specific mutation in GALC gene or detect the case of Saposine A deficiency. In SapA -/- patients, the reduced GALC activity is indeed not due to a defect in the GALC gene, but to the loss of function of Sap A, which is essential for GALC function. Seventy-eight variants of the more common GALC sequence have been identified to date (The Human Gene Mutation Database at the Institute of Medical Genetics in Cardiff – update: February 2011). Many patients have two different mutations in the two alleles of the gene, thus resulting in a wide range of clinical feature that makes difficult propose genotype-phenotype correlation.

1.1.3.3 Prenatal diagnosis and newborn screening for GLD

Prenatal diagnosis is extremely accurate using a direct chorionic villus sample, cultured trophoblasts and cultured amniotic fluid cells, providing rapid and accurate results early in gestation. Unfortunately no reliable carrier detection exists for individuals who do not have a family history of KD. While each parent carries one normal and one mutated *GALC* allele, the measured GALC enzyme activity can range widely in carriers because of polymorphisms in the normal copy of the gene. Although some parents have quite low GALC enzyme activity measured *in vitro*, none has had clinical disease. The carrier frequency in the general population is about one in 150 (Wenger, 2000). Newborn screening is currently performed in high-throughput way in the state of New York and Illinois and Missouri are developing plans to begin the same. The quantification of GALC activity is measured by tandem mass spectrometry on dried blood spots. Samples with less than 10% of normal activity values are considered positive and DNA analysis for GALC mutations starts. In order to avoid false positive screening, GALC deficiency is confirmed by a second assay performed on blood. When the diagnosis is confirmed, the infant is referred for consideration of a cord blood (CB) transplant. Currently, the transplant centre with the most experience of neonatal GLD is Duke University Medical Centre (North Carolina). Last year has been released a systematic evidence review regarding the benefits and harms of newborn screening for GLD. The authors identified several critical gaps in the knowledge: 1) the inability to determine shortly after a positive screen which children would benefit from urgent transplantation and 2) the lack of long-term follow-up data for those children who have received transplants, especially neurodevelopmental outcomes (Kemper et al., 2010). Recently the use of DTI with quantitative tractography was used to identify in neonates early changes in major motor tracts before clinical symptoms develop (Escolar et al., 2009). The importance of prenatal or newborn screening is great, considering the fact that accumulation of the toxic substrate Psy in tissues has been noted as early as 21 weeks' gestation in a fetus (Ida et al., 1994).

1.1.4 GALC: the gene and the enzyme

The GALC gene was mapped in 1990 by restriction fragment length polymorphism (RFLP) studies: it lies at 14q31 and spans 17 exons over a 60 kb interval (Luzi et al., 1995). The 5' UTR region, considered as the promoter region, contains 13 GGC sequences and binding sites for SP1, YY1, E2F and AP3 transcription factors (Sakai et al., 1998). CAAT sequences or TATA box, present in the promoter regions of other lysosomal enzymes, are absent in the GALC promoter. GALC is also expressed at a low level in the nervous system, where the first substrate of GALC, GalCer is present in high concentration (Luzi et al., 1997). The GALC cDNA, encodes a 669 residue protein of about 80 kDa with a 26 amino acid leader sequence (Wenger et al., 1997). In the lysosome, this pro-enzyme is further cleaved to a 50 kDa amino terminal and a 30 kDa carboxy terminal subunits. These subunits associate to form the functional enzymatic complex (Nagano et al., 1998). The rearrangement of glycosylation chain and the event of proteolysis take place after the release of the precursor from endoplasmic reticulum (ER) in Golgi apparatus and in the acidic lysosomal environment, respectively. The subunits aggregate into a multimeric high molecular weight hydrophobic complex of 600-700 KDa, wich is believed to be the active form (Ben-Yoseph et al., 1980). GALC works within the lysosome at low pH (between 4 and 4.4), together with activators such as Saposine A and C (Harzer et al., 2001). The main substrates of GALC are GalCer and Psychosine (Psy): GalCer is hydrolysed to ceramide (Cer), while Psy is hydrolysed to Sphingosine (Sph). Other substrates of GALC are Monogalactosyldiglyceride (MGD) and Lactosylceramide (LacCer)(Wenger et al., 2000)(Fig. 2).

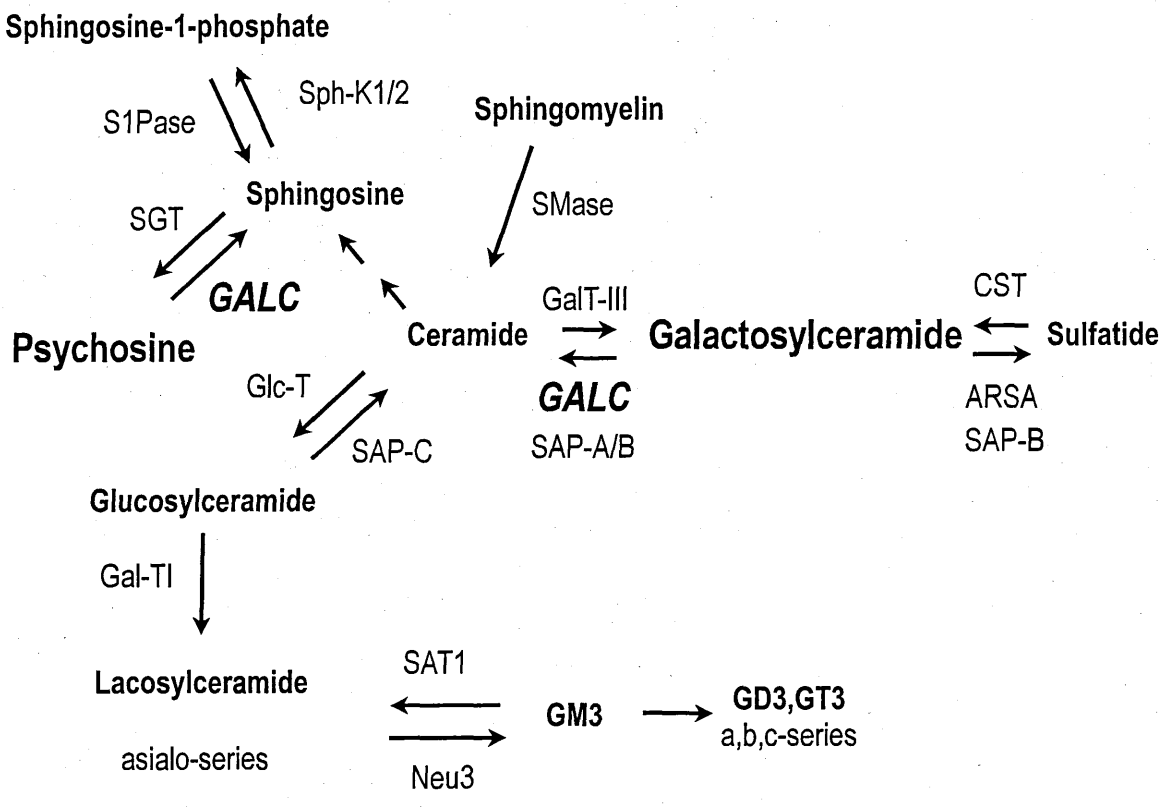

Figure 2. Simplified scheme of the sphingolipid metabolism.
The cartoon illustrates the activity of GALC enzyme within the sphingolipid pathway.
ARSA, arylsulfatase A; CST, cerebroside sulfotransferase; GALC, galactosylceramidase; GalT-I, LacCer synthase; GalT-III, GalCer synthase; GlcT, GlcCer synthase; SAP, saposin; SAT1, GM_3 synthase; Neu3, sialidase; Sphk-1/2 sphingosine kinase1/2; S1Pase sphingosine phosphatase; SGT sphingosine-galactosyltransferase; SMase sphingomyelinase.

The most relevant of these substrates is GalCer, produced from Cer by Ceramide-Galactosyltransferase (CGT) in the endoplasmic reticulum and from sulfatide by Arylsulfatase A (ARSA) in the lysosome. GalCer and sulfatides represent one third of the whole lipidic myelin mass (Norton, 1984). Moreover, GalCer is implicated in the transduction of signals for oligodendrocytes differentiation and in axon-glia interaction at paranode level (Marcus and Popko, 2002). Although GalCer is the first substrate of GALC, it does not accumulate in GALC deficient tissues, likely due to the activity of a different galactocerebrosidase. GALC deficiency is actually responsible for Psy accumulation up to at least 100 fold normal levels in human infants and animal models. This toxic storage has been shown to kill oligodendrocytes by an apoptotic mechanism, resulting in a greatly diminished amount of myelin and astrocytic gliosis and the

production of the characteristic globoid cells (for details, see paragraph 1.1.5.2).

1.1.5 Pathogenesis

1.1.5.1 Mutations

More than 70 mutations have been identified in the *GALC* gene. The most common disease-causing mutation in European origin individuals is a 30 kb deletion starting from exon 10 and proceeding until the end of the gene, found in 40-50% of the cases. Other relevant mutations comprises missense mutations (i.e. 1538C>T and 1652A>C) found in about 5-8% of patients and deletions, 1424delA and 809G>A, found in about 2-5% and in the 1-2% of patients, respectively. For the remaining 32-47% of the affected population, mutations are more heterogeneous. It appears that most of disease-causing missense mutations result in the production of unstable *GALC* protein that is rapidly degraded. Deletions, instead, result either in frame shifts and premature stop codons or in lack of a significant portion of the gene. Especially for late onset forms, it is difficult to make genotype-phenotype correlations, even if some mutations in homozygosis or coupled with deletions in the other allele seem to be correlated with (or more represented) in the infantile forms of KD (Wenger et al., 2000).

1.1.5.2 Psychosine

The unique biochemical feature of GLD is a lack of abnormal accumulation of galactosylceramide in the brain, contrary to what is expected from the enzymatic defect. This paradoxical phenomenon has been firstly explained by the exclusive presence of galacosylceramide in myelin sheath and the rapid lost during the progression of the disease of myeling forming cells. However there is the abnormal accumulation of a related toxic metabolite, Psychosine (Psy) or galacosylsphingosine and it is a key element in the pathogenesis of the disease. GalCer might be

converted to Psy by N-Deacilase, but the existence of this alternative pathway has never been demonstrated (Miyatake and Suzuki, 1972). Psy is also obtained through galactosylation of sphingosine by UDPGalactose: sphingosine1-β-Galactosyltransferase (Suzuki, 1998). In physiological conditions, GALC converts Psy to sphingosine and hydrolyses GalCer to Cer; in the absence of GALC, GalCer could be hydrolysed by Galactosylceramidase II. This enzyme, deficient in GM_1 Gangliosidosis, has a low affinity for Psy, which is not metabolized and accumulates in the white matter and, to a lesser extent, in other tissues (Kobayashi et al., 1985). Actually, however the biosynthesis of Psy is not clearly understood.

Psy accumulation in myelin forming cells, such as oligodendrocytes and Schwann induces cell death, however despite the toxic effect has been extensively studied, it is not fully understood. Psy specifically inhibits cytocrome C oxidase in mitocondria and alters mitochondrial membranes (Tapasi et al., 1998). Moreover it is able to trigger apoptosis by initiation of caspase 9 and effector caspase 3 activation (Haq et al., 2003; Jatana et al., 2002). Further studies have shown that Psy-induced cell death also involves the activation of secretory phospholipase A2 (sPLA2), which generates lysophosphatidylcholine and arachidonic acid. sPLA2 activation also leads to oxygen-reactive species (ROS) production and oxidative stress (Giri et al., 2006). In addition, Psy down-regulates survival pathways including nuclear factor-kB and PI3K-Akt. Several studies have reported the expression of pro-inflammatory cytokines and chemokines in cell cultures from GLD patients and Twitcher mice, a murine model of GLD. Moreover, expression of iNOS and glial fibrillary acidic protein (GFAP) in activated astrocytes in the CNS of GLD patients indicates the involvement of an inflammatory process in the pathogenesis of GLD. In astrocytes, Psy maintains the production of inflammatory mediators by inducing the nuclear translocation of the transcriptional factor C/EPB, which, in turn, stimulates the production of IL-6, IL-1β and TNF-α (Giri et al., 2006). The inflammatory condition could be both cause and consequence of Psy action. In fact, it is demonstrated that Psy may act as a pro-inflammatory stimulus. Even if the mechanism of action is not completely clear, a link has been demonstrated between the accumulation of Psy and the production of cytokines that promote inflammation, like TNF-α

(Formichi et al., 2007; Pasqui et al., 2007). Psy also induces alterations at the level of peroxisomes, involved in the biosynthesis of plasmalogens (important constituents of myelin), in β-oxidation of fatty acids and in detoxification from H_2O_2. (Haq et al., 2006). Interestingly, a modification of lipid raft structure due to Psy accumulation has been described in oligodendrocytes and neurons derived from GLD animal models and from human tissues (White et al., 2009). Psy accumulation and disruption of lipid rafts resulted in inhibition of PKC activity, contributing to the metabolic perturbation that characterizes GLD (White et al., 2009). Psy also accumulates into microglia, leading to the formation of globoid cells (GCs). GCs have been observed in CNS lesions of GLD patients by histology: these cells of the monocytic lineage, are positive to PAS-staining and display microglia-specific markers, such as vimentin and ferritin (Itoh et al., 2002). The origin of GC seems to be caused by the effect of Psy on the cell cycle regulation: Psy inhibits cytokinesis without inhibiting cell division (Im et al., 2001; Kanazawa et al., 2000), leading to the formation of giant GC, filled with nonmetabolized material. As a direct consequence, the cellular debris cannot be cleared, thus further worsening neuroinflammation. Psy action as "neurotoxin" seems to represent the critical biochemical pathogenic mechanism responsible of cell death in the brains of GLD patients and animal models.

1.1.6 Animal models of GLD

Spontaneous mutations resulting in GALC deficiency occur in several mammalian species, such as mice, dogs, and non-human primates. Firstly, a canine model of GLD was discovered (West Highland White terriers) (Kurtz and Fletcher, 1970; Victoria et al., 1996), presenting characteristic pathological features such as weakness, tremor, deficiency of GALC activity and Psy accumulation in brain. Secondly, the murine model of GLD, known as Twitcher (Twi) was identified at the Jackson Laboratory (Kobayashi et al., 1980). These Twi mice on the C57BL/6J strain, appear normal at birth, but start to develop clinical signs, such as ataxia, twitching and hind leg weakness at around 3 weeks of age. Neurological deterioration both in CNS and in PNS is

very fast, leading to a progressive hind leg paralysis, concomitant with weight loosing that lead to death at about 40 days of age. Twi mice present no GALC activity and Psy accumulation in CNS and PNS, with the appearance of multinucleated globoid cells (Tanaka et al., 1989). The disease-causing mutation in this model is a non-sense mutation, caused by a naturally occurring G>A transition at cDNA position 1017 in the GALC gene on both alleles. It results in the formation of a premature termination codon (PTC) (W339X) that abolishes enzymatic activity (Sakai et al., 1996). The truncated form of GALC expected to be produced in these animals is not detected, because of degradation of GALC mRNA due to non-sense mediated mRNA decay (NMD) (Lee et al., 2006). Other mouse models are available, including a transgenic mouse, the trs, obtained by homologous recombination (Luzi et al., 2001). The missense mutation responsible for the disease results in a substitution of a Cysteine with a Histidine. While this mutation in humans decreases GALC activity to only 80% of normal values, in the mouse it results in a more severe reduction of GALC activity (10 to 20% of normal values). Trs mice present a phenotype similar to the one observed in Twi mice, but with a delayed onset of about 10 days: twitching and tremors start around day 30 and the life span is about 50 days. A model resembling the phenotype observed in human late-onset forms of GLD, obtained by Cre/lox knock out of Saposine A (Sap A), an activator essential for GALC functionality. SapA-/-mice develop a slowly progressive hind leg paralysis, with clinical onset at about 70 days and survival up to 5 months (Matsuda et al., 2001).
A non-human primate model of GLD (Rhesus monkeys) with pathological signs consistent with a diagnosis of GLD is also available. Affected monkeys present tremors of the head and limbs, deterioration of walking abilities and ataxia. With disease progression, the animals also display a decreased nerve conduction velocity, severe demyelination in both CNS and PNS, accumulation of globoid cells in the white matter and severe gliosis(Baskin et al., 1998; Borda et al., 2008).

1.1.7 Treatment of LSDs

1.1.7.1 Rationale

In the last years, much progress has been achieved in the field of lysosomal storage disorders. In the past, no specific treatment was available for the affected patients; management mainly consisted of supportive care and treatment of complications. Nowadays, successful treatment are available mainly for those LSDs with no CNS involvement, e.g. Gaucher disease type I (Desnick, 2004). The treatments are based mainly on two concepts: 1) increasing residual enzymatic activity pharmacologically or 2) providing the enzyme ex-novo. This second approach relies on the widespread availability of the enzyme that can be achieved by the cross-correction mechanism typical of lysosomal enzymes. The notion that LSDs could be treated by replacing the effective enzyme with its normal counterpart was first suggested by de Duve in 1964 (de Duve, 1964, 2005). The discovery that newly synthetized lysosomal glycoproteins were targeted to the lysosome by the mannose 6- phosphate (M6P) receptor-mediated pathway provided the rationale for the treatment of non-neural LSD by ERT. This phenomenon was first observed on fibroblasts from patients affected by MPS I and II: the metabolic defect of these cells was corrected by providing "factors" secreted by wild type cells (Fratantoni et al., 1968) that was further characterized as functional enzymes (Hasidic et al., 1980). This phenomenon is unique of lysosomal enzymes, as MP6 groups are added exclusively to the N-linked oligosaccharides of these soluble enzymes as they pass through the cis Golgi network. After being modified, the lysosomal enzyme binds the M6P receptor in the trans Golgi network (TGN) and is sorted to the late endosomes to reach the lysosome. About 40% of the enzyme escapes this pathway and is secreted in the extra-cellular space: this enzyme can then bind the M6P-R on the membrane to the producer cell or surrounding cells and can be endocytosed and sorted to the lysosome (Sabatini, 2001). Importantly, only 1-5% of normal intracellular activity was required to correct the metabolic defects in enzyme-deficient cells (Cantz and Kresse, 1974). These studies indicated the

feasibility of ERT and, in particular, that low levels of exogenous enzyme could gain access to intracellular lysosomal sites and metabolize the accumulated substrate(s). Many therapeutic approaches for LSDs are based on cross-correction (Fig.3): in enzyme replacement therapy (ERT), the enzyme, administered through intra-venous injections, can reach the affected tissues with blood, while in tem cell transplant (SCT), the lysosomal enzyme is provided by normal cells of donor origin.

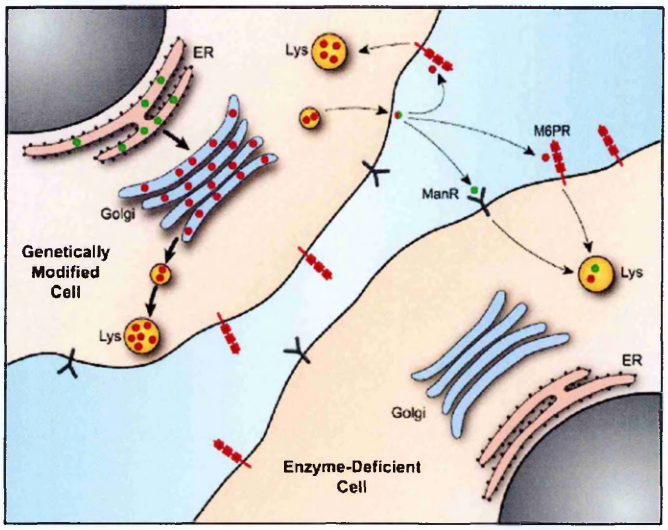

Figure 3. Cross-correction of defective cells by wild type cells. The lysosomal enzyme is released in the extra-cellular space where it is up-taken by defective cells through the M6P-R and sorted to lysosomes (Sands and Davidson, 2006).

1.1.7.2 Enzyme Replacement Therapy

ERT consists of the parenteral administration of the recombinant or purified enzyme and represents a valuable approach for non neurophatic LSDs. ERT is currently used in clinical practice for Gaucher disease type 1 (Desnick, 2004), and Fabry disease (Barbey et al., 2004) and it is under investigation for a number of LSDs, including, MPS I, II, IVB, VI and VII and Pompe disease (Rohrbach and Clarke, 2007). Enzyme replacement therapy for Gaucher didease type I, with glucocerebrosidase purified in large scale from human placentae, was introduced in 1991 (Grabowski et al., 1998). The primary cellular site of pathology in this disease is the macrophage/

monocyte system and the bone marrow and reticuloendothelial organs of affected individuals become infiltrated with lipid-laden 'foam' cells, known as 'Gaucher' cells. Patients develop massive enlargement of their livers and spleens, pancytopenia, and severe skeletal disease causing bone pain and pathological fractures. ERT significantly alleviates hepatosplenomegaly and haematological manifestations (Desnick, 2004). In order to develop an efficacious ERT for LSDs, the differences between the affected tissues should be taken into consideration. Various cell types express different receptors for the uptake of lysosomal enzymes: the hepatocyte membrane contains galactose receptor; macrophages require mannose residues for uptake, whereas most cells bind exogenous enzymes via the M6P-R. Moreover, diversity in the membrane density of the M6P-R of different cells and tissues has been observed: the highest concentration of receptors was found in the heart and kidneys, the lowest in muscles and the brain (Wenk et al., 1991). Therefore, since successful ERT requires targeting of multiple cell types, the ideal drug may be the one that includes enzymes with various sugar residues and isoforms, to take advantage of the many cellular receptors involved in endocytosis. Recombinant enzymes are currently obtained from cultures of over-expressing Chinese Hamster Ovary (CHO) cells or human fibroblasts. The genes for almost all of the lysosomal enzymes have been cloned and theoretically their encoded proteins could be produced in large quantities.

A major limitation of ERT is the inability of the enzyme provided, to efficiently cross the blood brain barrier (BBB), with a consequent ineffectiveness of this treatment for LSDs with severe CNS involvement (Schiffmann, 2010). However, recent studies challenged this dogma and suggest that, in some disorders, the modified or the native enzyme may be able to do so. Recently it has been tried to conjugate of the enzyme with molecules recognized by a specific BBB carrier, such as IGF-2, the Fc fragment of antibodies, ApoB, or the TAT protein transduction domain (Boado, 2008). Other approaches being developed to improve the transport across the BBB aim to extend the circulating half-life of the administered enzyme, such as by removing M6P residues and thus inhibiting uptake via M6P receptor by peripheral organs (Boado, 2008). Preclinical results on a mouse model of Metachromatic leukodystrophy (Matzner et al., 2005) suggested the

opening of a clinical trial for ERT; however, the outcome was not successful in humans and the clinical trial changed to a direct intratechal delivery approach (Shire HGT). Another limitation of ERT is the frequent occurrence of immune responses against the injected protein. In LSDs characterized by a complete absence of the enzyme, parenteral administration could result in the recognition of the protein as a non-self antigen, thus triggering a humoral response with IgG production. As a consequence, alteration of the pharmacokinetic, hypersensitivity and very occasionally, neutralization of the administered enzyme, were observed (Brooks et al., 2003). Recently the use of immunomodulatory gene therapy, i.e. the use of liver specific promoters to induce immune tolerance, has been proposed to overcome this issue (Koeberl and Kishnani, 2009). Finally, the high cost of the recombinant enzymes, the need for life-long treatment and the frequency of injections are significant issues for many patients and their families.

1.1.7.3 Enzyme Enhancement Therapy

In addition to ERT, current efforts are focused on the development of other strategies such as EET or Pharmacological Chaperon therapy (PCT). In most lysosomal disorders, certain missense mutations produce mutant proteins with a small amount of residual enzymatic activity (even less than 1%). These mutations result in milder phenotypes than those that have no residual enzyme function. The presence of residual activity presumably results from a small amount of the mutant glycopeptide that was properly folded, assembled, post-translationally modified, and trafficked to the lysosome. Such mutations are excellent candidates for EET. The hypothesized mode of action of these chaperones consists of reversible binding to the active site of a missense mutant enzyme, correcting protein misfolding and enhancing delivery to the lysosome. In the acidic lysosomal environment and in the presence of substrate, the chaperone would be released and the mutant enzyme would function better (Fan and Ishii, 2007). Recently, Suzuki and colleagues reported the rescue of β-galactosidase activity in deficient human and murine cultured fibroblasts and in a transgenic mouse model of GM_1-gangliosidosis, using the galactose derivative N-octyl-4-epi-β-

valienamine (NOEV), (Matsuda et al., 2003). The clinical efficacy of pharmacological chaperones has been investigated in the 'cardiac variant' of Fabry disease, obtaining evidence of improvement (Frustaci et al., 2001). Thus this type of treatment has shown to be promising, however these molecules work for some type of mutations and not for all of them.

1.1.7.4 Substrate reduction therapy

Substrate reduction therapy (SRT) is design to reduce the synthesis of the accumulating glycosphingolipids and the presumed offending metabolite (Cox, 2005; Platt and Jeyakumar, 2008). The concept of SRT was proposed by Norman Radin as a potential treatment for type 1 Gaucher disease, which is characterized by deficiency of glucocerebrosidase, leading to accumulation of glucocerebroside (Radin, 1996). The imino sugar Miglustat has been effective in treating mild to moderate systemic manifestation in patient with Gaucher disease (Pastores et al., 2005). Miglustat showed promise in animal models of GM_1 and GM_2 gangliosidosis and Niemann-Pick type C (Elliot-Smith et al., 2008; Jeyakumar et al., 1999; Zervas et al., 2001). Because SRT with Miglustat inhibits ceramide glucosyl transferase, neuronopathic Gaucher disease was theoretically the best candidate for this therapy (Platt and Jeyakumar, 2008), indeed there is evidence that Miglustat crosses the blood–brain barrier. However, a clinical trial did not show any effect of Miglustat on the neurological aspects of patients with type 3 (chronic neuropathic) Gaucher disease (Schiffmann et al., 2008). This failure may have been due to the limited potency of Miglustat or to the irreversible nature of the neurological deficit in this disease. Thus far, SRT has been shown to be somewhat effective only in patients with Niemann–Pick type C disease (Patterson et al., 2007). Even though the use of substrate synthesis inhibitors might influence the presence and distribution of sphingolipids, which play a number of important functions in cellular metabolism, it is likely that new molecules useful for SRT, with greater specificity and improved delivery to the brain, will be developed.

1.1.7.5 Stem cell transplant

The transplant of stem cells of different origin (neural, hematopoietic and mesenchymal stem cells) based its feasibility on the secretion of a functional lysosomal enzyme from the donor cells (Lee et al., 2007a; Lee et al., 2008; Orchard et al., 2007; Orchard and Tolar, 2010).

1.1.7.5.1 Hematopoietic stem cell transplant (HSCT)

An increasing number of patients with LSDs are undergoing HSCT in attempt to slow the course of the disease, prevent the onset of clinical symptoms and improve some pathological findings. The most promising results are obtained when HSCT is performed in pre-symptomatic patients, identified in the uterus or at birth because of family history (Peters and Steward, 2003). The rationale of HSCT is to reconstitute a patient's hematopoietic system with normal stem cells that are able to produce the missing enzyme. Hematopoietic Stem Cells (HSCs) are somatic stem cells that give rise to all blood cell lineages. Human HSCs can be isolated mechanically from the BM, where they reside, or from peripheral blood upon mobilization. An alternative HSC source is the cord blood. Initially, bone marrow was used as a source of stem cells but more recently, cord blood is the preferred cell source. The HSC pool is generally identified through the expression of the surface marker CD34, but selection using this marker provides a heterogeneous population of stem and committed progenitor cells. The most accurate definition of HSC is according to their function, measured as their ability to repopulate the hematopoietic system of a myeloablated host. Following systemic injection, HSCs circulate in the bloodstream, cross the vasculature and seed in the BM niche. This process is called *homing* and it is an active mechanism with many complex steps (Whetton and Graham, 1999).

Preclinical studies showed that donor-derived cells of the monocytic lineage infiltrate different tissues of the recipient, replacing the local macrophage population. These cells are not only the major effectors contributing to the clearance of the stored material throughout the tissues, but also act as reservoirs, synthesizing and secreting lysosomal enzymes which can be taken up by

neighbouring cells (cross-correction)(Biffi et al., 2004). HSCT has been tried in a certain number of LSDs but it seems to be effective only in a few of them (i.e. MPS I, non-neuropathic Gaucher disease) (Aldenhoven et al., 2008; Hoogerbrugge et al., 1995). HSCT might in principle be effective in halting the neurodegeneration in LSD in which there is a severe CNS involvement. This efficacy is related to the fact that perivascular and parenchymal microglia in the brain derives from bone marrow precursors and after HSCT the brain starts to be repopulated by the microglia derived form the donor. The newly constituted microglia starts a mechanism of cross-correction, secreting the missing enzyme that can be internalized by neighbour cells (Biffi et al., 2008; Krivit et al., 1999b). This process might be accelerated or in the presence of a strong inflammation or neurodegeneration, because of the potential increase of BBB permeability (Rodriguez et al., 2007; Simard et al., 2006). The myeloablative-conditioning regimen applied before HSCT is essential to allow engraftment of exogenous HSC, and could play a fundamental role in the timing and extent of reconstitution. In fact, irradiation or administration of chemotherapic agents promotes microglia reconstitution by increasing the permeability of the BBB (Ajami et al., 2007). One of the intrinsic limitations of this approach is time required to achieve full microglia replacement following HSCT. In mice, the time required to obtain extensive microglia reconstitution in the CNS is estimated around 1-6 months or more, according to the myeloablative regimen used and the underlying disease. In humans this is a very slow process and can need even years to be completed (Krivit et al., 1995). For this reason, even in the LSDs that better respond to HCT (e.g. Hurler), delivery of the missing enzymes to hardly accessible tissues (e.g. bone and, most importantly, CNS) is still suboptimal. In the rapidly progressive infantile forms with severe neurodegeneration this rather slow turnover might hamper the possibility to obtain therapeutic levels of enzyme in the time window of post-natal CNS development that is critical for myelination and neurogenesis, and for the correct development of CNS connections in the time window when the disease is more rapidly progressing. HSCT is associated with fairly high morbidity and mortality, which limits its use in conditions that are already life threatening. Major causes of morbidity and mortality are engraftment failure (i.e. inability of the transplanted HSC to

engraft and repopulate the recipient), regimen-related toxicity, graft versus-host disease (GvHD) and sepsis. Engraftment failure might be related to HSC or to the recipient. Several studies analysed the risk factors (such as HLA mismatch or T cell depletion) related to engraftment failure for example for MPS I-Hurler disease (Fleming et al., 1998). Due to these evidences HSCT does not constitute a valuable therapeutic option for many LSD patients. The use of CB HSCs greatly has influenced the outcome of HSCT in LSDs. When allogeneic HSCT is performed using BM HSCs, donors are usually siblings and often they are heterozygous/carrier for LSD. Transplantation of CB-derived HSCs, increases the number of available donors since a lower standard of histocompatibility between donor and recipient, is acceptable (Orchard and Tolar, 2010). The possibility to engineer autologous HSCs to over-express the relevant enzyme, thus combining stem cell transplantation with gene therapy could maximise the therapeutic benefits and simultaneously reduce the limitation and risks associated with allogeneic HSCT (see below).

1.1.7.5.2 Neural stem cell transplant

Transplanting neural stem/progenitor cells (described in paragraph 3.4) that intrinsically secrete missing or therapeutic gene products, may provide a strategy for long-term treatment of central nervous system manifestations of a number of neurogenic diseases (Snyder and Wolfe, 1996). Multipotent neural progenitors or stem cells (or cells that mimic their behaviour) can engraft as integral members of normal structures throughout the host central nervous system without disturbing other neurobiological processes. The feasibility of this neural stem cell-based strategy has been demonstrated in several animal models of neurodegenerative diseases (Lindvall and Kokaia, 2006; Shihabuddin and Aubert, 2010; Windrem et al., 2004). While NSC were initially thought as good candidates for cell replacement strategy, it is becoming clear that the therapeutic benefit of NSCs is mediated by a number of indirect, by-stander mechanisms, which are alternative and/or complementary to the expected cell replacement. In particular, NSCs can promote survival and function of endogenous glial and neural progenitors, following a

pathological insult. When transplanted in murine or non-human primate model of a chronic inflammatory neurodegenerative (Einstein et al., 2003; Pluchino and Martino, 2008a; Pluchino et al., 2003), ischemic (Bacigaluppi et al., 2008; Ballabio and Gieselmann, 2009), haemorrhagic (Lee et al., 2008) or traumatized (Park et al., 2002). CNS environment, NSCs can play an immunomodulatory and neuroprotective role that ameliorates pathological conditions (Jaderstad et al., 2010; Shihabuddin and Aubert, 2010).

Preclinical studies of NSCT have been made in several animal models of LSDs. In Sandhoff disease study, clinical improvement in the mice resulted from neonatal transplants using mouse or human neural stem cells. The transplantation delayed disease onset, preserve motor function, reduced pathology and prolonged survival. The limited cell replacement alone could not account for the improvement suggesting that the clinical benefit most likely resulted from multiple mechanisms (Lee et al., 2007a). Preclinical data about human NSC transplantation in a mouse model of infantile NCL, also known as Batten disease, showed that when transplanted in a mouse model of infantile NCL, human NSC engraft, migrate and continuously secrete the missing lysosomal enzyme. This results in a significant reduction storage build-up, protection of critical host neurons and delayed loss of motor function (Tamaki et al., 2009). On the basis of these pre-clinical studies, Stems cell's HuCNS-SC® product (an highly purified composition of human neural stem cells isolated from the human fetal brain that are prepared under controlled conditions) has been used in the first clinical trial based on the use of NSCT for a genetic neurodegenerative disorder. This clinical trial showed unclear results in terms of safety and efficacy (ClinicalTrials.gov identifier, NCT00337636). FDA allowed the phase II clinical trial to start.

A combined gene and NSC-based therapy approach might exploit the direct/by-stander effects provided by NSC with the possibility of producing high levels of the deficient enzyme. Genetically modified NSCs have been used in preclinical studies for MPS VII (Meng et al., 2003), Niemann Pick A disease (Shihabuddin et al., 2004) and Sandhoff disease (Jeyakumar et al.,

2009), with promising results in terms of reduction of storage, improve pathology and function, as better detailed below.

1.1.7.6 Gene therapy

LSDs are generally well-characterized single gene disorders, thus making them particularly attractive candidates for intervention by gene therapy. Moreover the possibility to modify a small number of cells that can produce and secrete supra-physiologic levels of the deficient enzyme coupled to cross-correction allow metabolic correction of a wide range of cell types. The potential efficacy of gene therapy approaches in LSDs is also related to the fact that even a low level of enzyme can be therapeutic. Furthermore the potential long-term expression of the therapeutic protein and the availability for patients with rare conditions are other benefits (Cheng and Smith, 2003).

In vivo gene therapy refers to the injection of a gene transfer vector directly into a tissue or into the circulation. Systemic delivery involves mainly liver transduction, which becomes the principal source of the circulating enzyme. Intracerebral injection allows direct CNS correction and it is useful for LSDs with CNS involvement (Sands Davidson, 2006). Adeno-associated viral and retroviral vectors have been used extensively in various animal models of LSDs with brain involvement (Marshall et al., 2002; Salegio et al., 2010). Intracerebral gene delivery has been shown to achieve long-term protein expression and therapeutic benefits in several small and large animal models of LSD, including GM_1- and GM_2-gangliosidosis (Broekman et al., 2007; Cachon-Gonzalez et al., 2006), alpha-mannosidosis (Vite et al., 2005), mucopolisaccaridosis (Di Domenico et al., 2009), Niemann-Pick A (Passini et al., 2005) and neuronal ceroid lipofuscinosis (Cabrera-Salazar et al., 2007). Significant improvements have been done in vector design in order to have long-time expression of the transgene and to decrease the immunity response. Recently it is emerging the role of lentiviral gene transfer vectors as therapeutic tool thanks to their ability to transduce non-dividing cells efficiently and to mediate persistent *in vivo* expression (Deglon and

Hantraye, 2005) (Di Domenico et al., 2009; Lattanzi et al., 2010).

Ex vivo gene therapy aims to modify cells genetically *ex vivo* and transplant them into an affected patient to create a reservoir of enzyme that can be secreted into the circulation and correct the disease at distant sites. The main types of somatic stem cells used in LSDs *ex vivo* gene therapy approaches are bone marrow stem cells (BMSCs), hematopoietic stem cells (HSCs), neural stem cells (NSCs) and mesenchymal stem cells (MSCs) (Shihabuddin and Aubert, 2010; Shihabuddin et al.). Several pre-clinical studies have demonstrated the efficacy of HSC gene therapy on murine models of LSDs (Biffi et al., 2008). In particular, the excellent results in terms of safety and efficacy of some pre-clinical studies using HSC gene therapy have allowed recently moving forward to clinical application. A clinical trial based on *ex vivo* gene therapy with lentivirus and HSCs, is on going for ALD patients and very promising results were obtained in two patients after 30 months follow up (Cartier et al., 2009). Based on the good results obtained from ARSA overexpression in HSC in mouse model (Biffi et al., 2006), a phase I/II clinical trial using *ex vivo* HSC gene therapy in MLD patients is on going in San Raffaele Institute.

1.1.7.7 Combined therapy

Many neurodegenerative diseases, including LSDs, are characterized by CNS inflammation. Whether this is a secondary consequence of the storage, it represents a valuable target for adjunctive therapy (Jeyakumar et al., 2005). Proia and co-workers demonstrate the proof of principle by crossing Sandhoff disease mice (Hex-/-) with macrophage inflammatory protein 1α (Mip1α-/-)(Wu and Proia, 2004). On the same Sandhoff model other options were tested, such as NSAIDs (Jeyakumar et al., 2004) anti-oxidants (Jeyakumar et al., 2004), but also combination of HSCT and SRT (Jeyakumar et al., 2001), SRT and NSAIDs (Jeyakumar et al., 2004) with encouraging results. These studies clearly demonstrate the overlap between the pathology of LSDs and that of other neurodegenerative conditions, thus targeting the different aspects of the LSDs pathogenesis might be on benefit in the future therapy.

1.1.7.8 Treatments for GLD

ERT

Due to the neuropathic component of GLD, the possible benefits of ERT treatment are poor. Pre-clinical studies on systemic GALC injection in Twi mice demonstrated only slight improvement in lifespan, although enzyme activity was detected (Lee et al., 2005). Similar results were obtained with intracerebrovetricular injections (Lee et al., 2007b).

EET

Very recently it has been reported the first study on the use of GALC pharmacological chaperons. The authors characterized three different homozygous mutations on mammalian cells and tested the effect of α-lobeline. Partial rescue of one out of three was proven (Lee et al., 2010). In vivo studies and the broadening of activity will be required before considering it as alternative therapy.

SRT

SRT has been tested on Twi mice in combination with HSCT and resulted in a greater benefit than either treatment alone (Biswas and LeVine, 2002). The lack of any significant deleterious effects in the mice exposed to the drug may reflect the fact that the inhibition of substrate synthesis is a partial, rather than a full or complete block. However, the "genetic" substrate reduction in CGT-/-twi-/- double ko mice led to unexpected findings (Ezoe et al., 2000). In this mice GC are not present at any age, while a progressive neuronal pathology was observed in the brainstem and spinal cord after 45 days. This finding might suggest that either some unknown substrates of GALC are synthesized in the absence of CGT or some of the usual CGT products can be synthesized by other enzymatic mechanism.

HSC TRANSPLANT

HCT was initially tested on Twi mice. Transplanted mice displayed a sustained increase of GALC activity in the CNS, a stabilization of Psy storage and a reduction in both the number of globoid cells and demyelination (Ichioka et al., 1987). Preliminary evidence has shown that HSCT could be effective for patients affected by the infantile form of GLD, if applied within the first months of life. When the disease is diagnosed early and when an HSC donor is available, HSCT can delay

the onset of GLD and halt its progression. Pre-symptomatic and symptomatic children with the infantile form of GLD have been successfully transplanted with HSC from unrelated CB (Escolar ML, 2005). Preliminary results have shown a positive effect if patients have been transplanted very early in life before the onset of symptoms. In such patients, the progression of the disease has been slowed and their phenotype seems milder compared to untreated controls. However variable motor function, from nearly normal to an inability to walk without assistance, may be attributed to different rates of central myelination. The effects of cord blood transplantation on myelination may differ in the central and peripheral nervous (Escolar et al., 2005). In patients transplanted at a symptomatic stage, disease progression has been shown to be as fast as in non-transplanted children. Only partial results were also obtained when HSCT was performed in patients affected by the late-onset form (J and Ad) of GLD (Krivit et al., 1998; Lim et al., 2008). Moreover with this procedure the effect of irradiation on proliferating cells (i.e. neural progenitors) has to be taken into account. High doses necessary for transplant could be deleterious for this cell population.

NSC TRANSPLANT

Neural stem cells appear to be resistant to toxic metabolites, making them good candidates for therapies in metabolic disorders where the cellular environment is damaged (Taylor et al., 2006). In a previous study (Pellegatta et al., 2006) Twi mice were transplanted with cultured LV-transduced NSCs. Although the engrafted GALC-over-expressing cells did not survive well in the highly inflammatory Twi brain, they migrated appropriately to active sites of demyelination. The therapeutic effect of the treatment was modest, due to the clearance of transduced cells, likely due to the activated microglia. The hypothesis that the CNS of Twi mice could be a non-permissive environment for transplanted cells was also investigated by Snyder's group. The inflammatory milieu of Twi CNS was not found to be a limiting factor for NSC engraftment, but, rather, it appeared to serve as a recruiting factor, drawing transplanted NSC towards damaged areas (Zhao et al., 2007). Moreover, they investigated the sensitivity of NSC to the toxic storage of Psy, present in the CNS of Twi mice. NSC showed an increased resistance to the detrimental effect of

Psy, if compared with more differentiated cells, such as oligodendrocytic progenitor (Taylor et al., 2006). Therefore, in order to develop an effective cell/gene therapy strategy for the treatment of GLD, different aspects should be carefully considered, including the level of enzyme expression required to achieve benefit, the characteristics of the transplanted cells and the permissiveness of the environment.

GENE THERAPY

In vivo gene therapy approaches have also been tried in animal models of GLD, based on *in vitro* studies showing the feasibility of gene correction in different neural cell types derived form the animal models (Luddi et al., 2001; Rafi et al., 1996) and from fibroblasts from GDL patients (Gama Sosa et al., 1996).

Intraventricular injection of Adenoviral vector carrying human GALC (hGALC) transgene performed at birth in Twi mice resulted in increased GALC activity and partial correction of the pathology in the brain, but without a significant improvement of the phenotype. Instead, pathology correction was not observed when Twi mice were treated at 15 days, suggesting that the timing of intervention its fundamental (Shen et al., 2001). Similarly intraventricular injection of AAV1, AVV2 or AVV2/5 did not achieve improvements in phenotype (Lin et al., 2005; Rafi et al., 2005). In general, intracranial injection of viral vectors expressing GALC resulted in physiological or even supra-physiological levels of enzyme activity in the brain. This resulted in slow-down of disease progression, significant reduction of tissue storage and decrease of activated microglia and astroglia (Lattanzi et al., 2010).

The major limitation of this approach is the lack of efficacy at the level of the PNS. For this reason, the combination with a systemic approach, such as ERT or HSCT, which could provide the enzyme to the PNS, might give better results.

Ex vivo gene therapy has been shown in several preclinical studies. A combined gene and cell-based therapy approach aims at enhancing the production of the deficient enzyme by prior transduction of cells with gene therapy vectors before transplantation into the host. However, in the case of GALC it has been recently demonstrated that forced expression of high levels of the

enzyme affects HSC survival and the HSC niche by altering the delicate balance that regulates bioactive sphingolipids, posing additional problems of transgene expression regulation in the perspective of HSCT for KD (Visigalli et al., 2010). Nevertheless, few months ago the same group demonstrated that the insertion of a regulatory sequence for microRNA suppressed GALC expression in HSCs while maintaining robust expression in mature hematopoietic cells. This approach protected HSCs from GALC toxicity and allowed successful treatment of a mouse GLD model, providing a rationale to explore HSC-based gene therapy for GLD (Gentner et al., 2010). NSCs have been used also for *ex vivo* gene therapy. Pellegatta and co-workers transplanted Twi mice with cultured LV-transduced NSCs. Although the engrafted GALC-over-expressing cells did not survive well in the highly inflammatory Twi brain, they migrated appropriately to active sites of demyelination (Pellegatta et al., 2006). Other study however suggested that inflammation could be useful to guide transplanted cell (Zhao et al., 2007) and moreover that gene corrected NSC are less susceptible to Psy toxicity (Taylor et al., 2006).

COMBINED THERAPY

Anti-inflammatory therapy with NSAIDs was tested in trs mice, a transgenic model of GLD, showing increasing life-span of treated mice (Luzi et al., 2009), thus indicating a possible role for combined therapy in association with a source of enzyme. Other preclinical studies are ongoing or are been done in order to couple CNS and total body treatment, for example the combination of *in vivo* gene therapy with a systemic approach, such as ERT or HSCT. Combination of gene therapy in the CNS with HSCT was tried (Lin et al., 2007). Twi mice were injected with AAV vector expressing GALC in the CNS and underwent HSCT from wild type donors. Encouraging results were obtained, suggesting synergy between the two therapies. In a different study, bone marrow cells and GALC-LV vectors were administered intravenously without any preconditioning to newborn Twi (Galbiati et al., 2009). These types of treatment will allow multi-organ treatment with good bioavailability of the GALC enzyme in a relevant time window.

1.2 Bioactive lipids

1.2.1 Overview

Lipids were canonically considered molecules involved in the formation and regulation of cellular membranes. After 20 years of research, now they are more considered: it was introduced the concept of "bioactive lipids", that means that these molecules can have a role also in cellular functions and they are no more only structural elements. The demonstration of direct activation of protein kinase C by the lipid diacylglycerol (DAG) triggered the idea that a lipid could regulate cell signalling (Nishizuka, 1992). An important group of bioactive lipids are the sphingolipids (Fig.4).

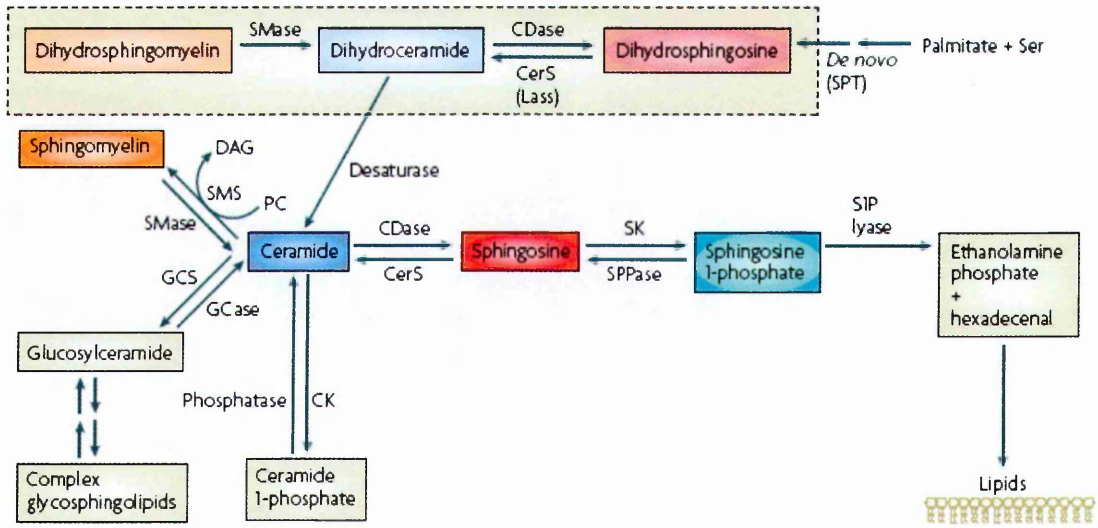

Figure 4. Sphingolipids metabolism and interconnection of bioactive lipids. Cer is considered to be the central hub of sphingolipids metabolism and is synthesized de novo from the condensation of palmitate and serine to form 3-keto-dihydrosphingosine (not shown). I turn, 3-keto-dihydrosphingosine is reduced to dihydrosphingosine followed by acylation by CerS. Cer is generated from the action of desaturases. From here, Cer can be converted to other interconnected bioactive lipid species. The only exit pathway is mediated by S1P lyase, which metabolizes S1P. CDase, ceramidase CK, Cer kinase; DAG, diacylglycerol; GCase, glucosylceramidase; GCS glucosylceramide synthase; PC, phosphatidylcholine; SK sphingosine kinase; SMaes, sphingomyelinase; SMS, sphingomyelin synthase; SPPase, sphingosine phosphate phosphatase; SPT, serine palmitoyl transferase. (Hannun ad Obeid 2008).

Sphingolipid metabolism has a unique metabolic entry point, which forms the first sphingolipid in the de novo pathway and a unique exit point, which breaks down Sphingosine-1-Phospate (S1P) into non-sphingolipid molecules. The multiple metabolic steps in between constitute a highly complex network that connects the metabolism of many sphingolipids. In this network, ceramide (Cer) can be considered to be a metabolic hub because it occupies a central position in the sphingolipid biosynthesis and catabolism (Fig.4). Enzymes of lipid metabolism are intimately related to each other, generating interconnected network that regulates not only the levels of individual lipids, but also their metabolic interconversion. Interestingly, the cellular levels of these bioactive sphingolipids render this scenario very likely. For example, in most cell types, sphingomyelin (SM) (Cer precursor) is present in concentrations that are an order of magnitude higher than those of Cer; therefore, small changes in SM can result in profound changes in Cer. In addition, Cer is often detected in concentrations that are more than an order of magnitude higher than those of sphingosine. Therefore, immediate hydrolysis of only 3–10% of newly generated ceramide may double the levels of sphingosine. Similarly, phosphorylation of 1–3% sphingosine may double the levels of S1Ps (Bielawski et al., 2006). Moreover, there are multiple pathways that can operate in parallel. In addition, bioactive sphingolipids exhibit hydrophobic properties; therefore their physiological environment is mostly restricted to membranes. Their subcellular localization and transport across and between membranes is indeed another element of complexity (Hannun and Obeid, 2008).

1.2.2 Sphingosine-1-phosphate

S1P is a key regulator of numerous physiological functions, including cell growth and survival, angiogenesis, cell motility and migration and lymphocyte trafficking (Maceyka et al., 2009; Spiegel and Milstien, 2003). S1P is formed intracellularly by two Sph kinases (SphK1 and SphK2) starting from Sph and sphinganine; it is important to not that these two molecules are not produced de novo and are only formed by catabolism of sphingolipids. S1P can be degraded

either by reversible dephosphorylation to Sph by phospahtases, including lysosomal phosphatses such as such as members of LPP family and two S1P specific phosphatases, SPP1 and SPP2 (Maceyka et al., 2007), or degraded by irreversible cleavage to ethanolamine phosphate and hexadecenal by S1P lyase (Bandhuvula and Saba, 2007).

S1P is a ligand for a family of five G-protein-coupled receptors (S1PRs), termed S1P1–5. In many cases, activation of these S1PRs appears to involve ''inside-out'' signalling whereby growth factors, cytokines, or cross linking of IgE receptors stimulates cytosolic SphK and induces its translocation to the plasma membrane where its substrate sphingosine resides (Spiegel and Milstien, 2003). This activation process produces S1P that may be secreted from specific types of cells, perhaps through the ABC transporter ABCC1 (Mitra et al., 2006) to stimulate S1PRs in an autocrine or paracrine manner. Whereas cell stresses, such as tumour necrosis factor-α, irradiation and anticancer drugs, induce accumulation of ceramide leading to apoptosis, many other stimuli, particularly growth and survival factors, activate SphK1, resulting in accumulation of S1P and consequent suppression of ceramide-mediated apoptosis (Cuvillier et al., 1996; Spiegel and Milstien, 2003). It has been suggested that the dynamic balance between intracellular S1P vs. sphingosine and ceramide, and the consequent regulation of opposing signalling pathways, is an important factor that determines whether cells survive or die (Cuvillier et al., 1996). This ''sphingolipid rheostat'' has important clinical implications for cancer treatment (Ogretmen and Hannun, 2004) and is evolutionarily conserved, as it also plays a role in regulation of stress responses of yeast (Saba and Hla, 2004).

Recently Wu and colleagues demonstrate a link between S1P receptor signalling pathway and neuropathic LSDs, using a model of Sandoff and Tay-Sachs disease (*Hexb* null mice). In these disorders an absence of lysosomal β-hexosaminidase A bloks the gangliosides degradation pathway, leading to substrate accumulation in neurons and triggering a sequence inducing neuronal cell death. The authors showed that genetic deletion of SphK1 or $S1P_3$ resulted in a milder disease course, with decreased glial proliferation and astrogliosis, thus suggesting a

regulation of these two phenomena during the terminal stage of Sandhoff disease by SphK1/ $S1P_3$ axis (Wu et al., 2008).

1.2.2.1 Sph kinases

In mammals both SphKs have a broad and overlapping tissue distribution, with SphK1 predominating in lung and spleen and SphK2 predominating in the heart, brain and liver (Kohama et al., 1998; Liu et al., 2000a). SpK1 and SpK2 are primarily cytosolic, although their distributions are altered in different cell types and by various signals (Strub et al., 2010). Homozygous single knock out mice of either enzyme are viable and there are no obvious phenotype. However, double mutants with all the four alleles missing, died in utero due to defective brain and cardiovascular system development (Mizugishi et al., 2005). This suggest that SpK1 and SpK2 are redundant in mammals for viability, but the functional redundancy may not apply to a variety of pathophysiological conditions, suggesting that isoenzyme-specific targeting of SphKs may be an effective means of disease control or prevention.

SphK1 is activated by diverse stimuli, including hormones, growth factors, immunoglobulin receptor crosslinking, cytokines, chemokines and lysolipids, including S1P (Spiegel and Milstien, 2003). Indeed, many of the pro-growth and anti-apoptotic effects observed by exogenous additions of S1P can be reproduced by overexpression of SphK1. On the contrary, SphK2 overexpression induced growth arrest, promotes apoptosis and chemosensitizes several cell types (Liu et al., 2003; Okada et al., 2005). The differential effects of the two SphKs on cell fate are due in part to their different roles in regulating Cer levels and in part to the different effects in transduction of signal from cell surface receptors (Strub et al., 2010).

1.2.2.2 Sph receptors

S1P is a ligand for five specific GPCRs $S1P_{1\text{-}5}$, formerly called endothelial differentiation gene (EDG) receptors, which are differentially expressed in different tissues. The cell types specific

expression of S1PRs as well as their differential coupling to different G proteins, explains the diverse signalling of S1P (Brinkmann, 2007). In many cases, the S1P produced activates cell surface S1PRs in a paracrine and/or autocrine manner, indeed many of the downstream effects of these stimuli require transactivation of one or more S1PRs, also called "inside-out" signalling (Alvarez et al., 2007).

$S1P_1$ is ubiquitously expressed, with high levels in brain, lung, spleen, cardiovascular system and kidney. Is it known that $S1P_1$ plays a key role in angiogenesis (Liu et al., 2000b), in maintaining endothelial barriers (McVerry and Garcia, 2005) and in immune cell function (Matloubian et al., 2004).

$S1P_2$ is also widely expressed in a variety of different cell types. It is required for proper development of the auditory and vestibular system (Kono et al., 2007), for mast cell degranulation (Jolly et al., 2004) and for increasing vascular permeability (Sanchez et al., 2007). $S1P_2$ is generally considered to be a repellent receptor as its activation inhibits cell migration and appears to work in opposition to $S1P_1$ and $S1P_3$, which both enhance cell migration (Lepley et al., 2005).

$S1P_3$ is expressed in the cardiovascular system, lungs, kidney, intestines, spleen and cartilage. It is an important regulator for vascular permeability (Sanchez et al., 2007) and for the heart rate (Forrest et al., 2004).

$S1P_4$ is primarily expressed in lymphoid tissues, including thymus, spleen, bone marrow, appendix and peripheral leukocytes. Its activation modulates the opening of intracellular calcium storages (Van Brocklyn et al., 2000).

$S1P_5$ is highly expressed in oligodendrocytes, however it is not clear if it plays a role in myelination (Jaillard et al., 2005).

1.2.3 Ceramide

Ceramide is considered to be the central hub of sphingolipid metabolism, and is synthesized de novo from the condensation of palmitate and serine to form 3-keto-dihydrosphingosine. In turn, 3-

keto-dihydrosphinsine is reduced to dihydrosphingosine followed by acylation by (dihydro)-ceramide synthase (CerS). Cer is generated by the action of desaturases. From here, Cer can be converted to other interconnected bioactive lipid species (Fig.4). In addition, Cer can be also produced by turnover of complex sphingolipids, such as sphingomyelin, GalCer and GlcCer, and Cer1P (Zheng et al., 2006). Although there are many signalling pathways that are affected by Cer, several appear to be direct targets: Phosphoprotein Phosphatases 1 and 2A (PP1 and PP2A) (Pettus et al., 2002), protein kinase C (PKC)(Kajimoto et al., 2004), Cathepsin D (Heinrich et al., 1999), stress-activated protein kinase (SAPK/JNK)(Huwiler et al., 2004). Moreover, the biophysical properties of Cer allow membranes to undergo structural changes that can be viewed as analogous to the activation or inactivation of a signalling target (Kolesnick et al., 2000).

1.2.4 Lactosylceramide

LacCer can be generated via different pathway: from ceramide generated by de novo pathway, from ceramide generated from other sphingolipids and from the catabolism of complex glycosphingolipids via the action of sialidases, galactosidase, sulfatase and fucosidase. Conversely LacCer plays a pivotal role as a precursor in the biosynthesis of the majority of glycosphingolipids. Briefly, Cer is converted in Glucosylceramide (GlcCer) by glucsylceramide synthase (GlcT), and then LacCer synthase (GalT-2) transfers a galactose moiety and GlcCer become LacCer. Moreover, it can be generated by catabolism of gangliosides via the action of sialidases. Until now four types of sialidases have been identified in human cells: lysosomal (NEU1), cytosolic (NEU2), plasma membrane (NEU3) and NEU4 (Chatterjee and Pandey, 2008). Among them the plasma membrane-bound sialidases have been shown to hydrolase gangliosides preferentially and are of great importance as they can rise the pool of LacCer and thus alter cell function (Miyagi et al., 2004). On the contrary, NeuAc LacCer a 2-3-sialyl transferase (SAT-1) catalyzes the formation of GM_3 ganglioside from LacCer.

LacCer plays a role in physiological processes such as smooth muscle cell proliferation (Bhunia et al., 1997), expression of adhesion molecules (Bhunia et al., 1998), angiogenesis (Rajesh et al., 2005) and in β1-integrin clustering and endocytosis (Ebadi and Sharma, 2003). Moreover it has been reporter that LacCer is an important signalling component for the induction of pro-inflammatory mediators and astrogliosis (Pannu et al., 2005; Pannu et al., 2004).

1.2.5 Sphingolipids and brain development

Sphingolipids and especially glycosphingolipids (GLS) are essential for the organism. For example, GlcT knockout mice are embryonically lethal and showed no cellular differentiation beyond the primitive cell layers (Yamashita et al., 1999). The crucial role of GLS in the development and maintenance of the proper functions of the nervous system has been demonstrated by lots of work (Piccinini et al., 2010; Yu et al., 2009).

GLS patterns undergo deep qualitative and quantitative modifications during the development of the nervous system: in rodent (Ngamukote et al., 2007) and human brains (Svennerholm et al., 1989) the total gangliosides contents increased several fold from the embryonic stages to the postnatal life. These increases were accompanied by a dramatic shift from simple gangliosides to more complex species. Along the adult life, a progressive loss of gangliosides with aging has been reported (Svennerholm et al., 1991). The expression of galactolipids such as GalCer and sulfatide, highly enriched in CNS and PNS, is also dramatically regulated during the development of the nervous system. During mid-embryonic stages of mouse brain development, GlcCer but not GalCer or sulfatide, is expressed (Svennerholm et al., 1989). Their synthesis starts in the embryonic development when oligodendrocytes enter terminal differentiation and is up-regulated during the postnatal extension of myelin sheaths (Pfeiffer et al., 1993). Moreover blockade of GLS biosynthesis by pharmacological inhibition of GlcT or CerS reduced axonal elongation and branching in cultured hippocampal and neocortical neurons (Harel and Futerman, 1993; Schwarz et al., 1995) and synapse formation and activity (Inokuchi et al., 1997).

1.2.6 Sphingolipids in LSDs

Lysosomal diseases are most frequently classified according to the major storage compound. Thus, disorders in which the accumulation of glysosamminoglycan fragments prevails are classified as mucopolysaccharidoses, those dominate by lipid storage as lipidoses. However, it is important to underlie that in most lysosmal diseases more than one compound accumulates and in some disorders for various reasons the stored material can be rather heterogeneous. The cellular consequences of substrate accumulation are determined by type of storage material, the extent of storage, the type of storing cells, and the direct or indirect consequences that lysosomal storage has on basic cellular processes such as intracellular trafficking and autophagy.

Compounds accumulating in LSDs can affect signal transduction pathways at different levels. Storage compounds can function as ligand for receptors, modify receptor response, alter subcellular organization of receptors and alter activities of enzymes involved in signal transduction cascades (Ballabio and Gieselmann, 2009). In GLD, Psy plays lots of these action: it binds TDAG8 receptor inhibiting cytokinesis, promoting the formation of globoid cells (Kanazawa et al., 2000); it is a reversible inhibitor of PKC, interfering with its activation (Yamada et al., 1996); it interferes with insulin growth factor-1 (IGF-1) signalling pathway increasing apoptosis (Zaka et al., 2005); it activates phospholipase A2, triggering the production of lysophosphatidylcholine (a mediator of apoptosis) and arachidonic acid (that generates ROX and free radicals)(Giri et al., 2006); it reduces the activity of AMP activated protein kinase, influencing the cell energy status (Giri et al., 2008).

Many pathways involve the release of calcium ions from the ER to the cytosol, and increased cytosolic calcium triggers a variety of cellular responses. In Gaucher disease, for example, GluCer storing neurons display an increased calcium release from the ER in response to a glutamate stimulus. This results in enhanced glutamate induced neurotoxicity which might explain partly the neurodegeneration seen in this disease (Korkotian et al., 1999). Moreover the dysregulated calcium homeostasis in the ER could affect the proper protein folding, as in the case of GM_1

gangliosidosi, where accumulation of GM_1 gangliosides elicit the unfolded protein response (Tessitore et al., 2004).

Synthesis and degradation of the various lipids must be fine tuned to maintain membrane homeostasis, thus storage of a particular lipid is likely to affect the metabolism of other lipid. As examples, the synthesis of phospholipids is reduced in GM_2 gangliosidosis as consequence of storage (Buccoliero et al., 2004), whereas in Gaucher disease, the GluCer storage activates enzymes of phospholipid synthesis (Bodennec et al., 2002).

In LSDs, the accumulation of membrane lipids affects also intracellular membrane flow and sorting. Since the endosomal and lysosomal pathway are functionally connected, it is not surprising that lysosomal storage affects intracellular sorting events. In cells of patients with LSDs, LacCer accumulates in the endosomal/lysosomal pathway, suggesting an alteration of the endosomal sorting common to all lipidosis. Indeed, in normal cells, LacCer is endocytosed and transported to the Golgi apparatus (Puri et al., 1999).

Finally, the lysosome plays a major role in an important degradation pathway, autophagy, which mediates the cellular turnover of proteins and organelles. Many studies established the presence of autophagosome accumulation in LSDs. This may be the result of either an induction of autophagy, or a defective autophagosome maturation (Cao et al., 2006; Fukuda et al., 2006; Settembre et al., 2008).

1.3 Neurogenesis, neurogenic niches and neural stem cells in the mammalian brain

Adult brain was supposed to be a stable and non-proliferative tissue for a long time. Evidence for postnatal neurogenesis was seen in the late '60s, from the first experiments performed by Das and Altman on proliferation of progenitors (Altman and Das, 1965a, b). However, from the late '90s it

was becoming clear that pieces of the embryonic development are retained for adult neurogenesis. In fact, stem cell self-renewal and progenitor differentiation is regulated by the specialized microenvironment—or "niche"—in which these cells reside. Such niches are composed of soluble factors as well as membrane bound molecules and extracellular matrix. During brain development, most stem cells and their niches are spatially ephemeral and temporally transient. In contrast, in the adult, neural stem cells and their niches are retained in restricted regions with their local developmental processes occurring for the life of the animal.

In the adult mammals brain, neurogenic stem cells are present in two specific regions, the subventricular zone (SVZ) of the lateral ventricle wall and the dentate gyrus subgranular zone (SGZ) of the hippocampus. Throughout adult life, cells born in the SVZ migrate long distance anteriorly through the rostral migratory stream (RMS) into the olfactory bulb (OB), where they differentiate into interneurons. Neurons in the dentate gyrus are born locally in the underlying SGZ and migrate a short distance to integrate in the dentate gyrus (Alvarez-Buylla and Garcia-Verdugo, 2002; Alvarez-Buylla and Lim, 2004; Alvarez-Buylla et al., 2002). Recently neurogenic niches have been described in the adult human brain.

In the following paragraphs we will discuss the concept of neurogenic niches and neural stem cells, focusing on the mammalian SVZ niche, which is the subject of our experimental work. However, the SGZ will be briefly discussed.

1.3.1 The neurogenic niches from the embryonic/ perinatal to the adult age

NSCs persist in compartments of the mature brain, providing a permanent source of newly generated cells that adapt their intrinsic cell program to the dynamic environment that underlies the transitions between pre-natal and post-natal and, ultimately, to the adult brain. NSC niches regulate neurogenesis during CNS development and provide, in adulthood, a sort of 'immature' environment in which the essential conditions for life-long neurogenesis are maintained. During early postnatal stages we observe the most relevant modifications in the structure and cell

composition of the niche microenvironments that ultimately result in the complex adult architecture (Bonfanti and Peretto, 2007; Gritti and Bonfanti, 2007) (Fig.5).

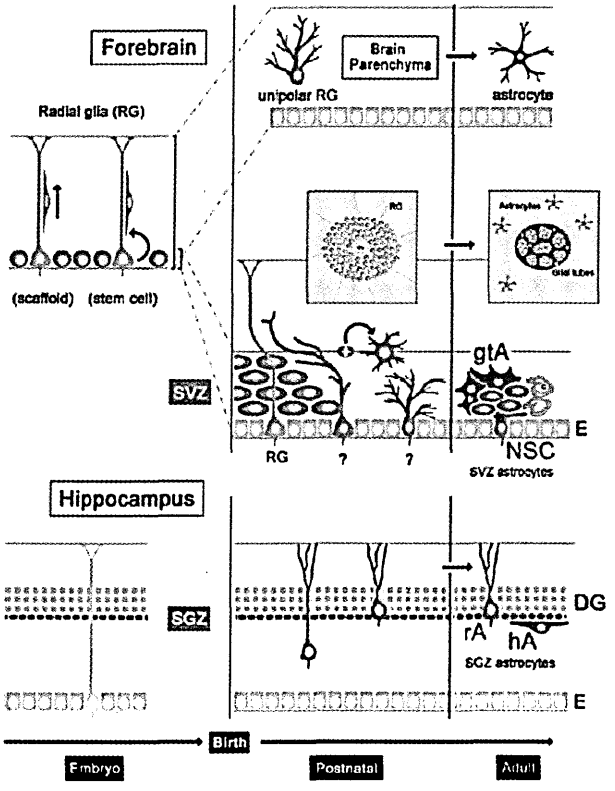

Figure 5. Niche development During embryonic development radial glia (light green) have a dual role, acting both as a scaffold for radial migration of neuronal precursors that leave the germinative layers (purple) and as stem cells capable of generating neurons and glia. After birth, radial glia transform into mature astrocytes (dark green) in the CNS parenchyma, and into astrocytes of the adult neurogenic sites, the forebrain subventricular zone (SVZ) and the hippocampal subgranular zone (SGZ). Abbreviations: E, ependyma; gtA, astrocytes of the glial tubes; hA, horizontal astrocytes; NSC, neural stem cells (type B cells, b); rA, radial astrocytes; RG, radial glia (Gritti and Bonfanti2007).

1.3.1.1 The SVZ niche

Central nervous system development is an intricate process relying on a series of mechanisms precisely regulated in time and space. In rodents, the majority of the cells presents in the adult brain are produced and migrate to their respective destination within an approximately one-week period during embryogenesis. The embryonic CNS is a dynamic structure, constantly increasing in size due to histogenesis, while the stem/precursor cell populations, which are responsible for building the brain, are retained in two distinct and relatively small proliferative areas. The first is the ventricular zone (VZ) where epithelial cells with NSC properties appear approximately at embryonic day (E) 8 and from which originate all cells of the developing and mature CNS,

including adult NSCs (Alvarez-Buylla et al., 2001). After a period of NSC/precursor expansion, as neurogenesis commences, a second progenitor population starts to be generated from asymmetrically dividing cells in the VZ and migrates basally. These cells, termed intermediate progenitors or basal progenitors, divide symmetrically to produce neurons and glia (Martinez-Cerdeno et al., 2006). The early NSC microenvironment consists of characteristic bipolar cells, termed neuroepithelial (NEP) cells, with one process (apical) attached to the ventricle and one longer process (basal) attached to the pial surface. NEP cells form the pseudo stratified VZ and are characterized by the periodic apico-basal translocation of their nucleus (interkinetic nuclear migration) which is regulated in such a way that mitosis occurs always at the ventricular surface, while S phase occurs at the basal-most area (Gotz and Huttner, 2005). The main structural constant of this early microenvironment is the ventricle, while the thickness of the neuroepithelium increases with time, accommodating the augmenting number of NEP cells and the occasionally generated neurons that quickly migrate towards the pial surface of the nervous tissue. Around midgestation, in rodents, NEP cells start to express glial markers and assume a more elongated morphology. Reflecting this transition, the emerging neural stem cell/progenitor type is now named a radial glial cell (RG) and retains the bipolar morphology and the interkinetic nuclear migration characteristic of NEP cells (Tramontin et al., 2003). As the thickness of the nervous tissue increases with the generation of large numbers of neurons, the basal process of the RG elongates in order to retain attachment to the pial surface (Rakic, 2003). The complexity of the mantle microenvironment increases as development proceeds, due to the generation of different neuronal cell types and the appearance of a dense network of blood vessels (Herken et al., 1989). A parallel increase in the VZ complexity is observed (Pinto and Gotz, 2007). Finally, to add to the complexity of the progenitor microenvironments, it should be noted that specific areas secreting growth factors or morphogens exist (named signalling centres) either within the VZ/SVZ or outside (Shimogori et al., 2004).

The SVZ is located next to the ependyma, a thin cell layer that lines the lateral ventricles of the brain (Fig. 6). Three types of precursor cells exist in the SVZ: type B SVZ-astrocytes, rapidly

dividing transit amplifying (type C) cells and committed migrating neuroblasts (type A). The cell lineage is type B to C to A, with the type B believed to be the self-renewing primary precursor (Doetsch et al., 1999a; Doetsch et al., 1997) Interestingly, the potential of SVZ progenitor cells appears to be limited, as the fate of their progeny is determined by the positional information established during early development of the central nervous system (CNS)(Merkle et al., 2007). Neuroblasts form clusters all along the ventricular length and migrate in chains towards the dorsal and posterior tip of each lateral ventricle in order to continue their migration within the rostral migratory stream (RMS) up to the olfactory bulb glomeruli, where they mature into local interneurons. In parallel, SVZ neural progenitors also generate oligodendrocyte precursors that migrate radially to the neighbouring white matter tracts of corpus callosum, septum and fimbria fornix and differentiate into myelinating oligodendrocytes (Gonzalez-Perez and Alvarez-Buylla, 2011; Gonzalez-Perez et al., 2009). The identification of SVZ progenitors was mainly based on morphological analysis by electron microscopy (Doetsch et al., 1997), but type C and A cells can also be identified by bromodeoxyuridine (BrdU) and ^{3}H-thymidine labelling and by specific molecular markers, such as Dlx2, doublecortin (DCX) and the polysialylated neural adhesion molecule (PSA-NCAM). Lineage tracing studies in adult mice have demonstrated that newborn neurons, astrocytes and sometimes oligodendrocytes can be derived from cells expressing a given molecular marker, such as Nestin, GFAP, GLAST and Sox2 (Breunig, 2007). However, these markers are expressed in heterogeneous populations of cells and it is not clear whether cells expressing these markers are the primary progenitors. Neither is it known whether a common progenitor exists in the adult brain for all three different types of progeny or if distinct progenitors are responsible for the generation of multiple neural cell types. NSCs have an astrocytic morphology and are situated adjacent to the multiciliated ependymal cells that line the lateral ventricles and are surrounded by other astroglial cells and type C and A cells. In addition, two multicellular structures are integrated into the SVZ: the astrocyte-constructed tubes in which neuroblast clusters migrate towards the rostral migratory stream and the numerous blood vessels with their endothelial cell/pericyte-derived walls and astrocyte endfeet on their surface.

Interestingly, the SVZ extracellular matrix (ECM) seems to be significantly different from that of the surrounding mature tissue. Recently it was described that extensions of the vessel basal lamina intrude the SVZ and branch around NSCs and progenitors (Mercier et al., 2002). These laminin and collagen I-rich ECM structures can be observed under the electron microscope and have been named fractones. Other ECM molecules that have been shown to be present in the SVZ are matrix metalloproteinases, tenascin-C (Jaworski and Fager, 2000; Kazanis et al., 2007), chondroitin/dermatan sulfate proteoglycans (Akita et al., 2008), as well as the trisaccharide LeX/SSEA-1/CD15 that is expressed on NSCs and type C cells. The expression of most of these molecules is normally down-regulated during early post-natal life resulting in the formation of the classic brain parenchymal ECM, characterized by the dominance of proteoglycans like brevican, neurocan and versicans (Bandtlow and Zimmermann, 2000). Therefore, the distinct nature of the SEZ niche is emphasized by the persistent presence of ECM molecules that are expressed during embryonic development or after injury (Bandtlow and Zimmermann, 2000).

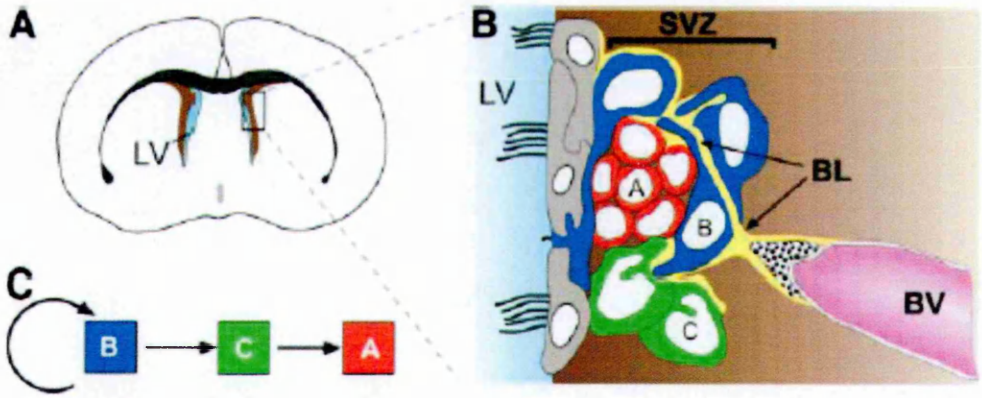

Figure 6. The SVZ

(A) Coronal section through the adult mouse brain. Light blue shows the lateral ventricle (LV) space filled with cerebrospinal fluid. Boxed area is shown enlarged in (B). (B) Architecture of the SVZ. B cells (dark blue) are the astrocytes that are the SVZ stem cell and also serve as niche cells. Some of the B cells contact the ventricle lumen and have a single cilium (shown). C cells (green) are rapidly dividing, transit-amplifying cells derived from the B cells. C cells give rise to A cells (red), neuroblasts that migrate to the olfactory bulb, where they become local interneurons. A blood vessel (BV, pink) is shown with a perivascular macrophage (dotted fill); a basal lamina (BL, yellow) extends from the BV and interdigitates extensively with the SVZ cells. (C) SVZ lineage. (Alvarez-Buylla and Lim, 2004).

1.3.1.2 The SGZ niche

Unlike in the SVZ, the hippocampal niche is not in direct contact with the ventricular cavities. In the SGZ, adult hippocampal progenitors are closely apposed to a dense layer of granule cells that includes both mature and newborn immature neurons, and develop locally into mature DG granule neurons (Gage, 2000). Within this microenvironment, there are also astrocytes, oligodendrocytes, and other types of neurons. Hippocampal astrocytes may play an important role in SGZ neurogenesis. They promote the neuronal differentiation of adult hippocampal progenitor cells and the integration of newborn neurons derived from adult hippocampal progenitors *in vitro* (Song et al., 2002). Blockade of the Wnt signalling pathway inhibits the neurogenic activity of astrocytes *in vitro* and SGZ neurogenesis in vivo, suggesting that hippocampal astrocytes may act through Wnt signalling (Lie et al., 2005).

At least two morphologically and antigenically distinct types of astrocytes (type B cells), exist in the adult SGZ (Seri et al., 2004): (1) horizontal astrocytes (GFAP+, Sox2+, S100β+), with the morphology of typical mature astrocytes, and (2) radial astrocytes (GAFP+, Sox2+, S100β-), which display a radial glia-like morphology. The latter extend a major radial projection into the granule cell layer and have extensive basal processes that form basket-like structures nestling clusters of neuroblasts (type A cells). Radial astrocytes give rise to small dark cells (type D cells; also referred to as type-2 cells in their higher proliferative state) (Steiner et al., 2006), which progress through three maturational stages as they translocate to the granule cell layer of the DG to become granule neurons (Seri et al., 2004). A recent study showed that type 2 Sox2+ cells can self-renew and that a single Sox2+ cell can give rise to a neuron and an astrocyte, providing the first *in vivo* evidence of stem cell properties of hippocampal neural progenitors (Suh et al., 2007). Because of the absence of tangential chain migration of neuroblasts, the architecture of the hippocampal neurogenic site is similar in postnatal and adult stages. By contrast, the location of cell proliferation differs, occurring in the hilus postnatally and in the SGZ in adults (Namba et al., 2005).

1.3.2 The niche microenvironment

The stem cell niche is defined as a microenvironment that facilitates the survival and self-renewing capacity of the stem cells, as well as (in the adult CNS) the production of actively dividing precursors leading to the generation of post-mitotic progeny (Morrison and Spradling, 2008). Similar relations have been described between hematopoietic stem cells and neighbouring osteoblasts (Yin and Li, 2006). At present there is no direct evidence to suggest the unique importance of any single interaction between the NSC and the cellular or parenchymal components of the SVZ or SGZ microenvironment. However, ependymal cells exert a supporting/regulatory function in the niche, since they can modulate the transport of ions and other factors from the cerebrospinal fluid (CSF)(Bruni, 1998). They are also a local source of neurogenic factors like pigment epithelium-derived factor (PEDF)(Ramirez-Castillejo et al., 2006) and the pro-neurogenic BMP signalling modulator noggin (Peretto et al., 2004), and they form gap junctions with SVZ astrocytes (Zahs, 1998). These factors may be required for the maintenance of neural stem cells. Indeed, ependymal cells are absent from the SGZ, this being the most distinct structural difference between the two adult neurogenic niches, and there is evidence suggesting that the ependymal-free SGZ contains neuronal progenitors with restricted self-renewing capacity rather than NSCs (Bull and Bartlett, 2005). In addition, the constant movement of the ependymal cilia is thought to contribute to the generation of gradients of soluble factors in the CSF and to regulate the migration of NBs (Sawamoto et al., 2006). Therefore any migratory cues provided by ependymal cells would be absent in the SGZ. However, SGZ progenitors do not migrate long distances and can probably acquire the necessary directional cues from the radial processes of the SGZ astrocytes (Seri et al., 2004). Three other cell types may also regulate NSC behaviour. *In vitro* data support the conclusion that the interaction between NSCs and blood vessel endothelial cells might be important in neurogenesis (Shen et al., 2004). Actively dividing cells have been shown to be positioned near blood vessels in the SGZ (Palmer et al., 2000) and in the SVZ (Tavazoie et al., 2008) and endothelial cells are a source of factors that have been suggested to control neurogenesis, like PEDF, leukemia-inhibitory factor and brain-derived

neurotropic factor. NSCs are also in close contact with their progeny: the induction of massive NSC mitotic activity in the SVZ after ablation of type C and A by intracerebrally infusing the anti-mitotic drug AraC (Doetsch et al., 1999b), indicates the existence of progenitor-dependent feedback loops controlling NSC proliferation, although the nature of this signalling remains elusive. Astroglia are the most abundant cell type in the SVZ but it is still unknown whether they can be segregated into distinct functional groups, such as astroglia with structural, supporting or neurogenic roles. Astroglia of the SGZ can be structurally separated into radial and horizontal astrocytes (Seri et al., 2004), while SVZ astroglia (or type-B cells) into two classes, type B1 and B2. B1 astrocytes reside adjacent to the ependymal cells and proliferate less than the smaller and basally located B2 astrocytes (Doetsch et al., 1997). Astrocytes are coupled with gap junctions and are able to networking and transport information from distant areas (Giaume and Venance, 1998). Thus they act as sensors and modulators of the microenvironment that become reactive, after AraC-induced depletion of the SVZ progenitors even before the mitotic activation of NSCs (Kazanis et al., 2007). Finally, it is important to note that a potentially important interaction exists between the NSC and the ventricular environment, as NSCs of the SVZ extend a monocliated process in between the ependymal cells enabling them to "taste" the growth factor and morphogen-rich CSF (Alvarez-Buylla et al., 2001; Doetsch et al., 2002). The importance of cilia in several signalling mechanisms has been recently highlighted (Singla and Reiter, 2006) and previous experimental work has revealed that essential components of the Shh signalling pathway are positioned at the primary cilium (Rohatgi et al., 2007). In the adult CNS, the significance of primary cilia in neurogenesis was highlighted by the finding that when the cilium was genetically ablated, proliferation in the SGZ was largely compromised (Han et al., 2008).

1.3.3 Neurogenic niches in the human CNS

The organization of the adult human SVZ is significantly different than that of rodents (Fig.7). In adult rodents, SVZ astrocytes (type B) are located next to the ependymal layer and ensheats

chains of migrating young neurons (Doetsch 1997b, Peretto 1997). In contrast, in the adult human brain SVZ astrocytes are not found adjacent to the ependyma and the presence of chains of migrating neuroblasts is strongly debated. Similarly, the same kind of features was also found in primates such as the common marmoset (Bunk et al., 2011). Human astrocytes are separated form the ependymal by a region largely devoid of cell bodies and very rich in process from astrocytes and ependymal cells, forming a ribbon that lines the lateral ventricles (Sanai et al., 2004). Although this organization appears unique to the adult human brain, some features may be comparable to that reported in other vertebrates (Rodriguez-Perez et al., 2003). The lateral ventricular wall consists of four identifiable layers throughout the length of the ventricle from the frontal horn to the temporal horn (Quinones-Hinojosa et al., 2006; Sanai et al., 2004). Layer I is a monocellular layer of ependymal cells. Layer II is a hypocellular layer consisting of minimal amounts of myelin and sporadic cells; this layer has a dense network of GFAP-positive processes. In comparison to layer II, layer III contains many more cell bodies, but the organization of this layer varies with localization. In this layer there are many cells with astrocytic characteristics. Further away from the ventricular surface, the astrocytic cellularity diminished and the appearance resembles that of underlying brain parenchyma, thus layer IV can be considered as a transitional zone. Moreover there are marked differences in the thickness of the hypocellular layer and the astrocytic ribbon along the rostrocaudal extent of the lateral wall (Sanai et al., 2004).

The RMS contains progenitor cells that migrate from SVZ to the olfactory bulbs (OB). This pathway is well described in rodents, rabbit and rhesus monkeys (Fasolo et al., 2002; Lois and Alvarez-Buylla, 1994; Pencea et al., 2001). It was firstly reported by Sanai and colleagues that there was no evidence of cells migrating in chains along the SVZ or olfactory peduncle to the bulb. Later on Curtis and colleagues reported the characterization of the human ventriculo-olfactory neurogenic system (VONS), containing the SVZ, the RMS, the olfactory tract and the OB, together with the presence of migrating progenitors (Curtis et al., 2007). Due to the difficulty of working on human brain tissues, the availability of samples and impossibility of using cell-tracking systems, these works relies mainly on histological analyses, and a strong debate between

the two findings was opened. However, recently it was reported a characterization of human RMS with some new findings: the presence of a four-layer arrangement in some parts of RMS (resembling SVZ); the presence of cilia in the cavities that surround the RMS (VONS structure); PSANCAM possibly migrating cells (Kam et al., 2009). Moreover the authors suggest that because the human olfactory bulb is only approximately 0.064% of total human brain weight, whilst the rat OB is about 20% of its total brain weight, should be expected that there is a lower drive for olfactory neurogenesis in the human brain, which is reflected in the lower number of neuroblasts within the human RMS as compared to the rat.

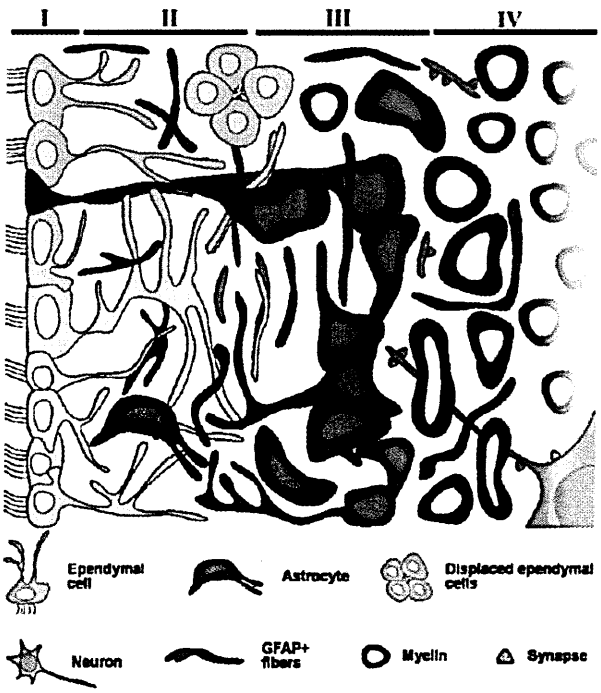

Figure 7. Proposed model of the human SVZ organization in the coronal plane.. Layer I, ependyma; Layer II, hypocellular gap; Layer III, ribbon of cells; Layer IV, transitional zone to the brain parenchyma. Astrocytes (blue cytoplasm and light-blue nucleus) with processes at the base of the SVZ mainly found in Layer III but some also in Layer II. Displaced ependymal cells (grey cytoplasm and light-grey nucleus) form clusters and are mainly found between Layers II and III. Neurons (red cytoplasm and light-red nucleus) are found mainly along the interface between Layers III and IV with processes sent to Layers II and III. In green are the synapses found in Layers II and III. (Quinones-Hinojosa, 2005).

1.3.4 Neural Stem Cells

Due to their relative rarity and lack of definitive markers, stem cells have traditionally been characterized on the basis of functional criteria. A putative stem cell in culture, must demonstrate the ability to proliferate, self-renew over an extended period of time and generate a large number of progeny that can differentiate into the primary cell types of the tissue from which it is obtained (Potten and Loeffler, 1990).

NSCs could be isolated from the adult brain, expanded and propagated by means of growth factors in floating cell clusters termed "neurospheres", and differentiated *in vitro* (Fig. 8) (Reynolds and Weiss, 1992). In the presence of mitogens such as epidermal growth factor (EGF) and fibroblast growth factor 2 (FGF-2), at low cell density and without cell adhesion substrate, most differentiating or differentiated cells are expected to die, whereas the NSCs respond to the mitogens, divide and form floating aggregates (primary neurospheres) that can be dissociated and re-plated to generate secondary neurospheres. This procedure can be repeated several times to expand the NSC population. The original method was then modified and refined and it is named as "NeuroSphere Assay"(NSA) (Gritti et al., 1999; Gritti et al., 2002; Reynolds and Weiss, 1996). By performing population analysis in long-term neurosphere cultures it was observed an overall enrichment and expansion of the stem population. This is likely due to the increased proportions of symmetric proliferative divisions over symmetric differentiative and asymmetric divisions (Morrison and Kimble, 2006), a mechanism driven by the positive selection induced by the NSA culture conditions within the relatively small stem cell population (Galli et al., 2002; Gritti et al., 2002). The three-dimensional structure and the cellular milieu of the neurosphere can be envisioned as the *in vitro* counterpart of the *in vivo* neurogenic compartment, a microenvironment that is relevant for stem cell maintenance, proliferation and differentiation. Notably, the cellular composition of niche environment is recapitulated also in terms of numerical proportions between the different cell types (few stem cells and a large population of committed progenitors). Due to this heterogeneity, *in vitro* markers for "stemness" have been searched. However, most of the molecules that have been suggested as potential specific NSC markers are likely expressed by subpopulations of immature neural precursors that could contain the stem cell population. The possibility of improving the neurosphere system and of finding alternative *in vitro* approaches, not only to enrich but also to select and clonally expand the *bona fide* stem cell population without loosing the original prevalent neuronal fate, has been a recurrent issue in the stem cell field. The artificial bi-dimensional structure ensured by monolayer adherent cultures might be sufficient to prevent lineage restriction of radial glia-like precursors, favouring niche-independent symmetric

self-renewal and expansion of a rather homogeneous cell population (NS cells) (Conti et al., 2005; Pollard et al., 2006; Spiliotopoulos et al., 2009). Establishment of *in vitro* settings necessarily results in disruption of the three-dimensional tissue structure, loss of specific cell-to cell contacts and modification of the extracellular environment and signalling. Thus, although the versatility shown by NSC cultures *in vitro* can be envisaged as an advantage in terms of therapeutic potential, caution is always necessary when considering the potential *in vivo* translation.

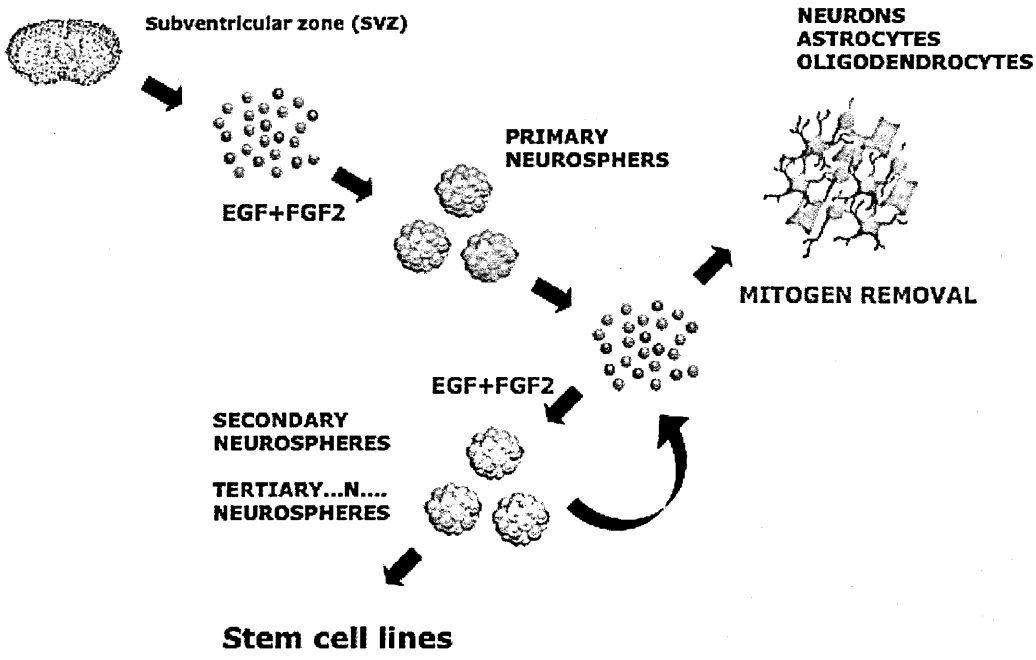

Figure 8. Neural stem cell derivation and long-term in vitro culturing and expansion. The cartoon illustrates the experimental protocol to establish neural stem cell (NSC) lines.

1.3.5 Neurogenesis and diseases

Most of the CNS insults lead to increased proliferation of progenitors in the neurogenic areas after a latent period and sometimes cause migration of newborn neurons to injury sites (Parent, 2003). Neurogenesis is induced, and the rate of proliferation of progenitor cells in the dentate gyrus can be profoundly accelerated by insults such as cerebral ischemia (Kokaia and Lindvall, 2003; Liu et al., 1998), seizures (Parent et al., 1997), and neurotoxic lesions (Gould and Tanapat, 1997).

Sustained neocortical neurogenesis has been documented also after hypoxic/ischemic injury (Yang et al., 2007). However, in cases of radiation injury, hippocampal neurogenesis was severely compromised (Monje and Palmer, 2003). Although the molecular mechanisms leading to increased neurogenesis following global or focal ischemia are not well understood, recently it has been reported that ischemic insults stimulate neurogenesis by the release of stem cell factor (SCF) and/or fibroblast growth factor-2 (FGF-2)(Jin et al., 2002).

In addition to acute insults to the brain, neurodegenerative disorders such as Alzheimer's and Parkinson's diseases are the other most common form of chronic neuropathology. The progressive neurodegeneration and subsequent atypical inflammatory response characterized by activation of microglia are a prominent feature in these diseases. The neurogenesis pattern in these disorders is also altered to a great extent. Interestingly, in the brains of human patients with Alzheimer's disease, increased neurogenesis in the SGZ of the hippocampus has been observed (Jin et al., 2004). This observation, though striking, perhaps represents the regenerative attempt by CNS to recover the neuronal loss and to restore the neuronal plasticity (Taupin, 2006). However, the neural progenitor pool is depleted in the other neurogenic area, SVZ, indicating that the pattern of neurogenesis in the two neurogenic areas of the brain is different with the disease pathology. Similar reports of enhanced NSCs regeneration and formation of immature neurons have been reported in MPTP mouse models of Parkinson's disease (Shan et al., 2006). The other type of neurodegenerative diseases where protein aggregates are the main culprits such as triplet repeat disorders (Huntington's disease) and Prion's disease also leads to increased cell proliferation as well as enhanced adult neurogenesis (Curtis et al., 2003b; Steele et al., 2006). These findings indicate that the diseased brain has the capacity for regeneration to compensate for the neuronal loss and thus provide therapeutic avenues by stimulation of endogenous neurogenesis to counteract the neurodegeneration.

1.3.5.1 Neuroinflammation

Inflammation is a complex cellular and molecular response to stress, injury or infection that attempts to defend against insults, to clear dead and damaged cells and to return the affected area to a normal state. Inflammation in the brain, however, is different from that in peripheral tissues in many ways such as initiation and sensitivity to inflammation. The brain is immune privileged because of its protection by the blood-brain barrier (BBB), which only allows certain molecules and cells to enter and exit. Because of the selective permeability of this barrier, only T cells, macrophages and dendritic cells can enter the CNS under normal physiological conditions (Hickey, 1999). Following damage or exposure to pathogen, an inflammatory process is initiated by the activation of resident microglia and astrocytes as well as infiltrating peripheral macrophages and lymphocytes. Activated microglia, astrocytes, macrophages and lymphocytes release a plethora of anti- and pro-inflammatory cytokines such as interferon gamma (IFN-γ), tumour necrosis factor alpha (TNF-α), interleukin-1 beta (IL-1β), interleukin-18 (IL-18) and interleukin-6 (IL-6); chemokines such as stromal cell-derived factor-1 alpha (SDF-1α) and monocyte chemoattractant protein-1 (MCP-1); neurotransmitters (i.e. glutamate) and reactive oxygen species (i.e. nitric oxide). These factors disrupt the BBB and recruit monocytes and lymphocytes to cross through the BBB to the site of inflammation (Hickey, 1999; Taupin, 2008) in addition to recruiting resident microglia and stimulating astrogliosis. These newly recruited cells become activated and release more inflammatory factors, creating a positive feedback loop that results in neuronal damage and changes in neurogenesis (Das and Basu, 2008). This process inadvertently causes further bystander damage to neurons and causes both detrimental and positive consequences to neurogenesis. Indeed inflamed brain microenvironment sustains a non-cell autonomous dysfunction of the endogenous CNS stem cell compartment and challenge the potential efficacy of proposed therapies aimed at mobilizing endogenous precursors in chronic inflammatory brain disorders (Pluchino et al., 2008).

1.3.5.1.1 Microglia activation

Microglia, the resident macrophages of the CNS, comprise 5-20% of the total glia in the brain. In the resting state, ramified microglia have multiple processes that interdigitate surrounding cells. Microglia are sentinels in the brain that change from resting to "activated" states injury (Becher et al., 2000) and activated microglia are a hallmark and driving force of brain inflammation. Microglial morphology changes from resting ramified to an intermediate semi-activated state (short thick processes, enlarged cells), and then to an amoeboid highly activated state (phagocytic).

Lipopolysaccharide (LPS)-induced microglial activation and associated inflammation enhances the integration of newly born neurons into the adult rat hippocampal neural circuitry (Jakubs et al., 2008). On the other hand, LPS activation of microglia was shown to strongly impair basal hippocampal neurogenesis (Ekdahl et al., 2003) partially through the production of TNF-α (Liu et al., 2005). LPS-induced inflammation resulted in an 85% reduction of newborn neurons in the hippocampus; the degree of impaired neurogenesis correlated with the number activated microglia (Ekdahl et al., 2003), thus indicating that uncontrolled inflammation is detrimental to neurogenesis. Suppression of activated microglia by Minocycline treatment resulted in increased numbers of new neurons in the hippocampus, demonstrating the significance of activated microglia in the reduction of neurogenesis by inflammation (Ekdahl et al., 2003). Further, anti-inflammatory treatment with Indomethacin restored neurogenesis that was diminished by irradiation-induced inflammation (Monje et al., 2003) and focal cerebral ischemia (Hoehn et al., 2005). This microglial inhibition of neurogenesis is mediated by activated, but not resting, microglia (Monje and Palmer, 2003)(Monje 2003). Interestingly it was recently reported that the relative state of activation in the SVZ resident microglia seems to be different from non-neurogenic areas. This population is constitutively activated, possibly due to presence of diffusible molecules in the CSF, and importantly is resistant to further activation after massive cerebral cortex brain injury. Moreover SVZ microglia are induce to migrate toward lesions and the greater constitutive microglial proliferation in the SVZ may, in part, serve to provide such

cells (Goings et al., 2006).

1.3.5.1.2 Astrocyte activation

Astrocytes constitute the majority of glial cells in the CNS, vastly outnumbering microglia, monocytes and lymphocytes and are classically identified as cell expressing the intermediate filament glial fibrillary acidic protein (GFAP). Astrocytes play a number of active roles in the brain, from clearing neurotransmitters from the synapse (Bergami et al., 2008) to regulate the function of oligodendrocytes (Ishibashi et al., 2006) and NSCs (Bundesen et al., 2003). In various CNS pathologies, astrocytes are likely to react promptly to the injury, leading to activation of astroglia or astrogliosis (Eng and Ghirnikar, 1994). Activated astrocytes release a plethora of inflammatory factors, growth factors and regulate extracellular levels of excitatory amino acids, which have both negative and positive effects on neurogenesis (Blasko et al., 2004; Song et al., 2002). Neuronal differentiation of adult rat NSCs increased tenfold when co-cultured with astrocytes, and both soluble and membrane-bound factors are responsible for this effect. In addition to directing the differentiation of NSCs to neurons, astrocyte co-culture also induced a twofold increase in NSCs proliferation (Song et al., 2002). The role of astrocytes in brain inflammation and its consequence on neuronal injury and neurogenesis during various CNS disorders has recently been intensely studied and continues to be thoroughly investigated.

1.3.5.1.3 NSCs and inflammation

The functional response of NSCs to inflammation indicates a precise relationship between the immune and the nervous system. One of the first evidence strongly supporting the concept that NSCs strongly interact with immune cells came from transplantation experiments aimed at using NSCs as therapeutic tool to counteract CNS inflammation (Pluchino et al., 2003; Pluchino et al., 2005). NSCs express immune-relevant molecules, such as cell-adhesion molecules, integrins and chemokine receptors that enable them to functionally interact with an inflamed CNS

microenvironment. For example NSCs express CXCR4 receptors, thus responding to the chemotactic signals by CXCL12 (Tran et al., 2004) and CCR2 receptor, whose ligand MCP-1 (CCL2) is an important chemokine for leukocyte trafficking to the brain, highly expressed in neuroinflammatory conditions (Tran et al., 2007). More recently it was found that inflammatory signals provided by activated microglia and/or activated antigen specific T cells regulate neurogenesis and gliogenesis within germinal niches (Monje et al., 2003; Ziv et al., 2006). Furthermore it was shown that TLR2 and TLR4 which regulate the immune response through the recognition of pathogen-derived molecules or pathogen-associated molecular patterns, are expressed in NSCs and pay an important role in hippocampal neurogenesis (Rolls et al., 2007). Thus, NSCs can be considered also immune-relevant cells in the brain; moreover immune system is an important regulator of proliferation, migration and survival of NSCs. Yet, as findings in this field are relatively recent, there exist a number of cytokines and chemokines to be investigated. Furthermore, signalling pathways involved in all these processes are to be elucidated.

2 AIM OF THE WORK

Globoid cell Leukodystrophy (GLD) is a rare autosomal recessive disorder caused by mutation in the lysosomal enzyme β-galactocerebrosidase (GALC). GALC is responsible for the degradation of specific galactolipids involved in the formation of myelin. Its absence results in accumulation of substrates and toxic metabolites that lead to the death of oligodendrocytes and Schwann cells. The most severe forms of GLD manifest early after birth with progressive brain damage and are fatal in few years. Demyelination is believed to occur as a consequence of Psychosine accumulation and neuroinflammation. However, the hypomyelination of the corticospinal tract described in asymptomatic neonates affected by Krabbe disease might explain the motor impairment present in some patients even before overt disruption of myelin. Most importantly, it might explain the clinical inefficacy of therapies on symptomatic patients as well as the poor improvement following early treatment in asymptomatic babies. These clinical observations, as well as the finding that neurodegeneration might be present in Twitcher mice, a relevant model of GLD, even in the absence of demyelination, strongly suggest GALC deficiency results in neural cell impairment long before the disruption of myelin driven by the overt CNS tissue storage and inflammation.

The goal of this study was to extensively characterize the role of GALC in regulating the function of NSC niches during the disease progression in Twitcher mice in order to test an even more challenging hypothesis, namely that GALC absence might result in functional impairment of neural stem/progenitor cell function in neurogenic niches and, consequently, in neurogenic and gliogenic processes occurring during pre-natal and early post-natal CNS development.

By morphological and functional analysis we showed altered cellular organization and loss of proliferating neuroblasts in the subventricular zone niche of Twi mice as a function of disease progression. These data were confirmed by *in vitro* experiments showing decreased numbers of primary neurospheres generated from Twi NSC/progenitors. Both defects were rescued to normal levels in post-natal day (PND) 40 Twi mice chronically treated with the anti-inflammatory drug

Minocycline starting from PND10. These results, as well as the up-regulation of several inflammatory molecules observed in Twi brains starting from the early symptomatic stage (PND20), suggested a major contribution by neuroinflammation at the late stages of the disease. However, these data did not rule out a direct contribution of GALC deficiency nor they excluded a role of GALC in maintaining a functional niche during CNS development. Indeed, our results indicate decreased proliferation of NSC/progenitors derived from PND2 and PND10 Twi mice, suggesting that GALC deficiency might lead to neurogenic impairment independently from CNS inflammation. Finally, lipid quantification in tissues and cells revealed increased amount of LacCer and low abundance of S1P. Metabolically, this resulted in different expression and activity of several enzymes related to GALC with consequent alteration of intracellular responses. Results of our work improve our understanding of the pathogenic mechanisms of GLD with important implications for therapy. In fact, an altered niche environment during CNS development might result in subtle but irreversible damage in CNS organization and function; this, in turn, might hamper the therapeutic outcome of both gene and cell-based approach currently available or under development. In addition, the peculiar biochemical pattern that we showed in Twi-derived NSCs and brain tissues has to be considered in the perspective of gene therapy approaches, since supraphysiological enzyme level as well as enzyme deficiency, could alter this fine-tuned metabolic balance.

3 MATERIALS AND METHODS

3.1. In vivo studies

3.1.1 Mice strain

Twitcher (Twi) mice were obtained from Jackson laboratories. Congenic FVB/N.B6Galc-(*twi/twi)* (FVB/Twi) mice were generated in our animal research facility by breeding Twi heterozygous (+/-) C57BL6 mice with wild type (+/+) FVB mice. FVB/Twi mice show a slower progressive form of GLD than the canonical Twi mice. Tremors develop at around PND 21, progressing to severe resting tremor, weight loss, paralysis and wasting of hind legs. At PND 40, severe PNS and CNS demyelination is observed. Death occurs at around 40-45 days. Mice were screened as indicated in paragraph 1.2 and heterozygous offspring were intercrossed to obtain an inbred strain. Mouse colony was maintained in the animal facility of the Fondazione San Raffaele del Monte Tabor, Milano, Italy. All procedures were performed according to protocols approved by an internal Animal Care and Use Committee (IACUC #314, 420) and were reported to the Ministry of Health, as per Italian law.

3.1.2 Genotyping

For genotyping mice, DNA extraction from tails biopsies is performed. Tissues are digested with Proteinase K (Roche) at the concentration of 1 mg/ml at 56°C over night (o/n) in lysis buffer containing TRIS 10 mM pH 7.2, EDTA 25 mM, NaCl 10 mM, SDS 10%. After inhibition of Proteinase 10' at 96 °C, specific PCR is carried out. . The forward primer for the reaction was designed on an intronic sequence 230 bp upstream the mutation (F: 5'- CACTTATTTTCTCCAGTCAT). The reverse primer has a complementary sequence of the exon downstream the mutation site and forms, in the mutant, a restriction site for the enzyme EcoRV (R: 5'- TAGATGGCCCACTGTCTTCAGGTGATA). Details of the PCR reaction are shown

below.

Buffer 5x (Promega) 5µl	step 1: 95°C 10' 1 cycle
Primer F 10µM (Primm) 0.5µl	step2: 95°C 30'' 38 cycles
Primer R 10µM (Primm) 0.5µl	54°C 30''
dNTPs 10µM (Roche) 0.6µl	72°C 30''
Go Taq (Promega) 0.25µl	step 3: 72°C 10' 1 cycle
H2O 14,65µl	
DNA 200ng	

The amplified fragment (260 bp) is then digested in presence of EcoRV enzyme at 37°C for 1 hour. Only when the mutant allele is present, a fragment 234 bp long appears. Details of the reaction are shown below.

Buffer B (Roche) 2.5 µl
EcoRV (Roche) 0.7 µl
H2O 11.8 µl
DNA (from PCR) 10 µl

PCR products were separated with electrophoresis in Metaphor 4% agarose gel. EcoRV digestion of WT DNA results in the generation of a band of 260 bp; heterozygous restriction pattern shows 2 bands: one corresponding to the WT allele (260 bp) and the other corresponding to the mutant allele (234 bp); homozygous restriction pattern shows only the band corresponding to the mutant allele (234 bp).

3.1.3 *In vivo* drug administration

Mice were injected IP with the anti-inflammatory drugs Minocycline and Indomethacin (Sigma-Aldrich). Drugs were dissolved in saline solution and used immediately at 40 mg/kg and 10 mg/kg, respectively. The treatments started at PND10 and finished at PND40 or until mice looses up to 50% of their weight (to monitor survival).

BrdU was administered IP every two hours for 8 hours at 50 mg/kg BrdU powder (Sigma-Aldrich) was dissolved in sterile water and immediately used.

3.1.4. Tissue collection and processing

A group of mice were killed by CO_2 exposure and decapitated. For biochemical and molecular assays the two brain hemispheres were separated and the word "total brain" correspond to half hemisphere. Brains were isolated and either quickly frozen in liquid nitrogen or immediately processed to obtain tissue extracts. Another group of mice were anesthetized with Avertine (11µl of stock solution, consisting of 1.25 g 2,2,2- Tribromoethanol 99% + 2.5 ml 2- Methyl-2-Buthanol 99% per 100 ml total volume/10 g body weight) and intracardially perfused via the descending aorta with 0.9% NaCl followed by 4% paraformaldehyde (PFA) in 0.1M PBS. Brains were collected and equilibrated for 24 hours in 4% PFA. Then they were included in 4% agarose. Serial coronal vibratome (6 series, 40 µm-thick) sections were processed for histology and immunofluorescence analysis as described below.

3.2 Immunofluorescence analysis

3.2.1 Tissues

After 3 washings with 0.1M PBS 1x of 5' each, free-floating vibratome sections were incubated with blocking solution (10% Normal Goat Serum NGS + 0.3% Triton X-100 in 0.1M PBS) for 1h at RT and then incubated overnight at 4°C with primary antibody diluted in blocking solution. After thorough 3 washings of 5' each, antibody staining was revealed using species-specific fluorophore-conjugated secondary antibodies diluted in 10% NGS in 0.1M PBS. Tissue sections were counterstained with 6-diamidino-2-phenylindole (DAPI, Roche) or ToPro-3 (T3605, Invitrogen) for nuclei, washed in 0.1M PBS, collected and mounted on glass slides using Fluorsave (CALBIOCHEM). See Table 1 for primary and Table 2 for secondary antibodies used.

3.2.2 Cell cultures

Coverslips were incubated with blocking solution (10% Normal Goat Serum NGS + 0.1% Triton

X-100 in 0.1M PBS, or without Triton, if permeabilisation is not necessary) for 30' at RT, then incubated o/n at 4°C with primary antibody diluted in blocking solution. After 3 washing of 5' each, antibody staining was revealed using species-specific fluorophore-conjugated secondary antibodies diluted in 1% NGS in 0.1M PBS. No detectable signal was observed in samples in which the primary antibodies were omitted. Coverslips were counterstained with 6-diamidino-2-phenylindole (DAPI, Roche) or ToPro-3 (T3605, Invitrogen) for nuclei, washed in 0.1M PBS, collected and mounted on glass slides using Fluorsave (CALBIOCHEM). See Table 1 for primary and Table 2 for secondary antibodies used

3.2.3 Wholemount staining

Brains were dissected under the stereomicroscope in order to reveal the SVZ and the lateral ventricle. Briefly, a coronally oriented cut was then made at the posterior most aspect of the interhemispheric fissure, allowing the caudal hippocampus to be visualized in cross-section. The hippocampus, which forms the medial wall of the lateral ventricle at this position, was then released from the overlying cortex and removed. Then, the lateral wall was completely exposed by removing any overhanging cortex dorsally and the thalamus ventrally. Wholemounts were immersion-fixed overnight in 4% PFA with 0.1% Triton-X100 at 4°C. The following morning, PFA was aspirated from the 24-well plate and the wholemounts were washed 3 x 5' each in 0.1M PBS with 0.1% Triton-X100. After washing, wholemounts were incubated for 1 hour at room temperature in blocking solution, containing 10% fetal bovine serum and 10 mg/ml BSA in 0.1 M PBS with Triton-X100, 2% or 0.5%. Next, the blocking solution was removed and primary antibodies diluted in the same blocking solution were added and incubated for 24 or 48 hours at 4°C. Primary antibodies were washed off initially by 2 quick rinses in PBS with 0.1% Triton-X100. Then we did 3 additional washes for 20' each at room temperature. Secondary antibodies were added in the same blocking solution used for primary antibodies and added to wholemounts to incubate for the same length of time as for primary antibodies at 4°C. For high-resolution

confocal imaging, following immunostaining the wholemounts needed to be sub-dissected to preserve only the lateral wall of the lateral ventricle as a sliver of tissue 200-300 mm thick. This step was performed under the stereomicroscope and then the slice was mounted onto a slide and covered with a coverslip in a flat manner. See Table 1 for primary and Table 2 for secondary antibodies used

3.3 Immunohistochemistry

3.3.1 BrdU

Slides or free floating vibratome sections were fixed for 10 min in 3% H_2O_2 in methanol; after washing in 0.1 M PBS (3 x 5' each), slides were incubated for 20' at 54°C in a denaturing solution (60% Formamide, SSC 2X- 0,3M sodium chloride, 30mM sodium citrate). Then, section was rapidly washed with SSC 2X and incubated with 2N hydrochloric acid for 30' at 37°C. Slides were equilibrated with 0.1M pH8.5 boric acid for 10' and then blocked with the blocking solution. Primary BrdU antibody was then added and incubated o/n at 4°C. After 3X10' washings with 0.1 M PBS, slides were incubated with biotinylated secondary antibody in 0.1 M PBS, 1% NGS. After 3X10' washings with 0.1 M PBS and 5' incubation with 100mM pH7.5 TrisHCl, slides were incubated 1 hour with the VECTASTAIN ABC kit (PK-6100Vector Laboratories). After 3X10' washings with 100mM pH7.5 TrisHCl, reaction with the substrate 3-3 diamino-benzidine tetrahydrochloride (DAB, 167µg/ml in Tris-HCl 100mM + H_2O_2 1:3000) was performed. Slices were dehydrated and mounted with EUKITT. Samples were visualized with a Nikon Eclipse E600 microscope. In case of double labelling, after the blocking passage was followed the protocol for tissue immunofluoresce.

3.3.2 Lectin histochemistry.

Slides were fixed for 10 min in 3% H_2O_2 in methanol; after washing in 0.1M PBS (3 x 5' each) we applied a blocking Kit (SP-2001, Vector Laboratories), followed by Avidin solution (15 min) and Biotin solution (15 min). Slides were subsequently incubated for 30' with blocking solution (0.1M PBS 0.3% triton 10% NGS) and then with Biotynilated Ricinus Communis Agglutinin I (RCA I, B-1085 Vector Laboratories; 1:200 in blocking solution) for 30'. After thorough washing (3 x 5') and 1 passage in 100 mM Tris-HCl (5'), staining was revealed using VECTASTAIN ABC kit (PK-6100Vector Laboratories). After washings in 100 mM Tris-HCl (3 x 5'), reaction with the substrate 3-3 diamino-benzidine tetrahydrochloride (DAB, 167µg/ml in 100mM Tris-HCl + H_2O_2 1:3,000) was performed. Slices were dehydrated and mounted with EUKITT. Samples were visualized with a Nikon Eclipse E600 microscope. Images were acquired using a Nikon DMX 1,200 digital camera and ACT-1 acquisition software (Nikon). Pictures of defined areas in each slice were taken and the total immunopositive area in each picture (expressed in pixels) was calculated using the ImageJ software. Tissue slices from untreated WT mice were used to set the signal threshold.

3.4. Image acquisition

Samples (cell cultures and tissues) were visualized with Zeiss Axioskop2 microscope using double laser confocal microscopy with Zeiss Plan-Neofluar objective lens (Zeiss, Arese, Italy). Images were acquired using a Radiance 2100 camera (Bio-Rad, Segrate, Italy) and LaserSharp 2000 acquisition software (Bio-Rad). Images were imported into Adobe Photoshop CS3 or Image J software and adjusted for brightness and contrast.

Wholemounts reconstructions were created by Adobe Photoshop CS3 software, with at least 12 images at low power (10X) for slice. Regarding cell cultures, 9 fields were acquired blindly for each coverslip, at least 2 coverslip for experiment. Immunopositive areas were calculated as: (area positive for selected marker/area positive for nuclei)*100.

3.5. Electron microscopy

Mice were perfused with 2% glutaraldehyde +1% paraformaldehyde in 0.1M PBS. After dissection, brains were post fixed for 2 h and cutted with a vibratome (300 μm). Vibratome sections were fixed in osmium-ferrocyanide for 1 h, stained with 1% uranyl acetate, dehydrated and embedded in Araldite. Ultra-thin sections were examined under a Philips CM10 transmission electron microscope.

3.6. RNA extraction

3.6.1 Cells

Total RNA from cells was extracted according to the manufacturer protocol of RNeasy mini kit (Qiagen). Briefly, pelleted cells were lysed with the provided buffer added of b-mercaptoethanol, mixed with 70% ethanol and loaded on column. Optional DNase digestion with RNase-free DNase (Qiagen) was performed.

3.6.2 Tissues

Total RNA from tissues was extracted according to the manufacturer protocol of TRIZOL Reagent (Invitrogen). Briefly, half brain was homogenised with 2 ml of Trizol, then the phase separation was performed adding chloroform. Then, RNA was precipitated with isopropyl alcohol and washed with 75% ethanol. The pellet was air-dried, dissolved in RNase-free water and stored at -80°C. Prior to use, an aliquot was quantified by spectrophotometer and cleaned from possible DNA contamination using DNase digestion with RNase-free DNase (Qiagen).

3.7. RT-PCR

3.7.1 Reverse transcription

mRNA reverse transcription was performed according to the manufacturer protocol of QuantiTect reverse transcription kit (Qiagen). Briefly, 1μg of RNA was mixed to gDNA Wipeout Buffer and RNase-free water, and incubated 2' at 42°C. Then, the mix is cooled on ice and added of reverse-transcription master mix (transcriptase enzyme, buffer and primers mix). The whole solution is incubated 15' at 42°C, 3' at 95°C and then used immediately or stored at -20°C.

3.7.2 PCR

PCRs were performed using as template 2 μl of cDNA. Each sample was run in duplicate in a total volume of 25μl/reaction, containing 2.5 μl of PCR Buffer 10X, 0.5 μl of 10mM dNTPS, 1 μl of each 10mM primer, 0.2 μl of TAQ DNA Polymerase (all Qiagen) and 17.8 μl of sterile water. The amplification steps were: step 1: 94°C 3' 1 cycle; step2: 94°C 30'', Ta 30", 72°C 30'', n cycles; step 3: 72°C 10' 1 cycle, were Ta (annealing temperature) was determined for each primer couple. The number of cycle was chosen in order to be in the exponential phase of amplification. Primers were designed using Primer-BLAST on line software, in order to span an exon-exon junction and with specificity only for the target sequence. The primers used are the following:

Gene	Forward	Reverse	Ta	n
ARSA	TGGACTACGGTTCACAGATTTC	TGGGAAGCACGTTAGGTTCTG	62°C	28
GlcT	TGCATTTCATGTCCATCATCTAC	GTCATCTGATTCACCATGGTTCA	62°C	28
GalT-I	TCTACTTCATCTATGTGGCTCC	AGAAGAGCTGATGGACTTCATC	62°C	28
GalT-III	CTGCAGAGGTGGGTAAGTGG	GCAGGTCATTTTGAGGCAGCC	62°C	28
CST	TTTCCTATTGCTGCTGTACTCC	TAGTCCTGCACCAGGCTTCG	62°C	30
SAT-1	GCTGGGTCACGCCCTCAACC	GCGAACCCAAAAGGGCAGGC	64°C	27
NEU3	CGGAGCCGAAGCCATGGAGG	CTCCCACACAGGGCAGGGGT	64°C	28

PSAP	TGTCCAAGACCCGAAGACATG	CTTGTTGGACTCAAGCTGCTGTTTC	62°C	27
SPK1	GCCAGGGAGCTGGTGTGTGC	TCATTAGTCACCTGCTCGTACCCAG	64°C	28
SPK2	TTGCTGGACGAGTCGCGTGG	CCTGGACCAGCCTCCAAGATCACA	64°C	28
SPly	GCCTGAGGAGACGCAGAGGC	CGCAATGAGCTGCCAGGGCT	64°C	27
SPph	ATGCCATGTCAGGCACCGCC	ACAAGAATCCAGCAATGACATCCAG	64°C	27
β-Actin	GGCATCGTGATGGACTCCG	GCTGGAAGGTGGACAGCGA	60°C	21

3.8. Real time qRT-PCR

qPCR was performed in Optical 96-well Fast Thermal Cycling Plates (Applied Biosystem) on ABI PRISM 7900 Sequence Detector System (Applied Biosystem), using the following thermal cycling conditions, one cycle at 95°C for 10 min, 40 cycles at 95°C for 15 seconds and 60°C for 30 seconds. After that, a melting curve was performed: the temperature is increased very slowly from a low temperature (60°C) to a high temperature (95°C). At low temperatures, all PCR products are double stranded, so SYBR Green I binds to them and fluorescence is high, whereas at high temperatures, PCR products are denaturated, resulting in rapid decrease of fluorescence. The fluorescence is measured continuously and a curve is created. Curves with peaks at a Tm lower than that of the specific PCR product indicates the formation of primer-dimers, non-specific product or smear. Each reaction well was checked to confirm specificity by using the melting curve. Each sample was run in triplicate in a total volume of 25µl/reaction, containing 12.5 µl 2X QuantiFast SYBR Green PCR Master Mix, 2 µl of template cDNA and 1 µM QuantiTect Primer Assays (all from Qiagen). Relative expression of mRNA for the target genes was performed by the comparative C_T ($\Delta\Delta C_T$) method using the βActin gene as control. The normalized C_T (ΔC_T) was obtained by subtraction of the C_T for bActin from the C_T for the gene of interest. The difference between the ΔC_T for Twi and wt samples gave rise to the $\Delta\Delta C_T$ value that was used for the calculation of the relative mRNA expression using the formula $2^{-\Delta\Delta CT}$. The relative mRNA levels were expressed as fold change in Twi over control.

3.9. Multi Analyte Profile ELISA

We performed ProdentMAP assay on total brain tissue samples. Samples were processed and analysed according to RBM standard operating procedures. Tissue samples were collected, weighed, and added to 9X volume of lysis buffer (50 mM Tris-HCL with 2 mM EDTA, pH 7.4) Following homogenization, the tissue preparation is centrifuged for 2 minutes in a microfuge at 13,000xg. All samples were stored at −80°C until tested. Briefly, using automated pipetting, an aliquot of each sample was introduced into one of the capture microsphere multiplexes of the RodentMAP, thoroughly mixed and incubated at room temperature for 1 hour. Multiplexed cocktails of biotinylated, reporter antibodies for each multiplex were then added robotically and after thorough mixing, were incubated for an additional hour at room temperature. Multiplexes were developed using an excess of streptavidin-phycoerythrin solution, which was thoroughly mixed into each multiplex and incubated for 1 hour at room temperature. Analysis was performed in a Luminex 100 instrument and the resulting data stream was interpreted using proprietary data analysis software developed at Rules-Based Medicine (RBM Plate Viewer version 1.1.1). For each multiplex, both calibrators and controls were included on each microtiter plate. Testing results were determined first for the high, medium and low controls for each multiplex to ensure proper assay performance.

3.10. Western blot

Cells and tissues were lysed with radioimmunoprecipitation assay (RIPA) buffer (50 mM Tris-HCl, pH 7.4, 150 mM NaCl, 0.5% sodium deoxycholate, 0.1% SDS, 2 mM EDTA) added with protease (Roche) and phosphatase (Sigma-Aldrich) inhibitors. Proteins were quantified by means of Bradford assay (BioRad) and normalized on an albumin standard curve. 40μg of total protein from brain tissue lysate were re-suspended in sample buffer, heated for 5 minutes at 95°C and separated via SDS-PAGE under reducing conditions. Western blotting was performed with

standard procedure and the PVDF membrane (Millipore) was hybridized using the antibodies indicated in table 1 and 2.

3.11. Neural stem cells

3.11.1 NSC isolation and culture

Neonatal (PND2), young (PND10) and adult (PND40) Twi mice and WT littermates were anaesthetized before being decapitated (using crushed ice and Avertin for neonates and adult mice, respectively). Brains were removed and transferred in a Petri dish containing 0.1M PBS + Glucose (0,6%) + Penicillin/Streptomicin (P/S) (1%). The olfactory bulbs were removed, a coronal slice comprising the periventricular subventricular zone (SVZ) of the forebrain lateral ventricles was cut and the periventricular tissue was carefully dissected using fine forceps (Gritti et al., 2002; Gritti et al., 2009). Briefly, tissues underwent two rounds of mechanical dissociation and primary cells were plated in chemically defined serum-free medium (DMEM/F12 1:1 vol:vol; control medium) containing basic fibroblast growth factor (FGF2) and epidermal growth factor (EGF) (Peprotech; 10 and 20 ng/mL, respectively; growth medium). The primary cell suspension is obtained pooling together tissues from 3-5 mice for each experiment.

In order to generate a NSC line, seven-day-old primary spheres were collected, mechanically dissociated to a single cell suspension, and plated in growth medium (3,500 cells/cm^2). This procedure was repeated twice; bulk cultures were then generated by plating cells in growth medium at a density of 10^4 cells/cm^2. NSCs lines up to the 5th passage were used in the experiment, where reported.

3.11.2 Primary spheres: NSA

Primary cells obtained as previously described, were plated in 24-well uncoated plates (Corning, 0.5 ml/well) at a density of 5,000 cells/cm^2 in growth medium, as previously described (Gritti et

al., 2002). Under these conditions, neurospheres are derived from single cells and return an index of the number of in vivo neural stem/progenitor cells (Morshead et al., 1994). The number of primary neurospheres with a diameter (∅) ≥ 100 μm in each well was counted 7 days after plating. Data were expressed as absolute number of primary neurospheres obrtained by each brain or as cloning efficiency (number of primary neurospheres in each well/total number of plated cells x 100) from a total of n≥ 3 independent experiments.

3.11.3 Primary spheres: NCFCA

Primary cells isolated as above from PND40 Twi and WT mice (n=6/group) were plated using the mouse NeuroCult neural colony-forming cell assay kit (StemCell Technologies) as per the manufacturer's instructions, at a density of 6,5 x 105 cells per 35 mm cell culture dish with 2 mm grid (Nunc), as described (Louis et al., 2006). The cells were then incubated for 21 days in humidified 5% CO2, and growth factors were added every 7 days. After 21 days in vitro, the colony diameters were measured using an eyepiece graticule on an inverted light microscope with phase contrast. Spheres were scored according to size.

3.11.4 Primary mixed neuronal/glial culture

Primary cells obtained as previously described from PND2 Twi and WT mice, were plated on 10-mm MATRIGEL 1:100 (BD) coated coverslip at 100,000 cells/cm2 density, in a chemically defined, growth factor free medium, in the presence of 2% Fetal calf serum (FCS) (Gritti et al., 2009). These cells were cultured for 20 days, then fixed with 4% PFA and processed for immunofluorescence. The primary cell suspension is obtained pooling together tissues from 3-5 mice for each experiment.

3.12. Lipid analysis

3.12.1 Tissue homogenization

The murine brain tissue samples were weighted and homogenized in cold 70% methanol in water. The homogenate concentration was adjusted to a final concentration of 100 mg tissue/ml.

3.12.2 Lipidomics analyses

The lipid analyses of murine brain tissue samples were performed according to the standard operating procedures (SOP), the Lab Method Sheets (LMS), and data Processing Method Sheets (PMS) of Zora Biosciences Oy. For ceramide and cerebroside, UHPLC system with CTC HTC PAL autosampler (CTC Analytics AG) instrument was used, whereas for Sph and S1P was utilised Rheos Allegro pump (Flux Instruments) and 4000 Q TRAP MS. Data were analysed using Analyst V1.5 and MultiQuant V1.1 software, with multiple reaction monitoring method.

For sphingolipid quantification, 10 µl of murine brain tissue homogenates in concentration of 100 mg/ml (*i.e.,* 1 mg) were used for lipid extraction (n=1). Briefly, lipids were extracted using a modified Folch lipid extraction. Samples were spiked with known amounts of non-endogenous Cer, LacCer, GlcCer, SPH, and S1P synthetic internal standards. After lipid extraction, samples were reconstituted in chloroform: methanol (1:2, v/v) and stored at -20°C prior to MS analysis. Molecular Cer, LacCer, Gal/GlcCer, SPH, and S1P were analysed on a hybrid triple quadrupole/linear ion trap mass spectrometer (4000 QTRAP) equipped with an ultra high pressure liquid chromatography (UHPLC) system (CTC HTC PAL autosampler and Rheos Allegro pump) using multiple reaction monitoring (MRM) –based method in positive ion mode

3.13. Thin layer chromatography

3.13.1 Treatment of cell cultures with [1-^{3}H]sphingosine

Cells were incubated with 3×10^{-8} M [1-^{3}H]sphingosine dissolved in cell-conditioned medium (5 ml/dish) for 2 h pulse followed by 48 h chase. After the pulse period, the medium was removed and replaced with cell-conditioned medium without radioactive sphingosine for the chase period. Under these conditions, free radioactive sphingosine was barely detectable in the cells and all cell sphingolipids, including ceramide, sphingomyelin, neutral glycolipids and gangliosides were metabolically radiolabelled. Tritium-labelled phosphatidylethanolamine was also obtained due to the recycling of radioactive ethanolamine formed in the catabolism of [1-^{3}H]sphingosine. The radioactivity associated with cells was determined by liquid scintillation counting: it corresponded to 145 nCi/mg.

3.13.2 Lipid extraction

Cell dishes were washed twice with ice cold PBS containing 0.4 mM Na_3VO_4 and then scraped in PBS and collected in centrifuge tubes. The cell pellets were obtained by centrifugation at 4°C at 1,600×*g* for 10 min and then resuspended in iced water to be snap frozen and lyophilised. Lipids from lyophilized cells were extracted with chloroform/methanol/water 2:1:0.1 by vol. This first extraction was performed by adding 1550 µl of the solvent system. The total lipid extracts were separated from the protein pellet by centrifugation at 13,400×*g* for 15 min. The cell pellets were subjected to a second lipid extraction by adding 250 µl of chloroform/methanol 2:1.

3.13.3 Phase partitioning

Aliquots of the total lipid extracts were further subjected to a two-phase partitioning, resulting in the separation of an aqueous phase containing gangliosides and in an organic phase containing all other lipids. Briefly: an amount of water, corresponding to the 20% of the total volume of lipid

extracts, was added to each total lipid extract. The solutions were centrifuged at 2,300×*g* for 15 min, obtaining the separation of two phases. The aqueous phases were transferred in other tubes and a similar volume of methanol/water 1:1 was added to the organic phases. The samples were mixed and the two phases were separated again by centrifugation. The organic and aqueous phases were then dried under nitrogen flow and then resuspended in a known volume of chloroform/methanol 2:1. The two phases thus obtained, as the total lipid extracts were used for the TLC separation and analysis.

3.13.4 Alkaline treatment on the organic phases

Alkaline treatment allows removing glycerophospholipids from the organic phases, breaking their ester bonds, and maintaining unaltered the amide linkage of sphingolipids. This procedure allows removing several chromatographic interferences. Aliquots of organic phases were dried under nitrogen flow and the residue was resuspended with 100 µl 0.6 M NaOH in methanol and allowed to stand at 37°C for three h and overnight at room temperature. The reaction was blocked by adding 120 µl 0.5 M HCl in methanol. Finally, after phase separation (by adding 1,050 µl of chloroform/methanol/water 70:18:17), the new organic phases were used for TLC analysis.

3.13.5 Mono-dimensional TLC

The lipid residue dissolved in chloroform-methanol, 2:1 by vol. was applied on a 3 mm lane at 1.5 cm from the plate bottom edge. Different samples were applied maintaining a 3–5 mm distance. The plate was immersed into the chromatographic solvent system (1 cm deep) and chromatographed in a closed tank allowing the solvent to reach the TLC top edge (TLC size, 10 × 20 cm). Chromatography was carried out at room temperature in the range of 20–25°C. The aqueous phases were analysed using solvent systems composed by chloroform/methanol/0.2% aqueous $CaCl_2$ 50:42:11 by vol. The organic phases were separated using the solvent system chloroform/methanol/water in the ratio of 110:40:6 by vol.

3.13.6 Radioimaging

Tritium metabolically radiolabelled glycosphingolipids and phosphatidylethanolamine were visualized by digital autoradiography performed with a Beta-Imager 2000 instrument (Biospace, Paris). Total 200–1,000 dpm were applied on the plate and the image was acquired for 24–48 h. Identification was accomplished by chromatographic comparison with standard radiolabelled gangliosides and phosphatidylethanolamine.

3.14 Sphingosine kinase activity assay

To measure SK activity, cell lysates (60 µg) were incubated (Olivera A. Anal Biochem 1994) in the presence of 50 µM D-*erythro*-sphingosine dissolved in 4 mg/ml BSA and 1 mM ATP. Reaction was initiated by addition of [^{32}P] γ-ATP (0.5 µCi, 1 mM) and 10 mM $MgCl_2$ and terminated after 30 min incubation at 37 °C by addition of 20 µl 1 N HCl and 900 µl of chloroform/methanol/HCl (100:200:1 v/v). 240 µl of chloroform and 240 µl of 1 M KCl were added, and phases were separated by centrifugation. 500 µl of the lower phase were dried under a stream of nitrogen and dissolved in 100 µl of chloroform/methanol (2:1 by volume). [^{32}P]S1P was separated by TLC using the solvent system 1-butanol/methanol/acetic acid/water (80:20:10:20, v/v) Radioactive lipids on HPTLC plates were detected and quantified by radioactivity imaging performed with a Beta-Imager 2000 instrument (Biospace, Paris, France) using an acquisition time of about 48 h. The radioactivity associated with individual lipids was determined with the specific β-Vision software provided by Biospace. SK specific activity was expressed in pmol/min*mg protein in experiments performed at least in duplicate.

3.15. Statistics

In vitro and *in vivo* cell counts and data obtained following the quantification of immunopositive area by the ImageJ software were analysed with Excel or GraphPad Software and expressed as the

mean ± std.error of the mean (SE, with n≥3*)*. Unpaired Student t-test or Mann Whitney test, 1 or 2-Way ANOVA followed by Bonferroni post-test (statistical significance: $p<0.05$) were used when appropriate. Non-parametric test were used in case of non Gaussian distribution of the data (evaluated by normality test). 1 way ANOVA was used to compare more than two sets of data and 2 way ANOVA was used in case of evaluating the effect of two variables; both were corrected with Bonferroni posst-test that allowed comparisons between all the data sets.

Log rank test was used for Kaplan-Meier survival curves.

3.16 TABLES

Table 1. Primary antibodies

PRIMARY AB		**DILUTION**		
Antigen		*Cells*	*Tissues*	*WB*
Glial fibrillary acidic protein (GFAP)	Dako Rabbit polyclonal	1:500	1:400	
Glial fibrillary acidic protein (GFAP)	Chemicon Mouse monoclonal IgG1			1:100,000
Ki67	Novocastra Mouse monoclonal Rabbit polyclonal	1:1,000	1:1,000	
Neuronal Class III β-Tubulin	Babco Mouse monoclonal, IgG2a, clone TUJ1 Rabbit polyclonal	1:500	1:500	
Oligodendrocyte marker O4	Chemicon (Millipore) Mouse monoclonal IgM, clone 81.	1:100	1:100	
CD68	Serotec Rat IgG		1:200	
Iba I	Wako Rabbit polyclonal		1:300	1:1,000
BrdU	Serotec Rat IgG		1:500	
Cleaved CASP3	Cell signaling technology Rabbit polyclonal	1:100		1:1,000
Doublecortin	Santa Crus Goat polyclonal		1:200	
p-ERK	Cell signaling technology Rabbit polyclonal			1:1,000
ERK (p44/42)	Cell signaling technology Mouse monoclonal			1:1,000

Table 2. Secondary antibodies

Secondary AB		**DILUITION**		
Antigen		*Cells*	*Tissues*	*WB*
Alexa 488 Alexa 546 Alexa 633-conjugate	Molecular probes Goat anti-mouse IgG; goat anti-rabbit IgG; goat anti-rat IgG	1:1,000	1:1,000	
Alexa 488 Alexa 594-conjugate	Molecular probes Donkey anti-goat IgG;	1:1,000	1:1,000	
Biotin-conjugate	Jackson lab Goat anti-rat		1:200	
HRP-conjugate	Santa Cruz Goat anti-mouse IgG; goat anti-rabbit IgG; donkey anti-goat IgG			1:1,000-1:200,00

4 RESULTS

4.1. Analysis of cell proliferation in the SVZ neurogenic niche

The neurological component of GLD is not fully understood and there are hints suggesting the presence of tissue damage before the overt demyelination (Escolar et al., 2009). During early postnatal stages we observe the most relevant modifications in the structure and cell composition of the SVZ niche microenvironment that ultimately result in its complex adult architecture (Gritti and Bonfanti, 2007). Recently, it was shown that variations in the expression levels of the lysosomal enzyme GALC perturb the homeostasis of the hematopoietic stem cell niche (Visigalli et al., 2010). Since the sphingolipid metabolism is particularly important in CNS tissues, especially during development, we thought to investigate the effect that GALC absence could elicit on neurogenic niches.

4.1.1 Impairment of cell proliferation in the SVZ neurogenic niche of Twi mice: *in vivo* studies

Proliferation of neuronal progenitors that eventually give rise to differentiated neurons within the adult central nervous system has been usually demonstrated using an exogenous cell tracer, 5'-bromo-2'-deoxyuridine (BrdU), in combination with endogenous neuronal markers. BrdU is a thymidine analog that incorporates into dividing cells during DNA synthesis, in the S-phase. Once incorporated into the new DNA, BrdU will remain in place and passed down to daughter cells following division (Nowakowski et al., 1989).

I first assessed by cumulative *in vivo* BrdU labelling whether the proliferation of SVZ precursors was altered in Twi mice as compared to WT littermates, also evaluating the potential effect of age. I injected asymptomatic postnatal day (PND) 10 and symptomatic Twi mice (PND30 and PND40) with BrdU (40 mg/kg, i.p., 1 injection every 2 hours for a total of 4 injections). Two

hours after the last injection mice were intracardially perfused, brains removed and processed for immunohistochemistry (IHC) using an antibody to BrdU, in order to visualize cells that incorporated the thymidine analogue. I decided to apply this multiple injection protocol in order to reach BrdU saturation and to label all the actively proliferative cells in the niche (Takahashi et al., 1992). I counted the number of BrdU+ cells in 3 sections/brain (n=6) and expressed the results as the average number of BrdU+ cells/section. Qualitative (Fig.9A) and quantitative (Fig.9B) analysis showed a significant decrease in the total number of BrdU+ cells in Twi mice as compared to WT littermates as a function of disease progression (20% and 50% decrease at PND30 and PND40, respectively).

Both SVZ neuroblasts (type A cells) and transient amplifying cells (type C cells) proliferate in physiological conditions, while type B cells (astrocytes) are considered as quiescent/slowly-dividing cells. In order to assess the cell type composition within the population of proliferating cells, I performed double label immunofluorescence with lineage specific markers. Doublecortin (DCX) is a marker of developing, immature neurons and is required for normal neuronal migration in the developing cerebral cortex (Meyer et al., 2002), thus being a useful marker to identify young, immature neurons, as type A cells. Double labelling for BrdU and DCX performed at PND40 (Fig.9C) revealed a significative decrease in the number of proliferating cells expressing DCX in Twi mice as compared to WT littermates (Fig.9D).

4.1.2 Impairment of cell proliferation in the SVZ neurogenic niche of Twi mice: *ex vivo* studies

In order to characterize the functional behaviour of type C and type B cells, which are less easily detected *in vivo* due to the lack of univocal specific markers, I resorted to an *ex vivo* experimental paradigm, namely the NeuroSphere Assay (NS-A) (Reynolds and Rietze, 2005; Reynolds and Weiss, 1992)

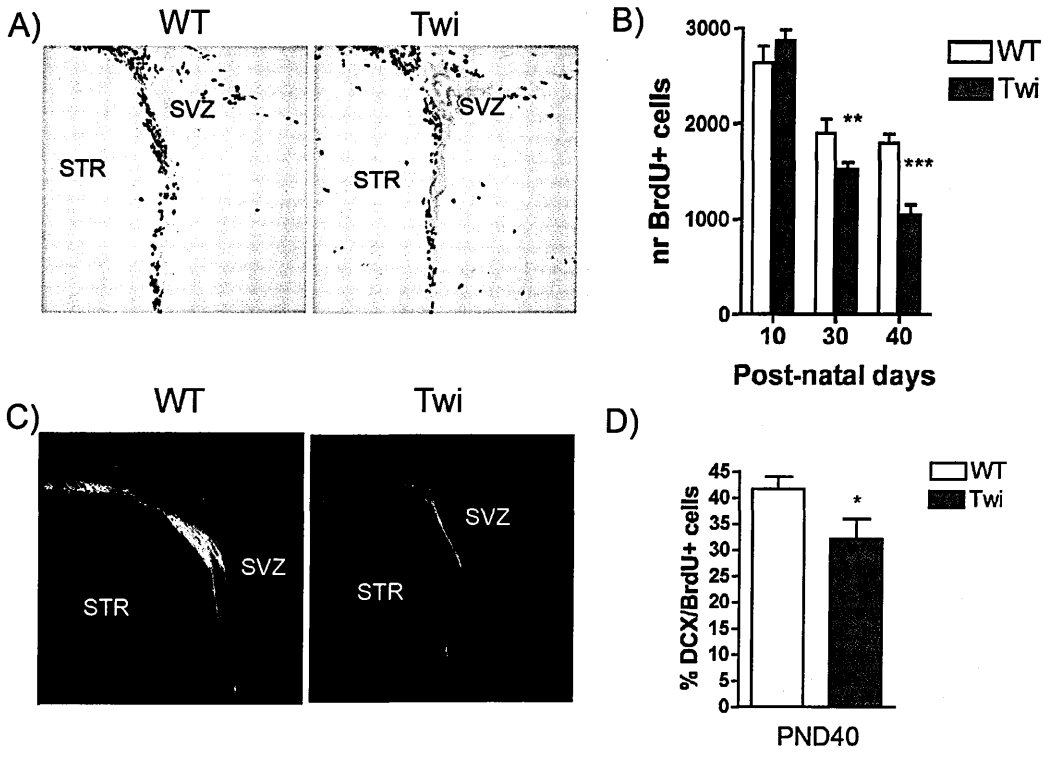

Figure 9. Impairment of cell proliferation in the SVZ of Twi mice

BrdU immunohistochemistry on brain coronal sections of PND40 WT and Twi mice. Decreased numbers of BrdU+ cells are present in the SVZ of Twi mice as compared to WT littermates. Note the presence of high numbers of BrdU+ cells in the brain parenchyma outside the SVZ in Twi mice. B) Quantification of the total number of BrdU+ cells per brain (n=6). *** $p \leq 0.001$; ** $p \leq 0.01$ (two-way ANOVA with Bonferroni post-test). C) Double labelling immunofluorescence for BrdU (red) and DCX (green) on brain coronal sections of PND40 WT and Twi mice. Double positive cells are less abundant in Twi brain as compared to WT (images were acquired by three-laser confocal microscope-Radiance 2100, BioRad; fluorescent signals from single optical sections were sequentially acquired and analysed by Adobe Photoshop CS software; magnification 10x). D) Quantification of the total number of BrdU+DCX+ in WT and Twi SVZ (n=6) * $p \leq 0.05$ (Mann Whitney test). Numbers are expressed as mean ± SEM

This assay allows isolating and propagating bona fide neural stem and progenitor cells in chemical defined culture conditions. I isolated primary cells from the SVZ of PND40 Twi and WT mice and plated them at clonal density (5000 cells/cm^2): the number of primary spheres counted 10 days after plating returned an index of the proportion of sphere-forming cells originally present in the tissue. I observed a significant decrease in the number of primary neurospheres derived from the Twi SVZ as compared to the WT counterpart (Fig.10A). The population of sphere-forming cells detectable with this assay includes primarily stem and precursor cells (type B and type C) but also committed progenitors (type A), which can undergo some rounds of proliferation under these culture conditions. In order to discriminate between the different sphere-forming cells I next applied a modified NSA assay (Neurosphere Cell Colony Forming Assay; NCFCA) (Louis et al., 2008) in which primary spheres are categorized based on their size (an index of proliferative potential) in order to differentiate spheres generated by bona fide stem cells (larger size) from those generated by committed progenitors (smaller size). Results showed a trend for decreased numbers of primary neurospheres having a diameter >2mm (likely formed by true stem cells) in Twi as compared to WT cultures as well as a significant decrease in the population of small size primary spheres (<2mm) (likely formed by precursor cells and progenitors) (Fig.10B, C).

Overall these data suggested that stem/progenitors cells in the SVZ of Twi mice are impaired in their proliferative and clonogenic ability

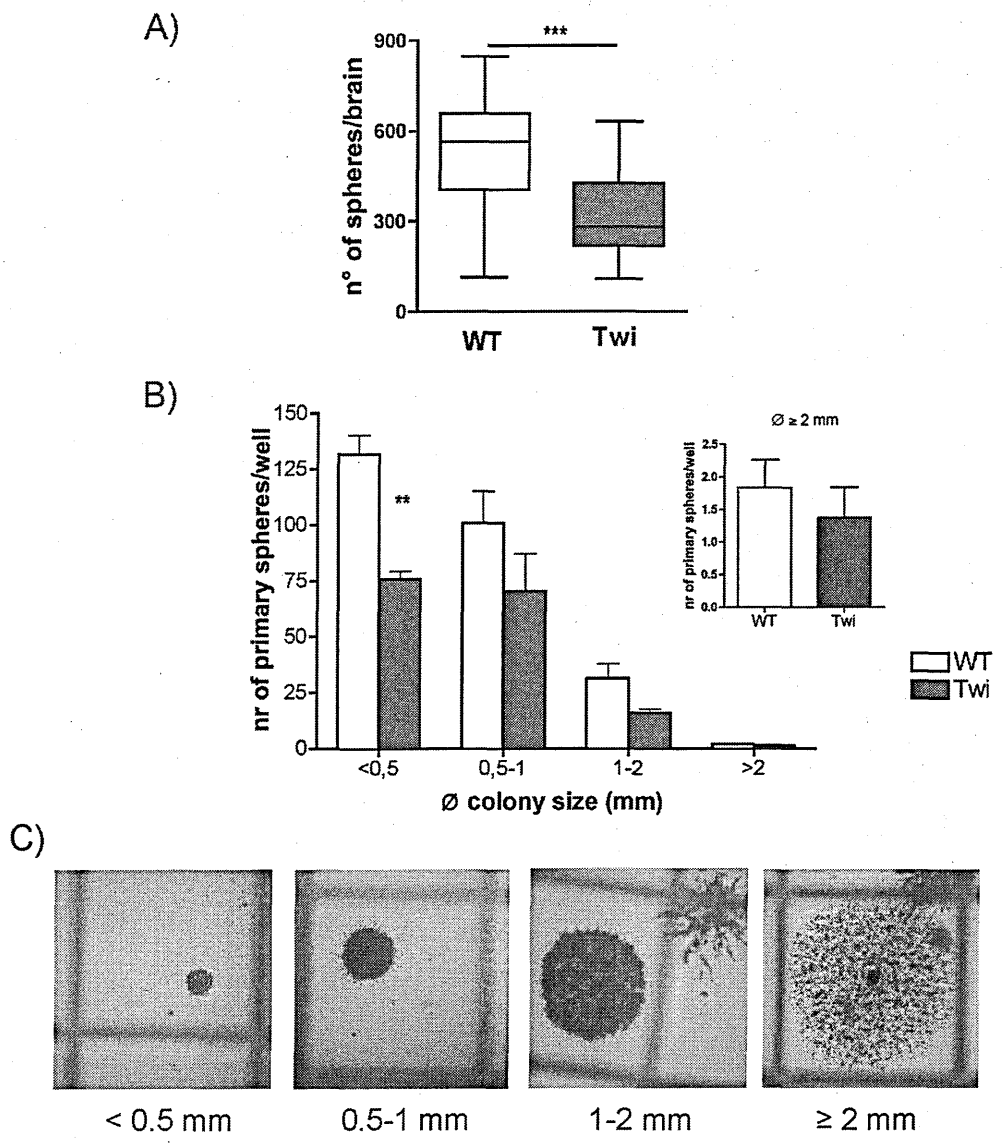

Figure 10. Impairment of SVZ-derived stem/progenitors cell proliferation assessed by NSA in Twi mice. A) Primary cells isolated from the SVZ of Twi mice (PND40) (n= 23) generate significant less numbers of primary neurospheres as compared to their WT counterpart (n=18). *** $p \leq 0.0001$ (Mann Whitney test). B) NCFC assay. The numbers of primary neurospheres are shown according to sphere size (n=8). Numbers related to the large size WT- and Twi-derived neurospheres are shown in the inset. *** $p \leq 0.001$ (two-way ANOVA with Bonferroni post-test). C) Representative pictures of primary neurospheres of different size (grid=2x2mm).

4.1.3 Alteration of neuroblasts' chain arrangement in the lateral wall of the forebrain lateral ventricles

I next sought to determine whether the morphological and ultra structural features of the Twi SVZ were also impaired. Wholemount approaches have provided several key insights into the germinal activity of the adult SVZ, providing a comprehensive, en-face view of this germinal region (Doetsch and Alvarez-Buylla, 1996; Mirzadeh et al., 2010; Mirzadeh et al., 2008). I sought therefore to use this technique to analyse the SVZ walls of PND40 Twi and WT littermates, to determine if the lower number of proliferating neuroblasts are associated with their altered structure and/or organization. I noted irregular features in the SVZ wall of Twi mice compared to WT littermates. In particular, I detected sparse chains with respect to well-defined chains observed in WT littermates, especially in the dorsal area. Moreover I observed occasionally tangled chains in the rostral/ventral part of the Twi SVZ as compared to the WT counterpart (Fig.11A, B). Interestingly, I observed the presence of microglial cell and monocyte/macrophage infiltrates in the SVZ of Twi mice that are almost absent in WT littermates (Fig.11C).

Figure 11. Alteration of neuroblast's chain arrangement.
A) Whole mount reconstruction (10X) of the later wall of the ventricle isolated from WT and Twi mice. DCX immunofluorescence (green) highlights chains of neuroblasts, GAFP (blue) and mouse IgG (red) stain astrocytes and blood vessels, respectively. Note the dorsal (a), ventral (b, d) and caudal (c) pattern. B) Higher magnification images of the different regions: (a) chains in the dorsal area are less abundant in Twi compared to WT mice (green: DCX; red: GFAP; blue: Ki67); (b) in the ventral area, tangles of chains can be found in Twi mice; (c) sparse chains are visible in the caudal area in Twi mice; (d) single cells migrating in Twi compared to WT mice (green:DCX; red: mouse IgG; blue:Ki67). C) Whole mount of the Twi SVZ revealed the presence of huge amount of microglial cells (Iba-1) and monocyte infiltration (CD68) compared to WT SVZ. Higher magnification images reveal the presence of CD68+ cell in between the neuroblast chains (DCX+) in Twi samples. Images were acquired by three-laser confocal microscope-Radiance 2100, BioRad; fluorescent signals from single optical sections were sequentially acquired and analysed by Adobe Photoshop CS software; magnification: A, 10x; a, 20X; b-d, 40X

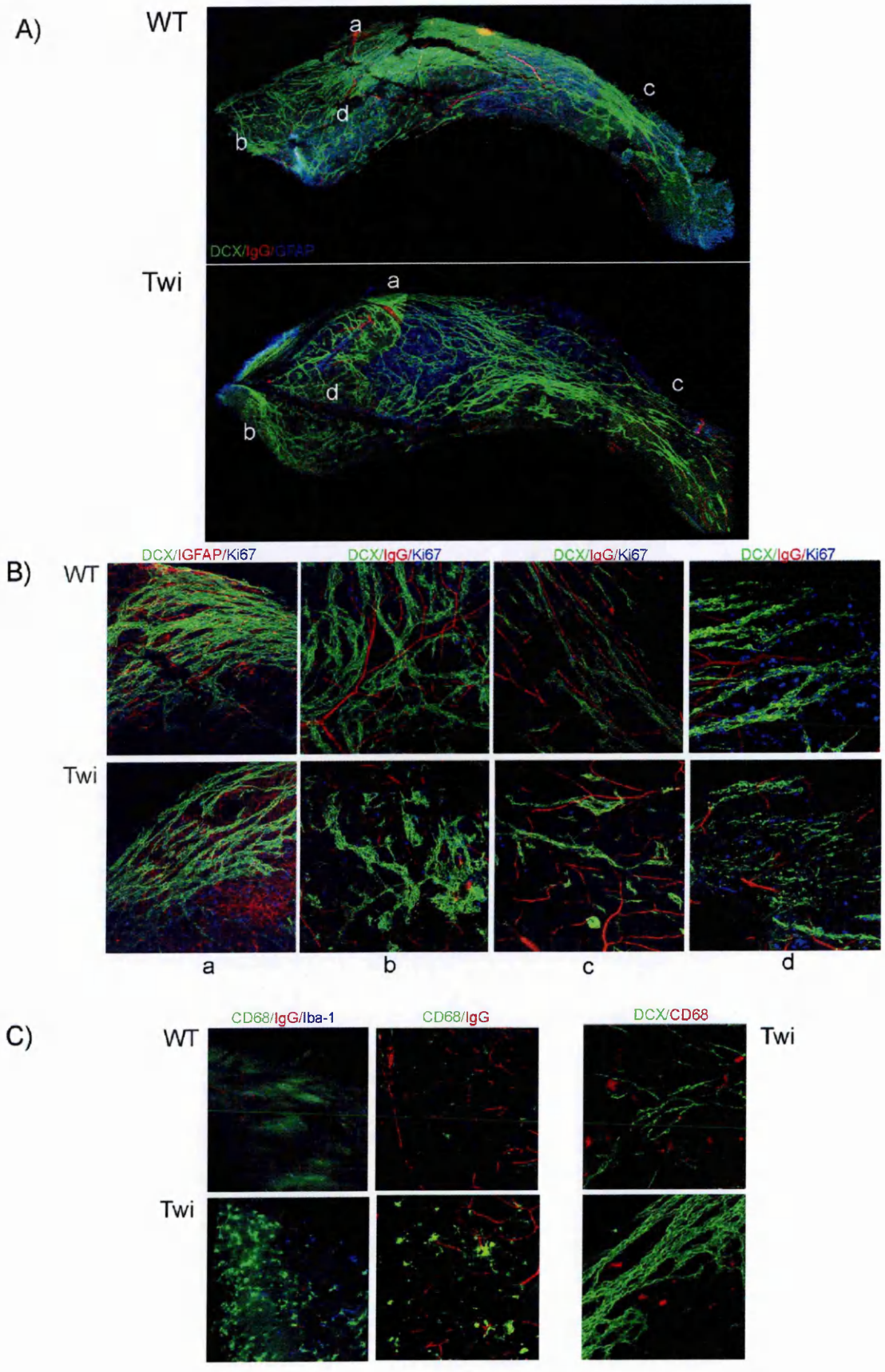
A)
WT
a
b
c
d
DCX/IgG/GFAP
Twi
a
b
c
d
B)
WT
DCX/IGFAP/Ki67
DCX/IgG/Ki67
DCX/IgG/Ki67
DCX/IgG/Ki67
Twi
a
b
c
d
C)
WT
CD68/IgG/Iba-1
CD68/IgG
DCX/CD68
Twi
Twi

4.1.1 Ultrastructural analysis of the SVZ neurogenic niche reveals modification in the cell type composition

To further characterize the morphological alterations observed in SVZ wholemounts at PND40, I performed electron microscopy (EM) analysis on coronal forebrain sections distinguishing the SVZ around the lateral ventricles (SVZ-LV) from the SVZ that spans in the rostral extension (SVZ-RE) in age-matched Twi and WT mice, quantifying the proportion of the different cell types (type A, B and C).

I did not observe significant differences in the ultrastructural morphology and proportions of type A and type B cells in the SVZ-LV of Twi mice as compared to WT littermates (Fig.12A). Interestingly, type C cells showed a moderate decrease in number (Fig. 12B). In contrast, Twi mice were characterized by a significant decrease in the number of neuroblasts at the SVZ-RE level (Fig. 12C), accompanied by loose chain organization (compare the grey areas in drawings of Fig. 12D). In addition, several unidentified cell types with ultrastructural morphology reminiscent of microglia were also observed in the entire SVZ of Twi mice (Fig. 12D), confirming the presence of cellular infiltrates in the SVZ, as shown with the wholemount technique.

Results from EM analysis support the idea that the SVZ progenitor cells; in particular, type A progenitors (neuroblasts) are less in number and less organized in Twi mice as compared to WT littermates. Considering the relatively normal morphology and cell type composition and the absence of cell accumulation of the SVZ-LV (not shown), our data suggest that the rate of neuroblast proliferation/death more than their migration could be impaired in the SVZ stem cell niche of Twi mice.

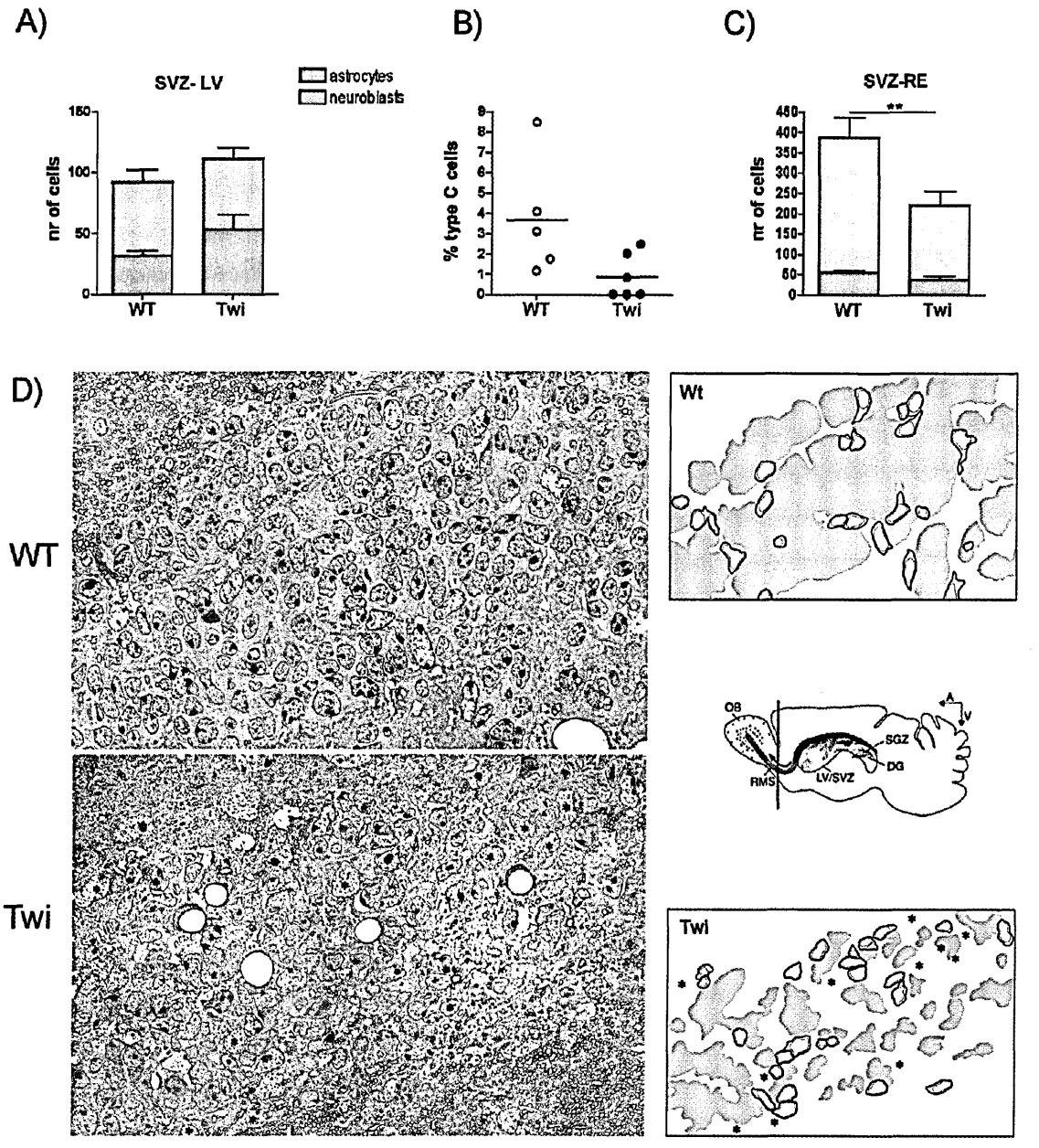

Figure 12. Cell type composition of the SVZ by ultrastructural analysis

A) The Twi SVZ-LV contains similar numbers of type A and B cells but decreased numbers of type C cells (B) with respect to WT SVZ-RE. (C) Significant decrease in the number of neuroblasts in SVZ-RE in Twi compared to WT mice. (D) Electron microscopy of the SVZ rostral extension (SVZ-RE) in WT and Twi mice (red area in the cartoon). In the masks, neuroblasts are represented in grey, astrocytes in white and the asterisk indicates putative microglia/macrophages cells. Numbers are expressed as mean ± SEM (n=3) ** $p \leq 0.01$ (Mann Whitney test).

4.2. The impact of neuroinflammation on the SVZ neurogenic niche

It has been reported that an inflammatory environment could be detrimental for neurogenesis and NSC functions (Pluchino et al., 2008). Since extensive microglia activation and reactive astrogliosis characterizes the Twi brain at the late stages of disease progression (Luzi et al., 2009) (see also below) I next sought to assess whether the functional impairment of the SVZ stem/progenitor cell compartment observed at PND40 might be consequent to the severe neuroinflammation associated with the disease progression.

4.2.1 Inflammatory profile in the Twi brain during disease progression: gene expression

I evaluated the inflammatory profile in total brain tissues isolated from Twi mice and WT littermates at different postnatal ages (PND2, PND10, PND20, PND30 and PND40) corresponding at different stages of the disease (from asymptomatic to fully symptomatic). I performed quantitative RT-PCR for a panel of selected cytokines and chemokines expressed by activated microglia and astrocytes as well as by neurons (CCL2, CCL3, CCL5 IL1α, IL1β, TNF-α, CXCL12 and CXCL10). These molecules are mainly pro-inflammatory cytokines and chemoattractants for monocyte/macrophages.

I showed an age dependent increase of mRNA expression of several of these molecules starting from the early symptomatic stage (PND20) (Fig. 13). In particular, I detected up-regulation of chemokines such as CCL2 (MCP-1) and CXCL10 (IP-10), which increase from 10- to 100-fold with respect to WT samples. Other pro-inflammatory cytokines, such as IL1α, IL1β and TNF-α, reached a maximum of 10-fold increase. It is important to note that CCL2 is expressed not only in neuroinflammatory conditions, but it is also constitutively expressed in the brain both by glial cells and neurons (Banisadr et al., 2005). Recent reports suggest that CCL2 could act as a modulator of neuronal activity and neuroendocrine functions (Conductier et al., 2010). Moreover the presence of its receptors (CCR2) on neural progenitors supports the idea that chemokines

might act locally as chemoattractan for these cells during the ontogeny of several brain structures (Tran et al., 2004). On the contrary, CXCL10 is generally not detectable and its expression is induced by other molecules, such as INF-γ, IL1β and TNF-α (Muller et al., 2010).

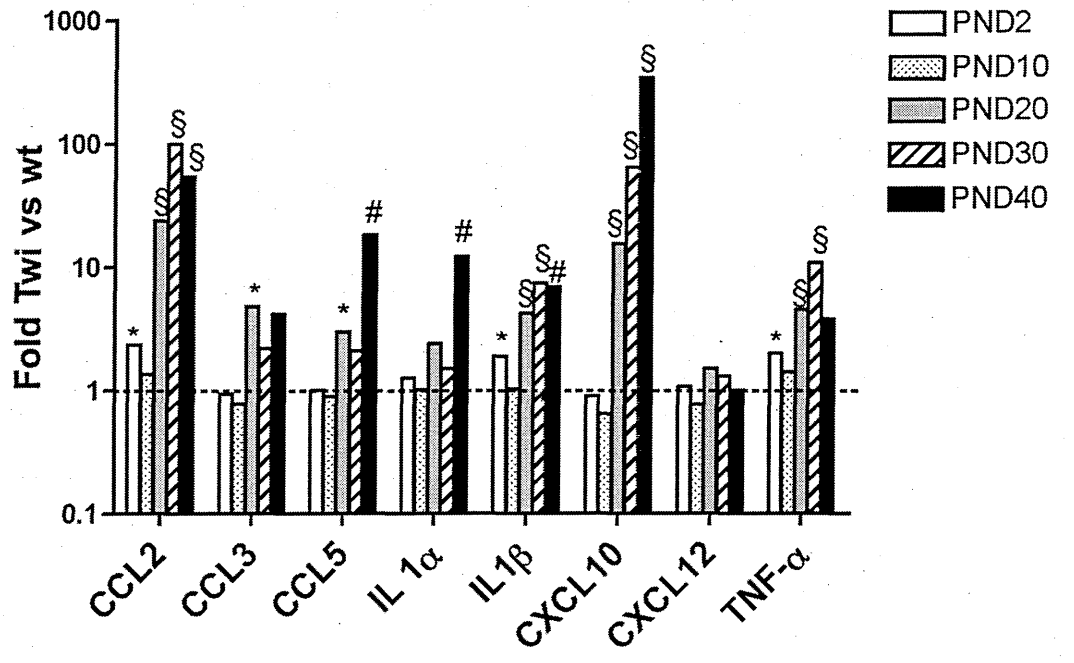

Figure 13. Inflammatory markers in total brain tissues of Twi mice as a function of age: mRNA levels

Total brain tissues of WT and Twi (n=3-5) mice were collected at different ages (PND2, PND10, PND20, PND30 and PND40). Sybr green RT-PCR was performed for several inflammatory markers. Values are expressed as fold increase to WT levels, using the housekeeping gene β-actin. § $p \leq 0.001$; # $p \leq 0.01$; * $p \leq 0.05$ (two-way ANOVA with Bonferroni post-test).

4.2.2 Inflammatory profile in the Twi brain during disease progression: protein levels

I next sought to confirm whether changes in mRNA expression levels were found at the protein level. Even though the correlation between mRNA and protein expression is not always linear, I expected to detect increased protein levels for the molecules in which I saw the highest fold differences in mRNA expression when comparing Twi and WT samples. I performed Multi Analyte Profile (MAP), a multiplex ELISA assay based on Lumina technology that detects

multiple molecules in the same brain tissue sample (Fig.14). For the highly expressed chemokines I corroborate the results obtained by qRT-PCR. Indeed, expression of CXCL10 protein is more than one order of magnitude higher in Twi brains compared to WT (17 pg/ml and 870 pg/ml for WT and Twi samples, respectively). Similarly, expression of MCP-1 (CCL2) protein is about 500-fold in Twi vs WT brain samples. For other molecules, such as IL-1β, IL-1α and TNF-α I detected minor increases in the protein levels with respect to mRNA expression. Interestingly, I observed a strong age-dependent increase in FGF-2 protein level in Twi samples, possibly indicating astrocyte iperthrophy and on-going astrogliosis, processes that are associated with microglia activation and inflammation in the Twi CNS.

4.2.3 Inflammatory profile in the Twi brain during disease progression: pathological features

In order to further investigate this issue, I performed Western blot analysis (Fig.15) on tissues samples from mice of different ages (from PND2 to PND40) for markers of astrogliosis (GFAP), microglia activation (IBA-1) and apoptosis (Cleaved Caspase 3). I decided to include a marker of apoptosis because it is known that astrocytes and microglia activation can trigger and foster the inflammatory response, inducing also cell death. Results from this assay showed an up-regulation of all the markers analysed, not only at PND40 (as expected), but also in tissues from PND2 and PND10 mice, thus indicating that Twi brains are characterized by precocious astrogliosis and inflammation.

These results strongly indicate that up-regulation of inflammatory molecules, likely a consequence of astrogliosis, microglia activation and apoptosis, are present before, or in close correspondence to the appearance of symptoms. This suggested a possible role of this process in the pathogenesis of the disease.

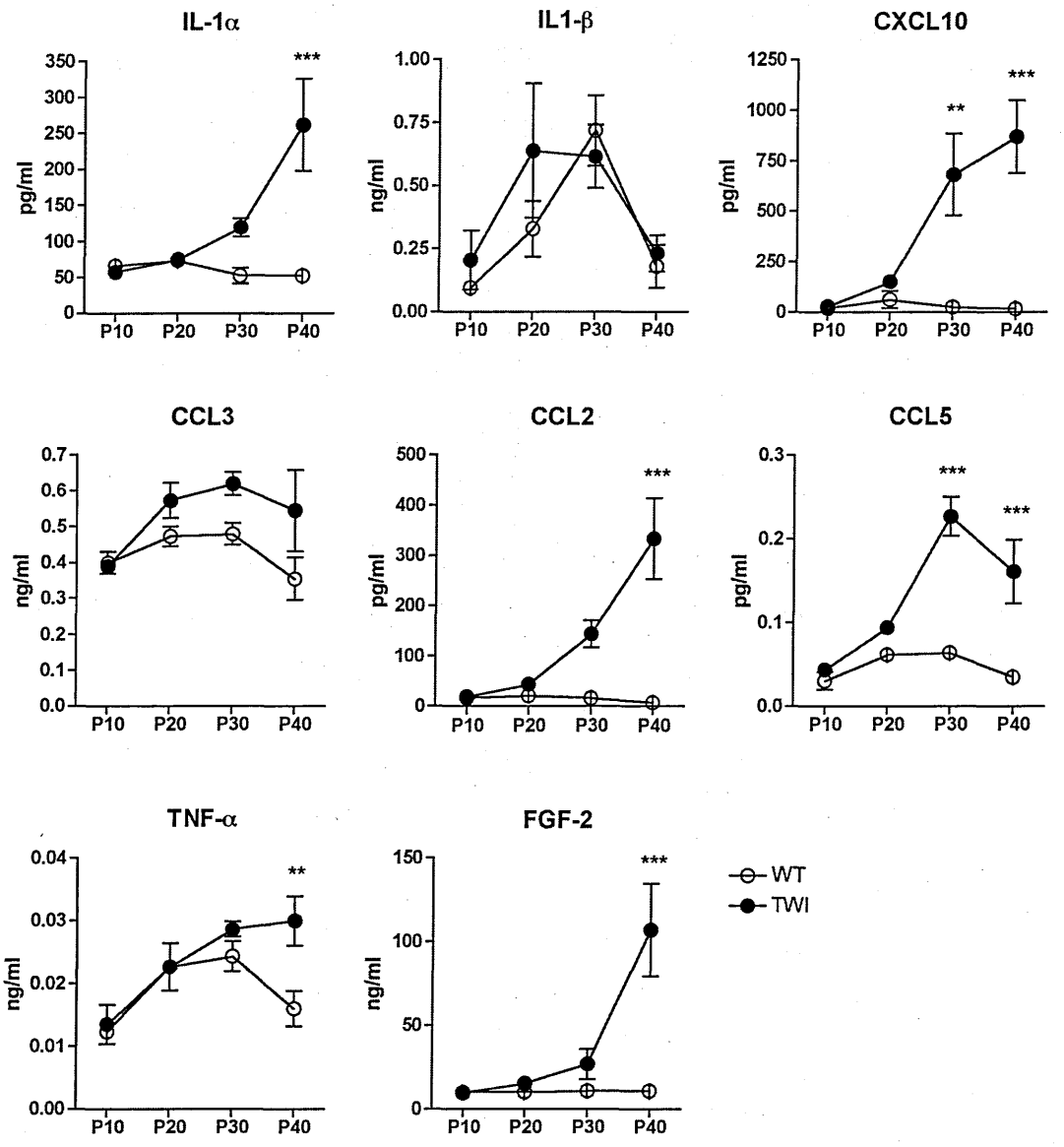

Figure 14. Inflammatory markers in the total brain tissue of Twi mice as a function of age: protein levels

Multi Analyte Profile (MAP) was performed on total brain tissue samples from WT and TWI mice (n=3) to detect the amount of several pro-inflammatory molecules. *** $p \leq 0.001$; ** $p \leq 0.01$ (two-way ANOVA with Bonferroni post-test).

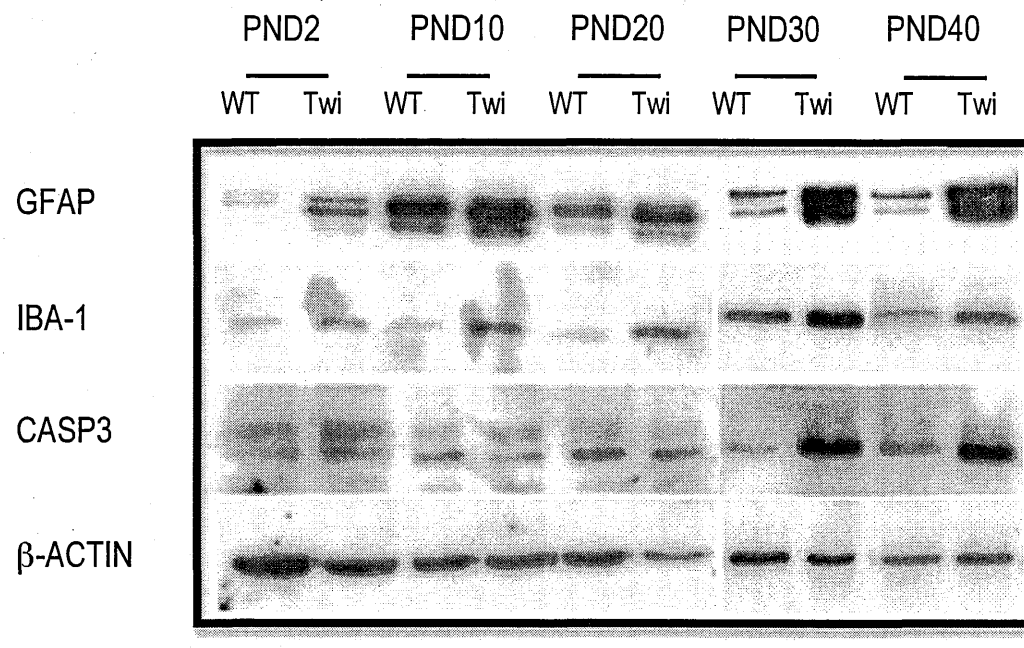

Figure 15. Astrogliosis, microglia activation and apoptosis are present in early symptomatic Twi brains

4.2.4 Modulation of inflammation in Twi brains: anti-inflammatory treatments

As described previously (see paragraph 1.1.7.7) combined therapies are designed to target different aspects of the pathology in LSDs and anti-inflammatory drugs have been successfully used in several of these diseases (Jeyakumar et al., 2004). I sought to test whether these compounds could benefit the Twi mice, modulating the inflammatory status that is pronounced not only at the latest stages of the disease, where CNS is already compromised, but also at earlier time points. I chose to test the effect of Minocycline, a tetracycline analog, capable to cross the blood brain barrier and with reported neuroprotective and anti-apoptotic activity, mainly due to inhibition of activated microglia (Domercq and Matute, 2004). As an additional control I used Indomethacin, a well-known non-steroidal anti-inflammatory drug that acts by inhibiting

cyclooxygenase. Twi and WT mice were administered the drugs daily starting from PND10 (40mg/kg and 10mg/kg for Minocycline and Indomethacin, respectively; intraperitoneal injection). Age-matched saline-treated mice served as controls. Mice were euthanized after 10, 20 and 30 days of treatment, at PND20, PND30 and PND40, respectively. Analysis of mRNA and protein levels were performed by qRT-PCR (Fig.16 A, B) and MAP (Fig.9) on the same panel of molecules analysed previously (see paragraph 2.1). mRNA expression of several pro-inflammatory molecules was partially down regulated in Minocycline-treated Twi mice (Fig.16A).

This effect was more pronounced at the earliest time points (10 and 20 days post-treatment) as indicated by the results of CCL2, CXCL10 and IL1-α, suggesting that the anti-inflammatory treatment is able to detoxify the brain environment effectively when it is not yet strongly compromised. On the contrary, Indomethacin-treated Twi mice showed major mRNA down regulation at the latest time point, suggesting that this drug requires more time to exert its activity (Fig.16B). Down-regulation of mRNA levels in drug-treated Twi mice did not closely correlate with down-regulation of protein levels (Fig.17). Only IL-1α, CCL3 and FGF2 protein levels showed a moderate down-regulation.

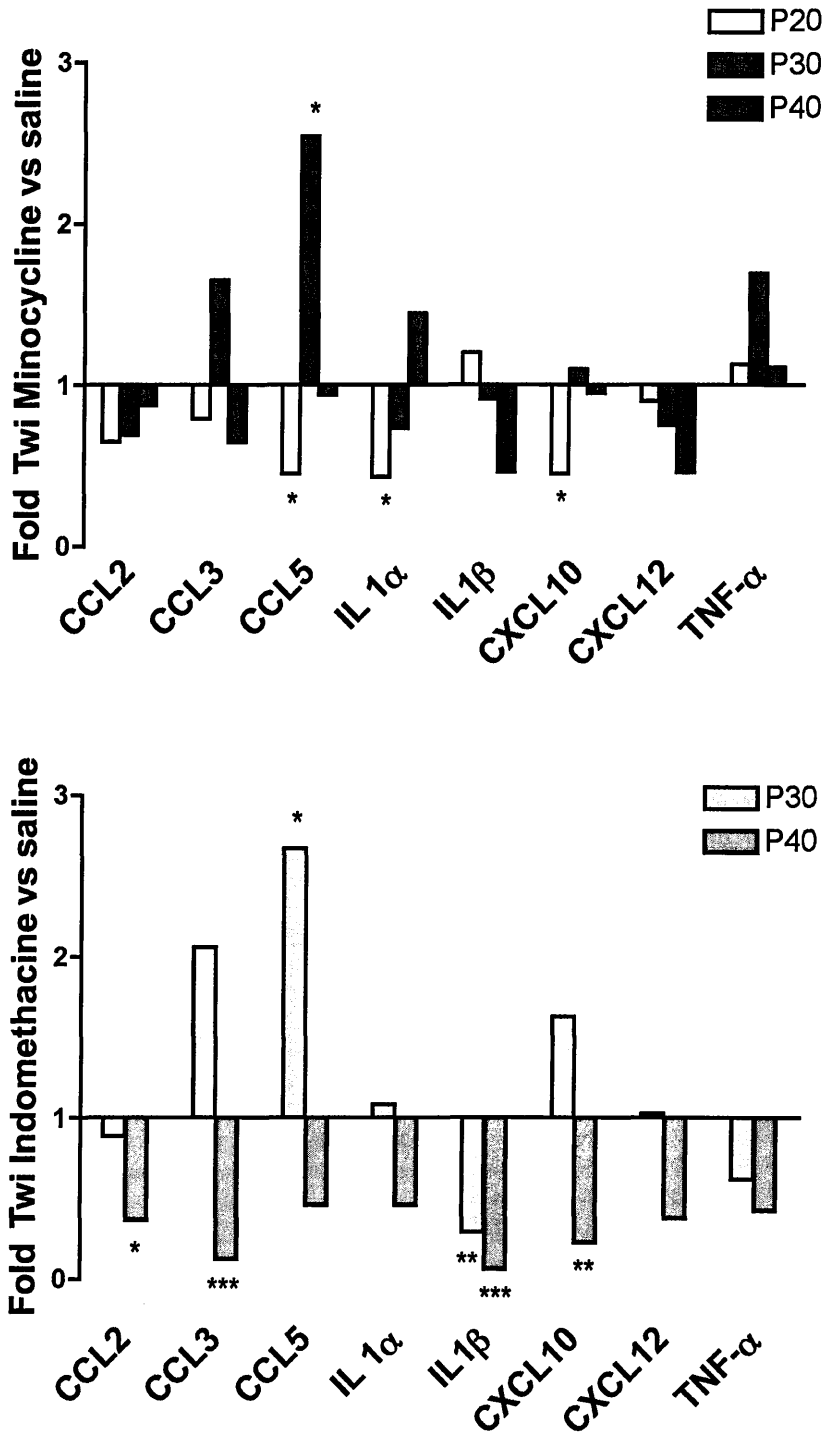

Figure 16. Modulation of the inflammatory profile of Twi mice treated with anti-inflammatory drugs: mRNA levels

Tissues from total brain of WT and Twi mice (n=3-5) were collected 20 (P30) and 30 days (P40) after daily treatment with Minocycline (A) and Indomethacin (B) started at PND10. Sybr green RT-PCR was performed for several pro-inflammatory molecules shown. Values are expressed as fold increase to untreated Twi levels, using the housekeeping gene β-actin as normalizer. *** $p \leq 0.001$; ** $p \leq 0.01$; * $p \leq 0.05$ (two-way ANOVA with Bonferroni post-test).

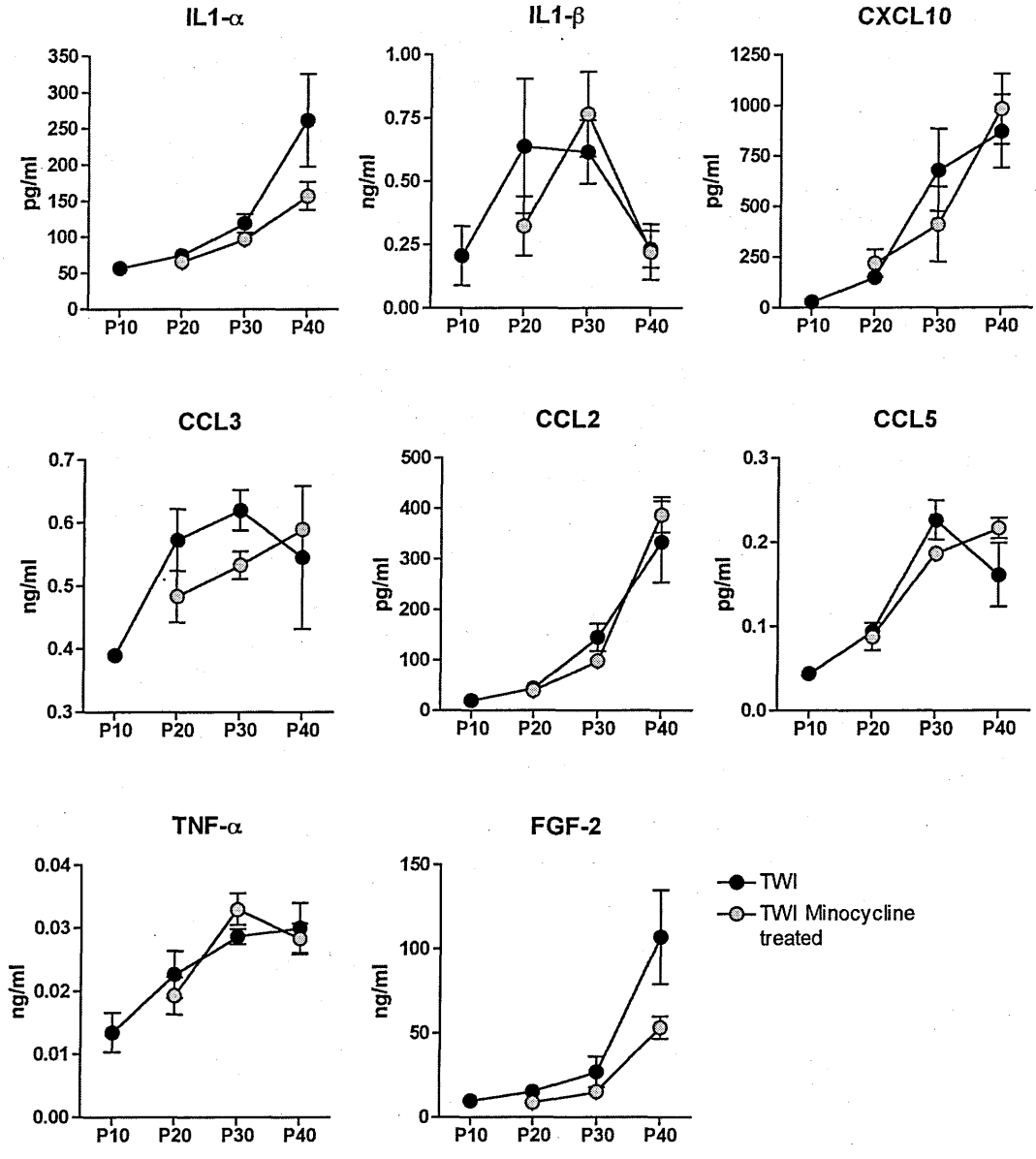

Figure 17. Modulation of the inflammatory profile of Twi mice treated with anti-inflammatory drugs: protein levels

Multi Analyte Profile (MAP) ELISA was performed on total brain tissue sample from WT and TWI mice (n=3) to detect the protein expression of several pro-inflammatory molecules.

4.2.5 Efficacy of the anti-inflammatory treatments on the pathological hallmarks

In order to evaluate whether the anti-inflammatory treatment could have an effect on the pathology hallmarks, I performed histochemistry and immunofluorescence on brain tissues of Minocycline-treated and untreated Twi and WT mice at PND30 and PND40 (Fig.18). I first analysed the pattern of lectin (RCA-1) staining in the cerebellum (Cb), pons and spinal cord (SC), which are the areas mainly affected by infiltrated globoid cells and glycolipid storage (Fig18, A). Lectins bind glycolipids and are considered a useful tool to visualize globoid cells in CNS tissues from murine and dog models of GLD (Alroy et al., 1986). Whereas at PND30 (not shown) I did not detect significant differences in lectin content (lectin immunopositive area) between Minocycline-treated and untreated Twi mice, at PND40 I observed a significant decrease of lectin positive area in the pons and SC of treated Twi mice, indicating clearance of tissue storage and globoid cells. Immunofluorescence analysis was then performed on selected rostro-caudal region (white and grey matter of the forebrain, Cb, pons and SC) using antibodies to CD68 (infiltrating macrophages) and Iba-1 (microglia). Quantification of the immunoreactivity for CD68 (Fig.18B) at PND30 (not shown) and PND40 revealed decreased presence of CD68+ cells for all the areas considered in Minocycline-treated compared to untreated Twi mice. Iba-1 immunoreactivity (Fig.18C) showed no significant differences at PND30 (not shown), while decreased Iba-1+ signal was found at PND40 in the forebrain of Minocycline-treated compared to untreated Twi mice.

These results indicate that, despite the moderate decrease in the mRNA expression and protein levels of the several pro-inflammatory molecules tested, Minocycline treatment was sufficient to partially clear storage and ameliorate pathology in the Twi CNS.

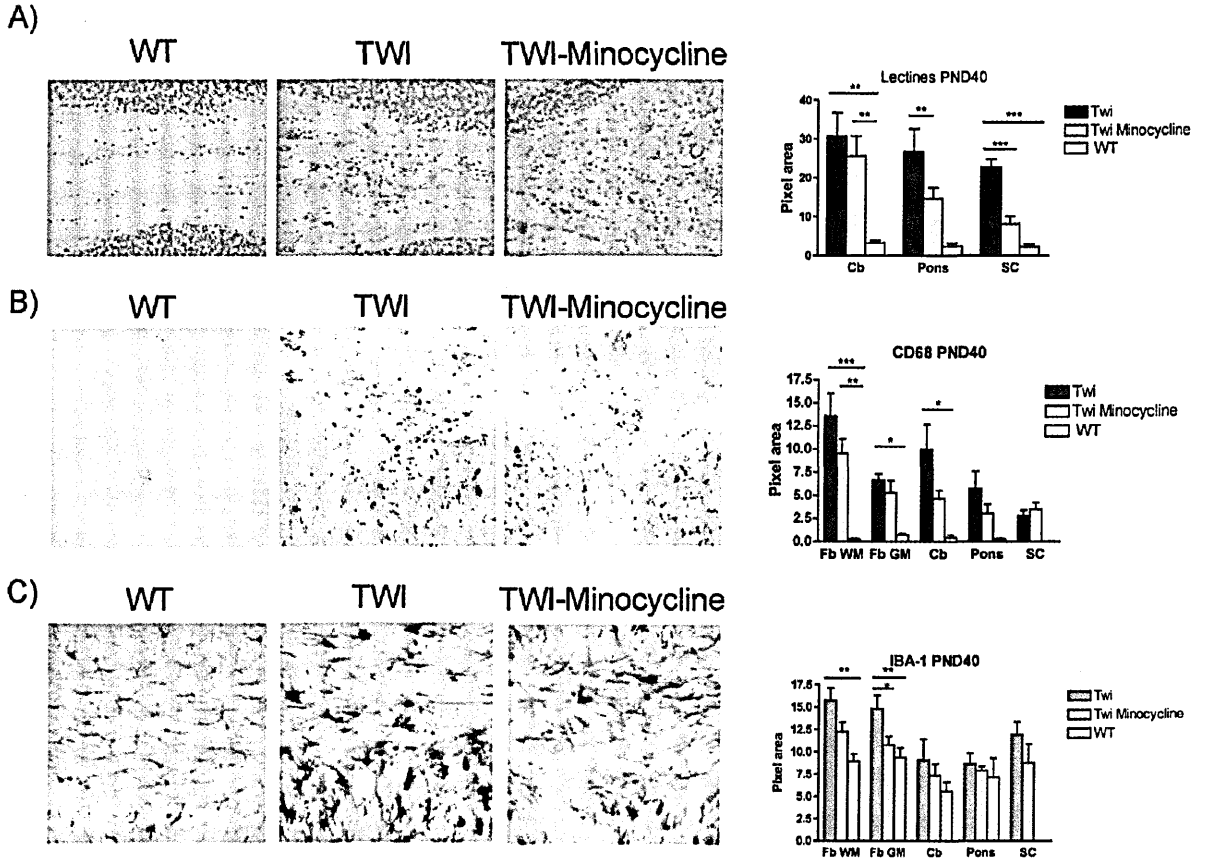

Figure 18. Anti-inflammatory treatment ameliorates storage and pathology.
Histochemistry using biotinylated lectins (RCA-1; glycolipid storage and globoid cells) and immunofluorescence analysis using CD68 anti-Iba1 (macrophages and microglia) antibodies were performed on selected region-matched rostro-caudal tissue slices PND40 WT and Twi (Minocyclin-treated and untreated) mice. Fb WM: forebrain white matter; Fb GM: forebrain grey matter; Cb: cerebellum; SC: spinal cord.
(A) Lectin histochemistry at PND40; (B) CD68 and (C) Iba-1 immunoreactitvity in PND40 forebrain. The total immunopositive area (expressed in pixels) was calculated using the ImageJ software using the WT parameters as threshold. 3-5 pictures were taken for each sections, at least 7 sections for brain considered (n=3)*** $p \leq 0.001$; ** $p \leq 0.01$ * $p \leq 0.05$ (one-way ANOVA with Bonferroni post-test)

4.2.6 Effect of anti-inflammatory treatment on the SVZ-neurogenic niche

To assess the impact of the anti-inflammatory treatment on the neurogenic compartment and to possibly discriminate between a cell-autonomous versus non-cell autonomous (environmental) origin of the NSC functional impairment, the morphological and functional features of the SVZ neurogenic niche were reassessed in Twi mice treated with anti-inflammatory drugs.

I performed the *in vitro* NSA and *in vivo* BrdU analysis on Minocycline-treated Twi and WT mice and untreated controls at PND40 (Fig19A, B). I decided to focus these studies on PND40 mice because this age corresponds to the fully symptomatic stage of the disease and to the latest point of the anti-inflammatory treatment protocol. A group of mice received BrdU injections at the day of euthanasia, according to the protocol described above, in order to evaluate the effect of the anti-inflammatory treatment on *in vivo* proliferation (fig.19A).

I found comparable numbers of BrdU+ cells in the SVZ of WT and Minocycline-treated Twi mice, thus indicating a rescue of cell proliferation due to the treatment. The *ex vivo* NSA assay (Fig.19B) gave similar results. In fact, the number of primary neurospheres derived from Minocycline-treated Twi mice was comparable to that of derived from WT mice. The NSA performed on SVZ primary cells from Indomethacin-treated mice gave similar results (Fig.19B). Importantly, no functional impairment was observed in the clonogenic ability of primary cells derived from Minocycline-treated WT mice (Fig.19B).

Ultrastructural analysis performed by EM did not show a clear increase in progenitor cell number and definitive rescue of SVZ morphology in Minocycline-treated Twi mice as compared to untreated Twi controls (Fig.20). Indeed, despite increased neuroblasts numbers in the SVZ-LV (Fig.20A) I observed no changes in the neuroblast proportions in the SVZ-RE (Fig.20B) and in the number of type C cells in the SVZ-LV (Fig.20C).

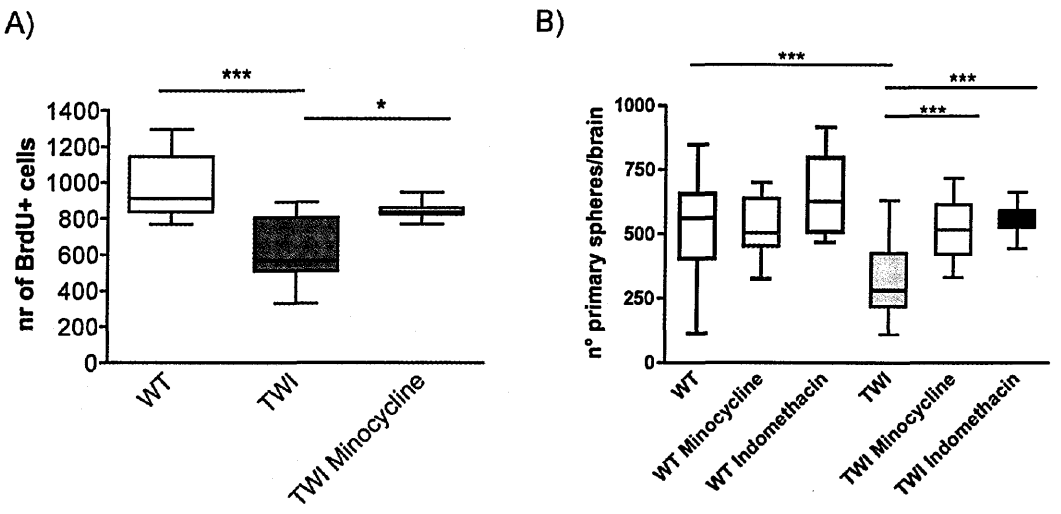

Figure 19. Assessment of *in vivo* and *in vitro* proliferation of SVZ stem/progenitor cells after anti-inflammatory treatments. (A) Quantification of the total number of BrdU+ cells in the SVZ in WT and Twi (Minocycline-treated and UT) mice (n=6) *** $p \leq 0.001$; * $p \leq 0.05$ (one-way ANOVA with Bonferroni post-test). (B) Number of primary neurospheres generated from the SVZ of untreated and drug-treated WT and Twi mice. Primary cells from the SVZ of treated mice (n= 9 for Minocycline; n=6 for Indomethacin) produces comparable numbers of neurospheres compared to those generated by WT SVZ, both UT (n=18) and treated (n=6 for both drugs) *** $p \leq 0.001$ (one-way ANOVA with Bonferroni post-test). Numbers are expressed as mean ± SEM.

Overall, these results suggest that anti-inflammatory treatment started at the asymptomatic stage is able to modulate the inflammatory status characterizing the Twi environment during the disease progression. The modulation provided by two different anti-inflammatory drugs, although far from rescuing the toxic Twi environment back to the non-inflammatory physiological environment, is sufficient to clear intracellular storage to ameliorate pathology, as detected at PND40, resulting in overall improved survival of treated Twi mice (Fig.21). Importantly, the anti-inflammatory treatment results in partial recovery of the functional defect affecting stem/progenitor cells in the SVZ niche.

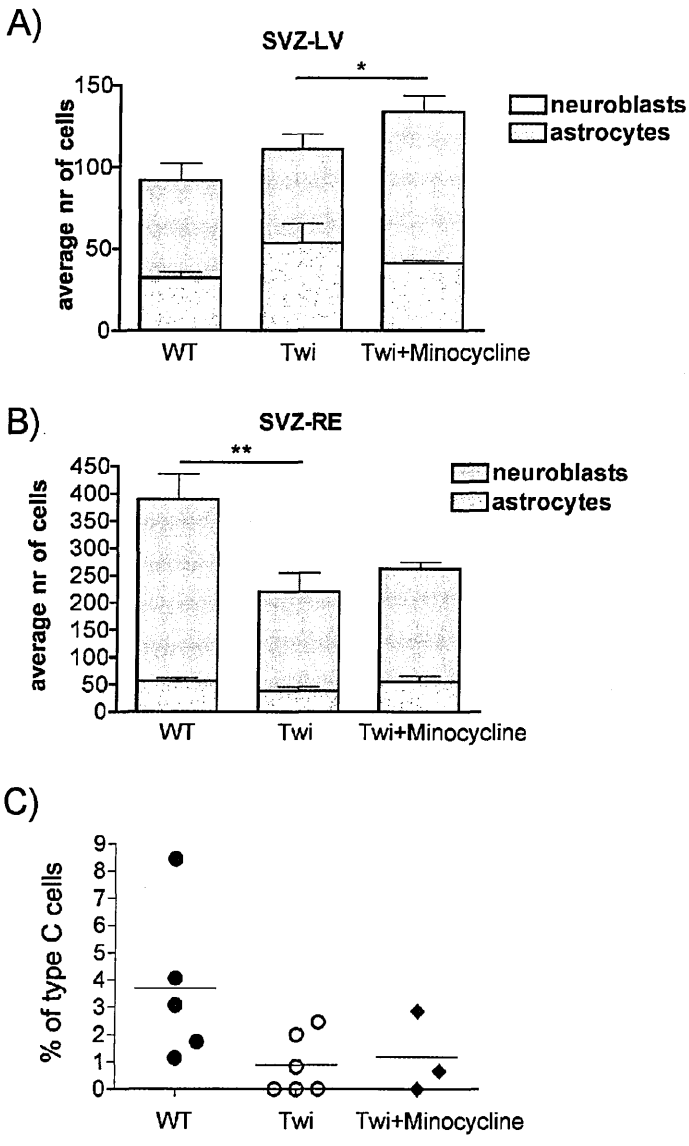

Figure 20. Ultrastructural analysis of the SVZ-LV and SVZ-RE regions of Minocycline-treated mice.

Electron microscopy analysis on the SVZ of PND40 WT and Twi mice, treated with anti-inflammatory drug. Quantification of the number of astrocytes and neuroblasts in the SVZ-LV (A) and SVZ-RE (B). (C) Percentage of type C cells in SVZ-LV. ** $p \leq 0.01$; * $p \leq 0.05$ (two-way anova with Bonferroni posttest). Numbers are expressed as mean ± SEM (n=3).

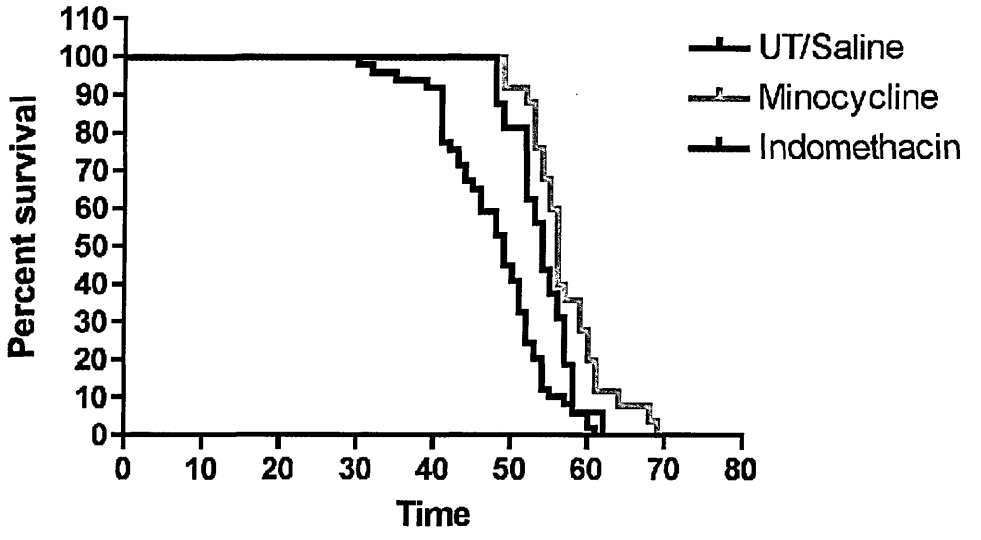

Figure 21. Prolonged survival of Twi mice treated with anti-inflammatory drugs
Kaplan-Meier survival curves of Minocycline- and Indomethacin-treated Twi mice are significantly different from the survival curve of untreated (UT)/Saline-treated Twi mice.
Average survival:
UT: 49 days (n=49)
Minocycline treated: 56 days (n=25)
Indomethacin treated: 54 days (n=16).
Log-rank test: Minocycline-treated vs UT: $p \leq 0.0001$
Indomethacin-treated vs. UT: $p \leq 0.0089$
Minocycline vs. Indomethacin: ns

4.3. Evaluation of the cell autonomous component affecting the SVZ neurogenic niche in Twi mice

The data shown so far underlie the relevance of the environmental contribution in determining the functional impairment in the SVZ niche, which is mainly evident at the latest stages of the pathology. Nevertheless, they do not conclusively rule out a direct contribution of the lysosomal enzyme GALC in maintaining a functional neurogenic niche during adulthood and, most important, during early post-natal CNS development.

In order to distinguish between the effect of the toxic environment and a potential cell-autonomous defect due to the genetic GALC deficiency, I assessed the function of the SVZ

compartment in neonatal/early postnatal Twi mice (PND2 and PND10). Indeed, despite no detectable up-regulation of inflammatory component was present in CNS tissues at these ages, WB data indeed suggested the presence of on-going astrogliosis and cell death. I therefore applied two *ex vivo* models (NSA and primary cultures) in order to evaluate the ability of self-renewal, proliferation, differentiation and maturation of the SVZ-derived stem/progenitor cell population.

4.3.1 Analysis of self-renewal, proliferation and differentiation

The NSA assay (Fig.22) showed a significant decrease in the number of primary spheres retrieved from the SVZ of Twi mice at PND2 and PND10 with respect to WT littermates, indicating impairment in clonogenic ability.

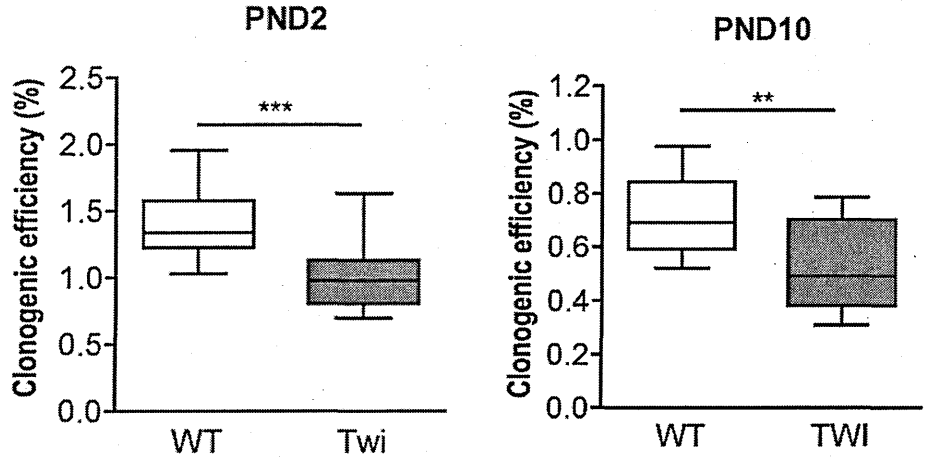

Figure 22. Impaired clonogenic efficiency in stem/progenitor cells derived from the SVZ of asymptomatic mice.
NSA assay was performed to evaluate the clonogenic efficiency of primary cells obtained from PND2 and PND10 WT and Twi mice (number of spheres generated/cells plated x100) *** $p \leq 0{,}0001$; ** $p \leq 0{,}001$ (Mann Whitney test) (n=4 experiments, 14-16 mice). Values are expressed as mean ± SEM

In order to better assess the proliferative ability of SVZ-derived progenitors and their multipotency I established primary mixed cultures from the SVZ of PND2 WT and Twi mice (Gritti et al., 2009). I plated freshly isolated primary cells in adhesion, in a growth factor-free

medium containing 2% foetal bovine serum. Two weeks after plating the cell type composition was assessed using immunofluorescence analysis. I evaluate the lineage commitment and differentiation using Tuj-1, O4 and GFAP antibodies for neuronal, oligodendroglial and astroglial cells, respectively (Fig.23A). I measured the immunopositive area for the different markers and I expressed the results normalised on the total nuclear area. A significant decrease of immunopositive areas for Tuj-1 and O4 was observed in Twi-derived primary cultures compared to the WT counterpart (fig. 23B,C). In contrast, no difference was observed in GFAP immunoreactivity (Fig.23D). In order to avoid possible false readout due to heterogeneity in cell density, I compared the total nuclear area and the total number of nuclei (by direct cell counts) in the different cultures, showing no significant differences between WT- ad Twi-derived cultures. Moreover, I confirmed the data obtained by area measurement with the data obtained with direct cell counts of neuronal progenitors (Tuj-1+) (Fig.24A) and oligodendrocyte precursors (O4+) (not shown)

4.3.2 Evaluation of proliferative/apoptotic markers

With the purpose of better understanding if the lower amount of neural and oligodendrocyte precursors is due to a defect in cell proliferation vs. cell death, I performed a time course analysis, counting the cells expressing the proliferation marker Ki67 and the apoptosis marker (Cleaved Caspase 3; CASP3). I did not observe any differences in the proliferative ability (not shown), whereas I detected an overall increase in cell death in Twi-derived primary cultures as compared to the WT counterpart (Fig. 24B). Interestingly, the majority of CASP3+ was comprised within the population of Tuj-1+ cells (Fig.24C, D). These data suggest that GALC deficiency affects the clonogenic and the proliferation ability of stem/precursor cells in the SVZ of asymptomatic mice. These progenitors showed altered differentiation capacity towards the neuronal and oligodedroglial lineage and are more susceptible to apoptotic cell death.

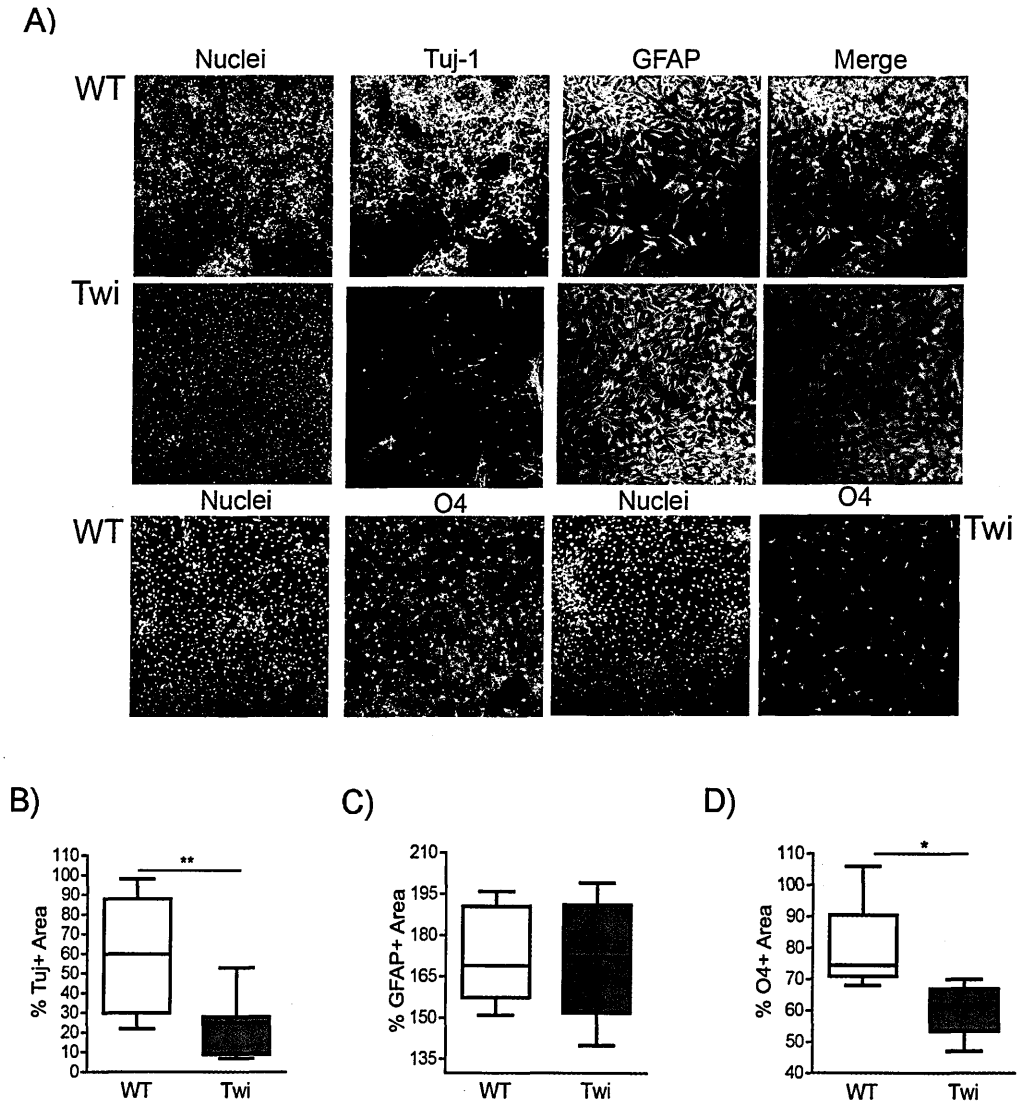

Figure 23. Cell type composition in primary cultures established from the SVZ of PND2 mice.

Analysis of multipotency and lineage commitment was performed by immunofluorescence, using antibodies to Tuj-1, GAFP and O4 for neurons, astrocytes and oligodendrocytes, respectively. (A) Representative images for the different lineage markers. (B-D) Immunopositive area (marker+ area/nuclei+ area x100) for the neuronal (B), astrocyte (C), oligodendroglial (D) antigens. Images were acquired by three-laser confocal microscope-Radiance 2100, BioRad; fluorescent signals from single optical sections were sequentially acquired and analysed by Adobe Photoshop CS software; magnification 20x. 9 fields for coverslip were taken and images were analysed for area measurements by ImageJ software (n=4 independent cultures, n=5-7 coverslip).

** $p \leq 0{,}008$. * $p \leq 0{,}02$ Mann Whitney test.

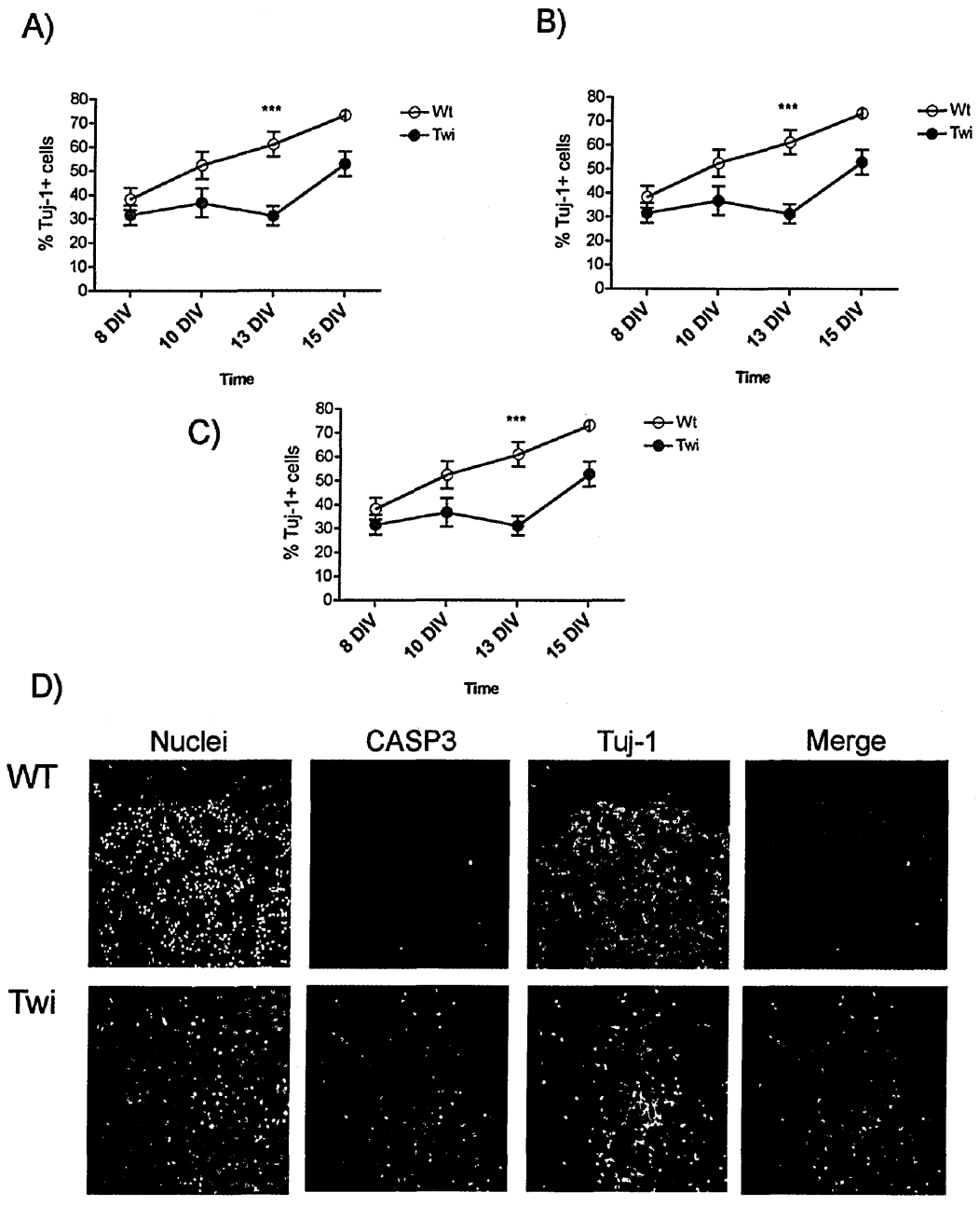

Figure 24. Time course analysis of SVZ derived primary cultures.
Primary cultures were analysed at 8,10,13 and 15 days in vitro (DIV) for the presence of Tuj-1 (neurons) and apoptotic cells (CASP3). (A) The number of Tuj-1+ cells increased as function of time in both WT and Twi-derived cultures, but the overall number of neurons is lower in mutant cultures at every time point considered. (B) The number of CASP3+ cells is higher in Twi with respect to WT cultures. C) The majority of CASP3+ cells is comprised within the Tuj-1+ population in Twi-derived cultures (n=2 independent cultures, counted at least 5000 cells/exp) *** $p \leq 0,01$; * $p \leq 0,05$ (two-way anova with Bonferroni posttest). Data are expressed as mean ± SEM. (D) Representative pictures of DIV13 primary cultures from the SVZ of Twi and WT mice. Images were acquired by three-laser confocal microscope-Radiance 2100, BioRad; fluorescent signals from single optical sections were sequentially acquired and analysed by Adobe Photoshop CS software; magnification 40x.

4.4. Analysis of the GALC metabolic pathway

Several sphyngolipids such as Cer, S1P and other molecules involved in the galactosylceramide synthesis and degradation are considered "bioactive lipids", strictly interconnected in a complex metabolic pathway. Unbalance of their mutual levels, which undergo tight regulation in physiological condition, might act directly or through activation of important signalling pathways to deregulate NSC functions. Thus, I sought to analyse whether GALC deficiency may result in unbalanced glycosphingolipid levels in our system.

4.4.1 Evaluation of lipid content in Twi brain

In order to evaluate the brain lipidic composition, I performed mass spectrometry to detect Cer, Cerebrosides (Glu/GalCer and LacCer), Sph and S1P in tissue samples from PND40 mice (total brain-TB and SVZ). As previously, I choose to perform this analysis on tissue samples from the fully symptomatic Twi mice, to verify end-point alterations and to match these results with *in vivo* and *in vitro* functional experiments.

The most abundant lipid species detected in both total (TB) and SVZ brain tissues were Gal/GlcCer (Fig.25A) Galactocerebrosides are typically found in neural tissue but with currently available mass spectrometry technique, these species cannot be separated from glucosylceramides. Levels of Gal/GlcCer and Cer s were similar in TB and SVZ samples of both WT and Twi mice (Fig.25A). In contrast LacCer levels were about 10-fold higher in samples obtained from Twi mice as compared to WT (Fig.25C). The LacCer (d18:1/18:0) was shown to be the most abundant LacCer species, with levels that were 20-fold higher in SVZ samples of Twi mice as compared to WT littermates (Fig.25D). S1P and sphinganines were detected in lower concentrations in TB and SVZ samples of Twi mice as compared to WT mouse brain (Fig. 25B). Also, it should be noted that levels of S1P were close to the lower detection limit and the levels of sphinganine-1-phosphate remained under the limit of detection. The elevated LacCer levels might be due to the broad specificity of GALC, which can metabolise also this molecule. In this study,

the sphingoid bases were generally detected in lower amounts in Twi mice, which could be explained by inhibition of the *de novo* sphingolipid synthesis due to the accumulating LacCer species.

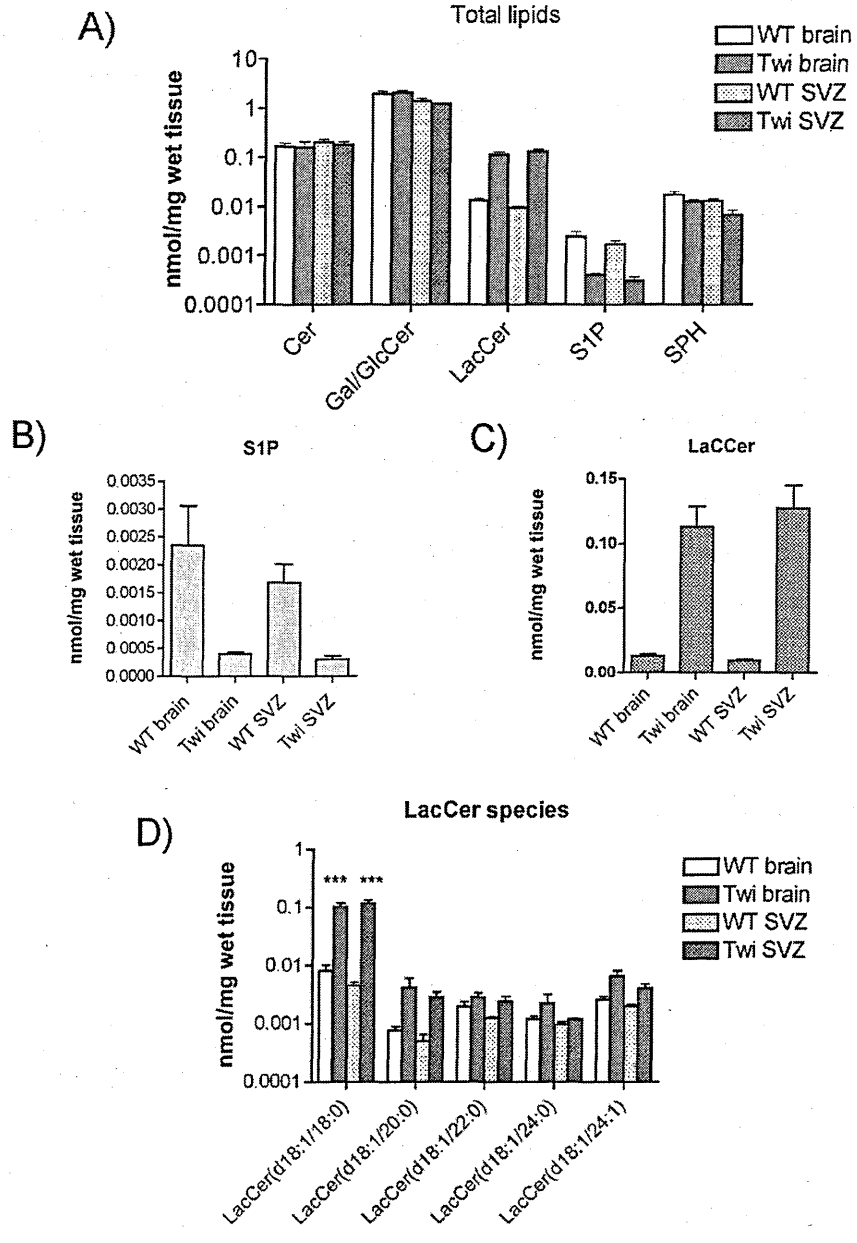

Figure 25. Mass-spectrometry analysis of brain lipid content

Total brain and SVZ tissues (n=2 pool of 4 mice/each) of PND40 WT and Twi mice were subjected to mass-spectrometry. (A) Quantification of the lipid species. (B) Decreased amount of S1P characterize Twi brains and SVZ tissues with respect to the WT counterparts. (C) Increased amount of LacCer in Twi brain and SVZ tissues compared to WT tissues. D) The increased LacCer amount is due prevalently to short-chain lipids. *** $p \leq 0{,}001$; * $p \leq 0{,}05$ (two-way anova, bonferroni post-test).

4.4.2 Evaluation of lipid content in SVZ-derived NSC

To assess the lipid component in the *ex vivo* SVZ-derived cells I used a different assay that allows to visualize the lipid steady state composition. I performed a pulse of radiolabelled sphigosine (SPH) (2 hours) followed by a 48-hour chase on NSC cultures derived from the SVZ of PND2 and PND40 WT and Twi mice. This labelling protocol is useful to check the distribution of SPH at steady state and to monitor its catabolic pathway. In the aqueous phase, where S1P and gangliosides are detected, I did not observe any changes between Twi and WT lipid pattern: unfortunately S1P is not detectable with this technique and gangliosides are expressed at low level in NSCs (Fig.26A). The organic phase revealed an increase in LacCer and Glu/GalCer in Twi samples of both ages with respect to their WT counterparts (Fig.26B). Quantification of the radioactivity revealed that the increment in the Glu/GalCer is similar for both ages, whereas LacCer is higher in NSCs derived from PND40 mice (fig.26C).

Thus, the analysis of the lipid pattern in both tissue samples and SVZ-derived NSCs, suggests the presence of unbalanced sphingolipid levels, with substrate accumulation (LacCer) and S1P decrease. It is interesting to note that the lipid pattern is similar in total brain and SVZ tissue, indicating that the neurogenic SVZ niche share the biochemical feature of the surrounding environment.

4.4.3 Analysis of S1P pathway

The different amount of S1P in Twi samples compared to WT prompt us to evaluate more in depth the S1P pathway. To test whether there could be an impaired signalling response in Twi mice, I first tested the presence of S1PRs in Twi and WT brain tissue and NSCs. I performed RT-PCR on total brain tissues from PND10 and PND40 mice and on NSC cultures derived from the SVZ of PND40 Twi and WT mice. The transcripts for the five receptors were present in all the samples, although with different levels of expression (Fig.27A, B).

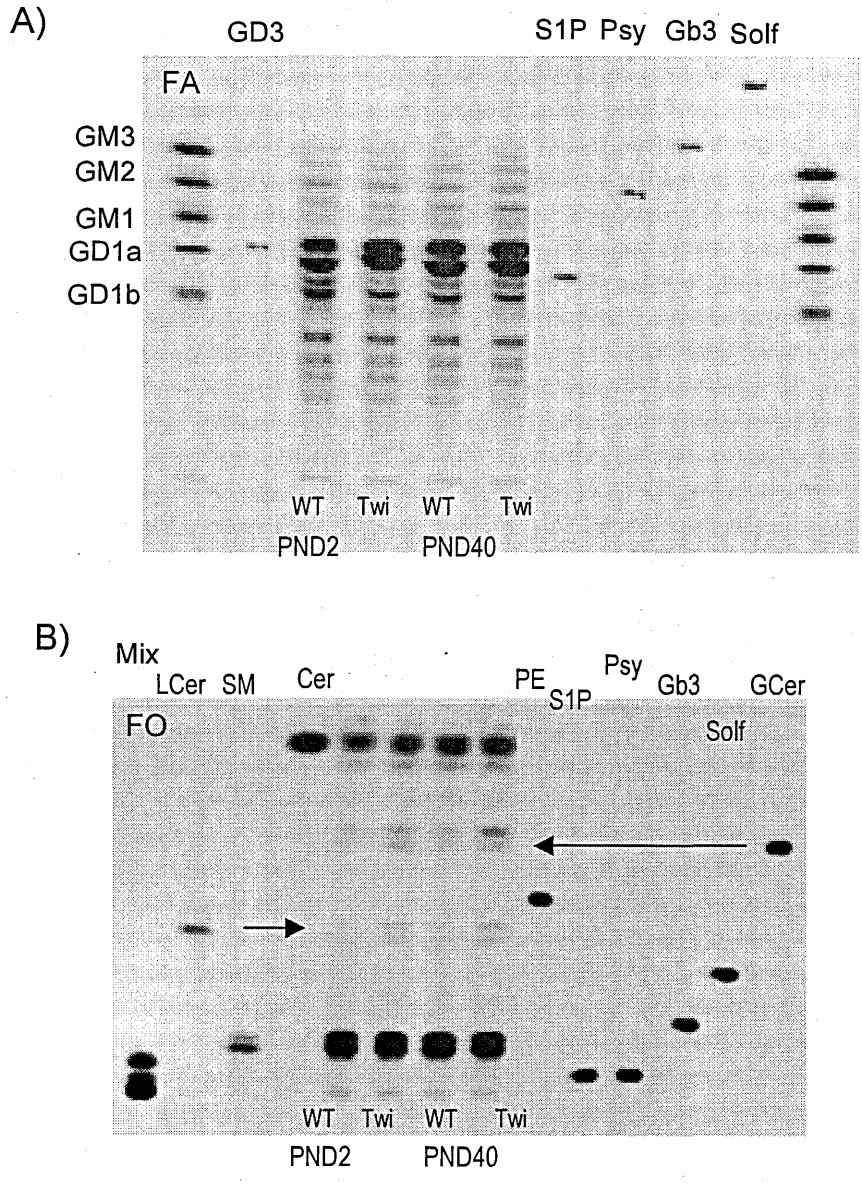

	PND2		PND40	
OP	**WT**	**Twi**	**WT**	**Twi**
Cer	25,9%	24,4%	28,2%	26,3%
Gal/GluCer	**4,2%**	**8,1%**	**4,4%**	**8,6%**
LacCer	**2,0%**	**2,9%**	**1,7%**	**4,1%**
Gb3	1,6%	1,9%	1,8%	1,5%
SM high	29,9%	26,4%	30,0%	30,9%
SM low	36,5%	36,4%	33,9%	28,6%
Total	**100,0%**	**100,0%**	**100,0%**	**100,0%**

Figure 26. Analysis of the lipid content in NSCs.
Thin layer chromatography after pulse-chase of labelled SPH on SVZ NSCs derived from WT and Twi mice at PND2 and PND40. (A) Aqueous phase showed similar gangliosides pattern between WT- and Twi-derived NSCs. (B) Organic phase (OP) showed increased amount of LacCer and Glu/GalCer in Twi NSCs compared to WT NSCs. (C) Quantification of the TLC bands showed in the organic phase.

While in brain tissues all the transcripts were similarly represented, regardless the post-natal age considered, S1P-R1 and S1P-R2 mRNA were most abundantly expressed in NSCs, reaching levels comparable to those found in CNS tissues. However, I did not detect any particular difference in expression levels between Twi and WT in all the samples analysed, possibly due the redundancy of these receptors (Fig.27A).

Nonetheless, I decided to test if there could be an alteration in the downstream signalling pathway. I performed western blot (WB) analysis on total brain tissue samples and NSCs from WT and Twi mice at PND10 and PND40 (Fig.27C). I detected a strong decrease in P-ERK in brain tissues derived from Twi mice, thus indicating a possible down-regulation in pathways in which ERK is involved, whereas no clear difference where detected in NSCs. These results in NSCs might be explained by the fact that the reduced pro-survival/pro-proliferative stimuli given by S1P might be overrun by the mitogen-enriched culture medium, which could trigger the activation of compensatory pathways.

4.4.4 Analysis of the expression of enzymes involved in GALC metabolic pathway

With the intent of evaluating the potential modulation of the enzymes involved in the GALC metabolic pathway, I performed gene expression analysis in total brain extracts and NSCs derived from the SVZ of PND40 WT and Twi mice (Fig.28A). I considered the following enzymes (see also Fig.2):

- ARSA (Arylsulfatase A)
- CST (Cerebroside sulfotransferase; sulfatide synthase)
- Gal-TIII (Galactosyltransferase III; galactosyl-ceramide synthase)
- PSAP (Prosaposin)
- Glc-T (Glucosyltransferase; glucosylceramide synthase)
- Gal-TI (Galactosyltransferase I; lactosylceramide synthase)

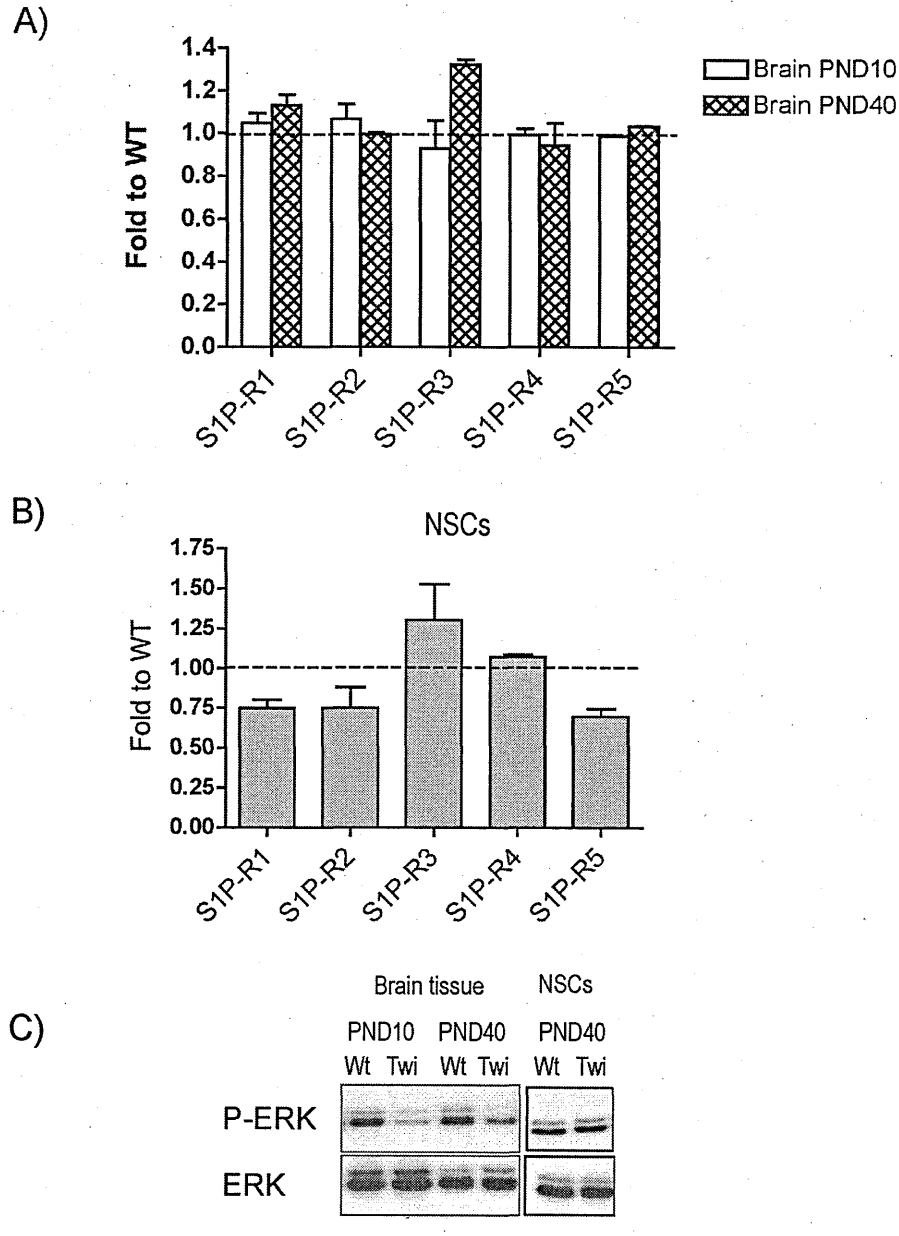

Figure 27. Signalling of S1P: S1P receptors and downstream pathway

(A) Semi quantitative RT-PCR was performed on tissue sample from PND10 and PND40 WT and Twi mice and on NSCs (B) derived form PND40 WT and Twi SVZ (n=3). No significant difference in S1PRs expression is observed between Twi and WT samples. mRNA relative expression is obtained using β-actin gene as normaliser and expressed as arbitrary unit. (C) Western blot analysis for the protein phospho-ERK is normalised with its non-phosphorylated counterpart (n=3).

- SphK 1 and 2 (Sphingosine kinase 1 and 2)

- S1P-Lyase

- S1P-Phosphatase

- NEU3 (Sialidase)

- SAT1 (Sialyl transferase)

Semi-quantitative RT-PCR showed increased expression levels of Galt-III and SphK1 in Twi samples compared to WT. GalT-III is the synthase that works in the opposite direction of GALC. Thus, it is possibly affected directly by GALC deficiency. Low levels of S1P could induce instead up-regulation of SphK1 expression.

To assess if increased gene expression had a functional correlation, I performed an enzyme activity assay for SphK1 on SVZ-derived NSCs (Fig.28B). I observed increased activity in Twi-derived NSCs cells with respect to WT, thus indicating a strong correlation between mRNA expression and protein activity.

Alteration in lipid content, transcript expression and activity of enzyme involved in the GALC pathway not only in brain tissues, but also in *ex vivo* isolated NSCs (free of tissue-derived environmental inputs) strongly suggest that GALC absence might impact on critical cell processes in neural cells, including stem/progenitor cells in the neurogenic niches, at the very early stages of the disease, before the overt cellular storage. The build up of storage, however, triggers neuroinflammation during the progression of the disease, which likely contributes to worsen the functional cell impairment, resulting in the extensive tissue damage that is typical of the latest stages of the disease.

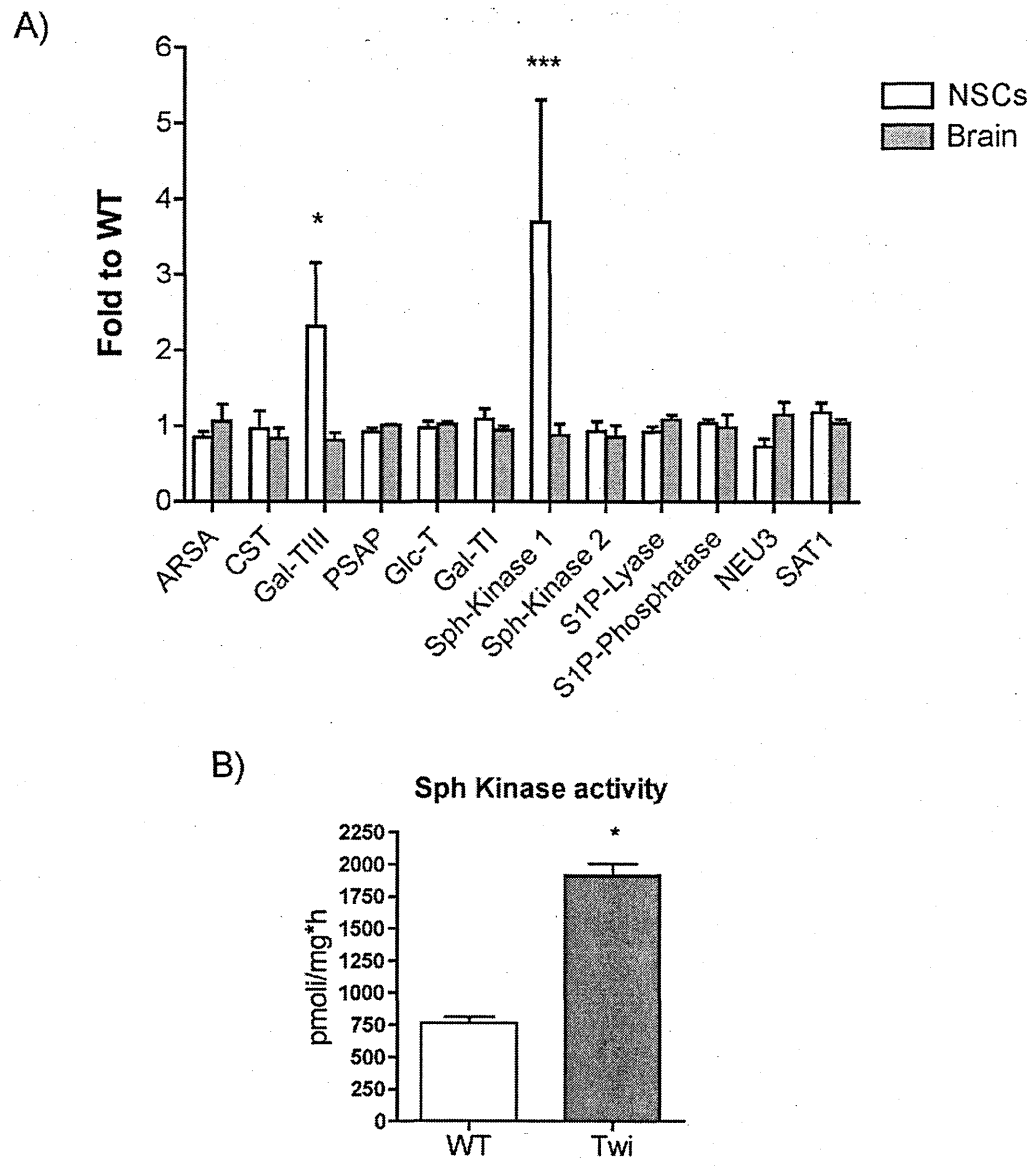

Figure 28. Analysis of enzymes present in the metabolic pathway of GALC

A) Semi quantitative RT-PCR were performed on total brain tissues from WT and Twi PND40 mice and on NSCs derived from SVZ of PND40 WT and Twi mice (n=3). SVZ derived Twi NSCs showed significant up-regulation of Gal-TIII and Sph-kinase I enzymes compared to WT derived NSCs. No significant differences are observed in tissue samples. Data are expressed as fold increase to WT values; normalisation was performed on β-actin gene as reference. Data are expressed as mean ± SEM *** $p \leq 0.001$; * $p \leq 0{,}05$. two-way ANOVA with Bonferroni post-test. (B) Sph kinase enzyme assay showed increased activity in NSCs derived from Twi mice. * $p \leq 0{,}05$ (Mann Whitney test) (n=2).

5 DISCUSSION

GLD is a severe genetic neurodegenerative Lysosomal Storage Disorder (LSD) with an urgent medical need. The only available treatment for GLD patients so far is allogeneic haematopoietic stem/progenitor cell transplantation (HCT) (Orchard and Tolar, 2010). This procedure is effective only if performed very early after birth or in asymptomatic patients (Escolar at al., 2005), and it is still accompanied by severe side effects. In addition, long-term follow-up data report that treated infants preserve cognitive function but still develop some degree of motor disability, which ranges from mild to severe (Escolar at al., 2005).

Recognition that defects in postnatal neurogenesis and neural stem cell compartments might be involved in the pathogenesis or maintenance of CNS disorders, including LSD (Curtis et al., 2003a; Yang et al., 2006), gives reason for considering NSC-based approaches as a therapeutic perspective. Yet, our knowledge concerning the mechanisms regulating the physiology of these neurogenic regions and of the resident stem cell compartments remains incomplete, particularly as regards their behaviour in the brain during the onset and progression of a neurodegenerative condition. This lack of knowledge largely hampers the possibility to fully exploit NSC therapeutic potential in the context of exogenous transplantation, as well as in the more fascinating option of endogenous stem/progenitor cell recruitment. In fact, an altered niche microenvironment, might negatively affect neurogenic and gliogenic processes during pre-natal and early post-natal CNS development. In this thesis I investigated the functional, biochemical and molecular properties of the neurogenic subventricular zone region and of SVZ-derived neural stem cells of Twitcher mice, a relevant murine model of GLD that recapitulates the human pathology, during the onset and progression of the disease, in comparison with non-affected littermates (controls). I showed impairment in the organization and function of neurogenic niches not only in symptomatic Twi mice (confirming the role of inflammation in this process) but also in early post-natal

(asymptomatic) animals, strongly suggesting a role of GALC in regulating neurogenesis and gliogenesis during CNS development. Our studies shed light on the basic biology of NSCs in health and disease, raising important points as regard the pathophysiology of leukodystrophies, possibly allowing understanding obstacles that need to be addressed for the future development of clinical gene/cell therapy.

Alterations in the neurogenic compartment of symptomatic Twi mice

Demyelination and tissue damage that characterizes the CNS environment in GLD patients and animal models is classically thought to be the consequence of tissue storage, psychosine accumulation and neuroinflammation (Suzuki, 1998, 2003). However, clinical observations indicate that functional impairment, demyelination and possibly neurodegeneration are present in GLD-affected newborns (Escolar et al., 2009). This suggests that GALC deficiency might result in impairment of neurogenesis, gliogenesis and myelination during pre-natal or early post-natal age CNS development, long before the disruption of myelination driven by the overt CNS tissue storage and inflammation, but this issue has been poorly addressed in pre-clinical studies so far. I took advantage of the Twi mouse model to test the challenging hypothesis that GALC deficiency might alter the neurogenic SVZ niche during the early CNS development, possibly affecting neurogenic and gliogenic processes and resulting in subtle but likely irreversible damage in CNS organization and function. Indeed, our *in vivo* and *in vitro* data support this hypothesis.

I report a significant decrease in cell proliferation within the SVZ neurogenic region as a function of disease progression. This impairment mainly affects the neuroblast compartment, which also appears to be highly impaired in its morphology and organization, as assessed by both classical ultrastructural analysis and by immunofluorescence on whole mounts of the lateral ventricle walls, a technique that allows appreciating the three-dimensional organization of the SVZ cell types, rendering a comprehensive, en-face view of this germinal region that is not possible using classical sectioning techniques for histological analysis (Doetsch and Alvarez-Buylla, 1996; Mirzadeh et al., 2010; Mirzadeh et al., 2008).

While these observation indicate a reduced neurogenic ability in Twi mice compared to age matched WT mice at the late stage of the disease, they do not allow to appreciate the potential involvement of the stem/transit amplifying cell population (type B and C cells) to this process. Due to the lack of univocal phenotypic markers for these cell types I resorted to move to *ex vivo* functional assays that better allow monitoring the proliferation and self-renewal of these cell population. Decreased numbers of SVZ-derived primary neurospheres obtained from Twi mice compared to WT littermates using the standard NSA and the modified NCFC assay (which positively correlates the size of the newly formed spheres to the stem properties of the founder cells) indeed confirmed *in vivo* data, indicating that not only committed progenitors but also the more immature stem/progenitor cell populations were affected in their proliferative and self-renewal capacity.

Inflammation contributes to the SVZ functional impairment at the late stages of the disease.

GLD is characterized by a severe inflammatory component both in human patients and in Twi mouse (Luzi et al., 2009; Wenger, 2000). It is known that inflamed brain microenvironment triggers and sustains a non-cell autonomous dysfunction of the SVZ stem cell compartment (Mathieu et al., 2010; Russo et al., 2011). In particular, the chronic inflammation present in a murine model of Multiple Sclerosis (EAE mice) affects both the proliferation and the migration of neuronal progenitors (Pluchino and Martino, 2008b). This functional impairment is rescued following *ex vivo* isolation and long-term culturing of the SVZ-derived stem/progenitor cells in vitro using the NSA, thus indicating a strong non-cell autonomous cell component underlying the defect. This aspect might challenge the potential efficacy of proposed therapies aimed at mobilizing endogenous precursors in chronic inflammatory brain disorders. On the other hand, data in the literature showed that inflammatory signals could recruit specifically transplanted and possibly also endogenous cells in areas of tissue damage, thus contributing to therapeutic benefit (Einstein et al., 2003; Pluchino and Martino, 2008a). Thus, timely modulation of inflammation, also by enhancing/inhibiting recruitment of specific populations of inflammatory cells, appears to

be a key issue to be considered in the developing of cell-based therapies for neurodegenerative diseases (Martino and Pluchino, 2006; Schwartz and Brick, 2008).

Previous results as well as results of this work indicate a strong up-regulation of pro-inflammatory molecules in the Twi brain as a function of disease progression. I clearly show that this up-regulation consistently starts between post-natal days 10 and 20, corresponding to pre/early symptomatic stages of the disease, indicating that inflammation might contribute to the development of the pathology besides being a consequence of the extensive tissue damage found at latest stages of the disease.

In this perspective a chronic anti-inflammatory treatment started at the asymptomatic stage could help to decrease the burst of inflammatory molecules and rescue function. I tested this hypothesis using Minocycline, a tetracycline analog able to cross the BBB and Indomethacin, a more classic anti-inflammatory drug. Indeed, treatment with both drugs resulted in down-regulation of several pro-inflammatory molecules. This action was likely underlying the moderate improvement that we saw when scoring the pathology hallmarks in the brain of treated Twi mice, such as monocyte infiltration, microglia activation and storage. Most important, the anti-inflammatory treatment was able to delay the onset of symptoms and to prolong lifespan (+5/7 days), in line with previous results reported in a milder murine model of GLD, the *trs* mice (Luzi et al., 2009). The extent of the therapeutic benefit provided by anti-inflammatory treatment was comparable to that provided by systemic and intrathecal administration of the recombinant enzyme (Lee et al., 2005; Lee et al., 2007b). These results further indicate the potential relevance of the inflammatory compartment as complementary/additional therapeutic target for GLD and similar LSDs.

Importantly, our data demonstrate that the anti-inflammatory treatment is effective in rescuing SVZ-derived stem/progenitor cell functional impairment in fully symptomatic Twi mice, both *in vivo* (number of BrdU+ cells) and *in vitro* (clonogenic activity), further confirming the strong non-cell autonomous contribution of the inflammatory environment on the neurogenic compartment at the latest stages of the disease. Nevertheless, these data did not exclude a cell-

autonomous contribution to the functional impairment, as also suggested by the very limited rescue in the SVZ ultrastructure and neuroblast number and morphology assessed by EM analysis.

Is there a cell autonomous component underlying NSC/progenitor functional impairment?

Several works describe functional defects in NSCs or progenitors derived from animal models of LSDs. Reduction in self-renewal activity by abnormal nitric oxide-mediated signalling was described in NSCs derived by NPC1-deficient mice (Kim et al., 2008). Also, defects in cholesterol traffic and neuronal differentiation are reported in NSCs derived from the same animal model (Kim et al., 2007). Thus, these studies suggest that the neurogenic impairment that I detected in Twi mice could be an intrinsic feature of the pathology and not only a consequence of a toxic environment.

In order to exclude the contribution of inflammation I tested the functional features of NSCs derived from the SVZ of newborn and pre-symptomatic Twi mice (post-natal day 2 and 10). *In vivo* BrdU labelling showed similar numbers of proliferating cells in Twi and WT mice at this ages, likely reflecting the high proliferation rate of cells in the developing SVZ brain at these ages (Peretto et al., 2005) that might mask potential subtle differences. Indeed, moving to the *ex vivo* NSA model, I detected significant lower number of newly formed primary neurospheres obtained from Twi mice as compared to WT mice (at both ages), strongly indicating that the impairment in stem/progenitor cell proliferation/self-renewal is already present in cells in the early post-natal SVZ niche.

Multipotency and differentiation potential are the other functional features that characterize stem/progenitor cells in addition to self-renewal and proliferation. I decided to investigate these features using mixed neuronal/glial primary cultures established from SVZ. The advantage of these cultures over the neurosphere cultures is that they mirror the cell type composition of the tissue from which they are established (Gritti et al., 2009) and allow monitoring cell differentiation/maturation over time. Evaluation of the cell type composition performed after terminal differentiation (15 days after plating) using specific cell lineage markers indicated that

SVZ-derived primary cultures from Twi mice are characterized by lower numbers of neurons and oligodendrocytes as compared to WT cultures. Defects in progenitor cell proliferation or survival, as well as delayed differentiation might be responsible for this result. Indeed, a time course analysis indicated that the lower number of neurons and oligodendrocytes in Twi cultures are due to increased apoptosis in the respective progenitor cell types. These observations indirectly support the results of western blot analysis showing increased expression of cleaved caspase 3 in brain tissues of Twi mice at the same ages.

Although this *in vitro* model is a simplified way to look at the SVZ maturation, still it allowed us highlighting impairment in primary SVZ cells due to cell intrinsic features, excluding major environmental influences related to inflammation. As reported in literature, oligodendrocytes are the most affected population by the pathology due to accumulation of Psy (Giri et al., 2008; Giri et al., 2006; Zaka and Wenger, 2004), and indeed I found decreased proportion of these cell type in our model. Interestingly, in line with the phenotype observed in our *in vivo* experiments, I observed also a strong decrease in cells of the neuronal lineage. Psy quantification in the different cell types would be useful to determine whether accumulation of this toxic substrate occur also at this early time point, inducing cell death of both population.

These results support our initial hypothesis that an altered niche microenvironment during early CNS development might negatively affect neurogenic and gliogenic processes. It would be interesting to evaluate whether loss of neuronal and oligodendroglial progenitors also occurs in non-neurogenic areas that are however characterized by post-natal cell proliferation, such as the cerebellum. This would further account for the functional impairment observed in patients before the peak of CNS tissue storage and inflammation (Escolar et al., 2009). This cell-autonomous defect could support the clinical inefficacy of therapies on symptomatic patients but could also explain the poor improvement of early treatment in asymptomatic babies, opening important issues regarding the time of treatment, with strong implication for therapies.

Cell autonomous defect: role of sphingolipids.

I measured up-regulation of markers of astrogliosis (GFAP) and activated microglia (Iba-1) in CNS tissues isolated from neonatal and early post-natal Twi mice, suggesting that the inflammatory machinery is activated in the Twi CNS environment at this early stages despite the absence of up-regulated pro-inflammatory markers. Storage in post-natal and fetal brain resulting from genetic deficiency has been previously described (Ida et al., 1994; Suzuki, 1998, 2003; White et al., 2009) and is likely to impact on critical cell functions before reaching the threshold required to trigger massive recruitment of the inflammatory machinery. Indeed, Psy accumulation before disease onset is low and below the threshold needed to kill oligodendrocyte but sufficient to affect the neural stem/progenitor cells compartment and possibly the structure of axons (Castelvetri et al., 2011; Olmstead, 1987).

GALC is a key enzyme in the catabolism of sphingolipids that are enriched in myelin sheets. The role of sphingolipids has been studied for many years in neurons and glia as well as in other tissues. Ceramide, the first product of GALC, can be considered as a metabolic hub, since it occupies a central position in the biosynthesis and catabolism of sphingolipids. Moreover, Cer and other molecules of this pathway, such as Sphingosine and Sphingosine-1-Phosphate, are considered "bioactive sphingolipids" since they act as signals regulating a vast number of cellular processes, including survival, proliferation, migration, differentiation and response to growth factors(Hannun and Obeid, 2008).

Interestingly, I detected increased amount of LacCer and Glu/GalCer in both tissues and cells derived from brain and SVZ tissues of Twi neonatal and postnatal mice compared to WT littermates, indicating that these molecules are likely substrates of GALC and that they are accumulating in Twi brains and neural stem/progenitor cells early in CNS development. LacCer is a signalling molecule implicated in several cellular processes, and changing in its levels could alter cellular response such as proliferation, adhesion and migration (Chatterjee and Pandey, 2008). Interestingly, it is also an important second messenger in neuroinflammation (Won et al., 2007). Moreover, I have to consider that besides accumulating in lysosomes, these lipids might

accumulate in the plasma membrane of cells, altering the balance of lipid composition and possibly affecting critical microdomains, such as lipid rafts (White et al., 2009). This might results in detrimental effects, both in neurons, in which membrane plasticity influences axon elongation and synapse formation (Ibanez, 2004; Niethammer et al., 2002), and in oligodendrocytes during myelination (Kramer et al., 1999), both processes being tightly regulated during early CNS development.

In addition to the vast number of processes that sphingolipids are associated with, further levels of complexity arise from the metabolic interconnection of bioactive lipids. It has been suggested that the balance between survival and death of many cell types may be affected by the equilibrium between the intracellular levels of inter-convertible sphingolipids such as Cer and S1P. Enzymes that either produce or degrade these sphingolipids control this equilibrium. Our analysis revealed a decrease amount of S1P in Twi samples, with concomitant increase of expression and activity of Sph kinase. This suggests that the cells are trying to counteract the lipid unbalance due to GALC deficiency.

Therefore, complex biochemical and signalling alterations are likely to be consequent to GALC deficiency (and possibly also to GALC over-expression that can be obtained upon gene transfer) (Visigalli et al., 2010), giving reason of the fact that variations in GALC expression levels perturb the survival and function of relevant components of stem cell niches, including the SVZ.

Conclusions

Early abnormalities of the corticospinal tract, a major motor pathway, detected by DTI were described in asymptomatic neonates affected by Krabbe disease and that may explain the motor impairment present in some patients before massive disruption of myelination by the lack of GALC. Most importantly, it might explain the clinical inefficacy of therapies on symptomatic patients as well as the poor improvement following early treatment in asymptomatic babies. These clinical observations, as well as the finding that neurodegeneration might be present in Twi mice even in the absence of demyelination (Galbiati et al., 2009) strongly suggested GALC deficiency

results in neural cell impairment before the clear onset of tissue storage and before the up-regulation of the classical pro-inflammatory signature that is typical of Twi CNS tissues. Results of our work support this concept. Also, they provide strong evidence supporting the more challenging hypothesis that the impairment in neurogenic and gliogenic processes occurring during early post-natal CNS development might be consequent to a functional impairment in neural stem cell/progenitor function in the neurogenic niches due to GALC absence. According to tables equating CNS development across species, the neonatal/early post-natal age (PND2-PND10) in mice correspond to the second trimester of fetal life in humans (Clancy et al., 2007). Thus, according to our data, GALC absence might impact on CNS functions very early in pre-natal life.

The comprehension of the role of GALC absence in the early neurogenic processes shed lights on the basic mechanism of the pathology and contributes to understand the limitations suffered by the current available treatments (HSCT) (Escolar ML, 2005; Krivit et al., 1999a), helping to develop new effective CNS-directed therapies for GLD.

7 ACKNOWLEDGEMENTS

I would like to thank my director of studies, Dr. Angela Gritti, who followed me during these years of PhD.

Prof. Timothy Cox, who supervised this work and gave me scientific and personal support.

Prof. Luca Bonfanti, for his help with electron microscopy experiments and very rich discussions.

Dr. Massimo Aureli for his precious collaboration in biochemistry.

People of Gritti and Biffi's lab for sharing this experience.

Rampoldi and Casari's lab members, especially Céline, Ilenia, Luca, Celia, Loredana for their friendship and support.

All my friends, particularly Elisa, Claudia, Beatriz and Laura, for their encouragement and for having sustained me during these years.

My family and Simone for their constant presence.

8 BIBLIOGRAPHY

Ajami, B., Bennett, J.L., Krieger, C., Tetzlaff, W., and Rossi, F.M. (2007). Local self-renewal can sustain CNS microglia maintenance and function throughout adult life. Nat Neurosci *10*, 1538-1543.

Akita, K., von Holst, A., Furukawa, Y., Mikami, T., Sugahara, K., and Faissner, A. (2008). Expression of multiple chondroitin/dermatan sulfotransferases in the neurogenic regions of the embryonic and adult central nervous system implies that complex chondroitin sulfates have a role in neural stem cell maintenance. Stem Cells *26*, 798-809.

Aldenhoven, M., Boelens, J.J., and de Koning, T.J. (2008). The clinical outcome of Hurler syndrome after stem cell transplantation. Biol Blood Marrow Transplant *14*, 485-498.

Alroy, J., Ucci, A.A., Goyal, V., and Aurilio, A. (1986). Histochemical similarities between human and animal globoid cells in Krabbe's disease: a lectin study. Acta Neuropathol *71*, 26-31.

Altman, J., and Das, G.D. (1965a). Autoradiographic and histological evidence of postnatal hippocampal neurogenesis in rats. J Comp Neurol *124*, 319-335.

Altman, J., and Das, G.D. (1965b). Post-natal origin of microneurones in the rat brain. Nature *207*, 953-956.

Alvarez, S.E., Milstien, S., and Spiegel, S. (2007). Autocrine and paracrine roles of sphingosine-1-phosphate. Trends Endocrinol Metab *18*, 300-307.

Alvarez-Buylla, A., and Garcia-Verdugo, J.M. (2002). Neurogenesis in adult subventricular zone. J Neurosci *22*, 629-634.

Alvarez-Buylla, A., Garcia-Verdugo, J.M., and Tramontin, A.D. (2001). A unified hypothesis on the lineage of neural stem cells. Nat Rev Neurosci *2*, 287-293.

Alvarez-Buylla, A., and Lim, D.A. (2004). For the long run: maintaining germinal niches in the adult brain. Neuron *41*, 683-686.

Alvarez-Buylla, A., Seri, B., and Doetsch, F. (2002). Identification of neural stem cells in the adult vertebrate brain. Brain Res Bull *57*, 751-758.

Bacigaluppi, M., Pluchino, S., Martino, G., Kilic, E., and Hermann, D.M. (2008). Neural stem/precursor cells for the treatment of ischemic stroke. J Neurol Sci *265*, 73-77.

Ballabio, A., and Gieselmann, V. (2009). Lysosomal disorders: from storage to cellular damage. Biochim Biophys Acta *1793*, 684-696.

Bandhuvula, P., and Saba, J.D. (2007). Sphingosine-1-phosphate lyase in immunity and cancer: silencing the siren. Trends Mol Med *13*, 210-217.

Bandtlow, C.E., and Zimmermann, D.R. (2000). Proteoglycans in the developing brain: new conceptual insights for old proteins. Physiol Rev *80*, 1267-1290.

Banisadr, G., Gosselin, R.D., Mechighel, P., Rostene, W., Kitabgi, P., and Melik Parsadaniantz, S. (2005). Constitutive neuronal expression of CCR2 chemokine receptor and its colocalization with neurotransmitters in normal rat brain: functional effect of MCP-1/CCL2 on calcium mobilization in primary cultured neurons. J Comp Neurol *492*, 178-192.

Barbey, F., Hayoz, D., Widmer, U., and Burnier, M. (2004). Efficacy of enzyme replacement therapy in Fabry disease. Curr Med Chem Cardiovasc Hematol Agents *2*, 277-286.

Baskin, G.B., Ratterree, M., Davison, B.B., Falkenstein, K.P., Clarke, M.R., England, J.D., Vanier, M.T., Luzi, P., Rafi, M.A., and Wenger, D.A. (1998). Genetic galactocerebrosidase deficiency (globoid cell leukodystrophy, Krabbe disease) in rhesus monkeys (Macaca mulatta). Lab Anim Sci *48*, 476-482.

Becher, B., Prat, A., and Antel, J.P. (2000). Brain-immune connection: immuno-regulatory properties of CNS-resident cells. Glia *29*, 293-304.

Ben-Yoseph, Y., Hungerford, M., and Nadler, H.L. (1980). The interrelations between high- and low-molecular weight forms of normal and mutant (Krabbe-disease) galactocerebrosidase. Biochem J *189*, 9-15.

Bergami, M., Santi, S., Formaggio, E., Cagnoli, C., Verderio, C., Blum, R., Berninger, B., Matteoli, M., and Canossa, M. (2008). Uptake and recycling of pro-BDNF for transmitter-induced secretion by cortical astrocytes. J Cell Biol *183*, 213-221.

Bhunia, A.K., Arai, T., Bulkley, G., and Chatterjee, S. (1998). Lactosylceramide mediates tumor necrosis factor-alpha-induced intercellular adhesion molecule-1 (ICAM-1) expression and the adhesion of neutrophil in human umbilical vein endothelial cells. J Biol Chem *273*, 34349-34357.

Bhunia, A.K., Han, H., Snowden, A., and Chatterjee, S. (1997). Redox-regulated signaling by lactosylceramide in the proliferation of human aortic smooth muscle cells. J Biol Chem *272*, 15642-15649.

Bielawski, J., Szulc, Z.M., Hannun, Y.A., and Bielawska, A. (2006). Simultaneous quantitative analysis of bioactive sphingolipids by high-performance liquid chromatography-tandem mass spectrometry. Methods *39*, 82-91.

Biffi, A., Capotondo, A., Fasano, S., del Carro, U., Marchesini, S., Azuma, H., Malaguti, M.C., Amadio, S., Brambilla, R., Grompe, M., *et al.* (2006). Gene therapy of metachromatic leukodystrophy reverses neurological damage and deficits in mice. J Clin Invest *116*, 3070-3082.

Biffi, A., De Palma, M., Quattrini, A., Del Carro, U., Amadio, S., Visigalli, I., Sessa, M., Fasano, S., Brambilla, R., Marchesini, S., *et al.* (2004). Correction of metachromatic leukodystrophy in the mouse model by transplantation of genetically modified hematopoietic stem cells. J Clin Invest *113*, 1118-1129.

Biffi, A., Lucchini, G., Rovelli, A., and Sessa, M. (2008). Metachromatic leukodystrophy: an overview of current and prospective treatments. Bone Marrow Transplant *42 Suppl 2*, S2-6.

Biswas, S., and LeVine, S.M. (2002). Substrate-reduction therapy enhances the benefits of bone marrow transplantation in young mice with globoid cell leukodystrophy. Pediatr Res *51*, 40-47.

Blasko, I., Stampfer-Kountchev, M., Robatscher, P., Veerhuis, R., Eikelenboom, P., and Grubeck-Loebenstein, B. (2004). How chronic inflammation can affect the brain and support the development of Alzheimer's disease in old age: the role of microglia and astrocytes. Aging Cell *3*, 169-176.

Boado, R.J. (2008). A new generation of neurobiological drugs engineered to overcome the challenges of brain drug delivery. Drug News Perspect *21*, 489-503.

Bodennec, J., Pelled, D., Riebeling, C., Trajkovic, S., and Futerman, A.H. (2002). Phosphatidylcholine synthesis is elevated in neuronal models of Gaucher disease due to direct activation of CTP:phosphocholine cytidylyltransferase by glucosylceramide. Faseb J *16*, 1814-1816.

Bonfanti, L., and Peretto, P. (2007). Radial glial origin of the adult neural stem cells in the subventricular zone. Prog Neurobiol *83*, 24-36.

Borda, J.T., Alvarez, X., Mohan, M., Ratterree, M.S., Phillippi-Falkenstein, K., Lackner, A.A., and Bunnell, B.A. (2008). Clinical and immunopathologic alterations in rhesus macaques affected with globoid cell leukodystrophy. Am J Pathol *172*, 98-111.

Breunig, J.J. (2007). Evolving methods for the labeling and mutation of postnatal neuronal precursor cells: a critical review (Cold Spring Harbor, NY Cold Spring Harbor Laboratory Press).

Brinkmann, V. (2007). Sphingosine 1-phosphate receptors in health and disease: mechanistic insights from gene deletion studies and reverse pharmacology. Pharmacol Ther *115*, 84-105.

Broekman, M.L., Baek, R.C., Comer, L.A., Fernandez, J.L., Seyfried, T.N., and Sena-Esteves, M. (2007). Complete correction of enzymatic deficiency and neurochemistry in the GM1-

gangliosidosis mouse brain by neonatal adeno-associated virus-mediated gene delivery. Mol Ther *15*, 30-37.

Brooks, D.A., Kakavanos, R., and Hopwood, J.J. (2003). Significance of immune response to enzyme-replacement therapy for patients with a lysosomal storage disorder. Trends Mol Med *9*, 450-453.

Bruni, J.E. (1998). Ependymal development, proliferation, and functions: a review. Microsc Res Tech *41*, 2-13.

Buccoliero, R., Bodennec, J., Van Echten-Deckert, G., Sandhoff, K., and Futerman, A.H. (2004). Phospholipid synthesis is decreased in neuronal tissue in a mouse model of Sandhoff disease. J Neurochem *90*, 80-88.

Bull, N.D., and Bartlett, P.F. (2005). The adult mouse hippocampal progenitor is neurogenic but not a stem cell. J Neurosci *25*, 10815-10821.

Bundesen, L.Q., Scheel, T.A., Bregman, B.S., and Kromer, L.F. (2003). Ephrin-B2 and EphB2 regulation of astrocyte-meningeal fibroblast interactions in response to spinal cord lesions in adult rats. J Neurosci *23*, 7789-7800.

Bunk, E.C., Stelzer, S., Hermann, S., Schafers, M., Schlatt, S., and Schwamborn, J.C. (2011). Cellular organization of adult neurogenesis in the Common Marmoset. Aging Cell *10*, 28-38.

Cabrera-Salazar, M.A., Roskelley, E.M., Bu, J., Hodges, B.L., Yew, N., Dodge, J.C., Shihabuddin, L.S., Sohar, I., Sleat, D.E., Scheule, R.K., *et al.* (2007). Timing of therapeutic intervention determines functional and survival outcomes in a mouse model of late infantile batten disease. Mol Ther *15*, 1782-1788.

Cachon-Gonzalez, M.B., Wang, S.Z., Lynch, A., Ziegler, R., Cheng, S.H., and Cox, T.M. (2006). Effective gene therapy in an authentic model of Tay-Sachs-related diseases. Proc Natl Acad Sci U S A *103*, 10373-10378.

Callahan, J.W., and Skomorowski, M.A. (2006). Diagnosis of Krabbe disease by use of a natural substrate. Methods Mol Biol *347*, 321-330.

Cantz, M., and Kresse, H. (1974). Sandhoff disease: defective glycosaminoglycan catabolism in cultured fibroblasts and its correction by beta-N-acetylhexosaminidase. Eur J Biochem *47*, 581-590.

Cao, Y., Espinola, J.A., Fossale, E., Massey, A.C., Cuervo, A.M., MacDonald, M.E., and Cotman, S.L. (2006). Autophagy is disrupted in a knock-in mouse model of juvenile neuronal ceroid lipofuscinosis. J Biol Chem *281*, 20483-20493.

Cartier, N., Hacein-Bey-Abina, S., Bartholomae, C.C., Veres, G., Schmidt, M., Kutschera, I., Vidaud, M., Abel, U., Dal-Cortivo, L., Caccavelli, L., *et al.* (2009). Hematopoietic stem cell gene therapy with a lentiviral vector in X-linked adrenoleukodystrophy. Science *326*, 818-823.

Castelvetri, L.C., Givogri, M.I., Zhu, H., Smith, B., Lopez-Rosas, A., Qiu, X., van Breemen, R., and Bongarzone, E.R. (2011). Axonopathy is a compounding factor in the pathogenesis of Krabbe disease. Acta Neuropathol.

Chatterjee, S., and Pandey, A. (2008). The Yin and Yang of lactosylceramide metabolism: implications in cell function. Biochim Biophys Acta *1780*, 370-382.

Cheng, S.H., and Smith, A.E. (2003). Gene therapy progress and prospects: gene therapy of lysosomal storage disorders. Gene Ther *10*, 1275-1281.

Clancy, B., Kersh, B., Hyde, J., Darlington, R.B., Anad, K.J.S., and Finlay, B.L. (2007). Web-based method for translating neurodevelopment from laboratory species to humans. Neuroinformatics *5*, 79-94.

Conductier, G., Blondeau, N., Guyon, A., Nahon, J.L., and Rovere, C. (2010). The role of monocyte chemoattractant protein MCP1/CCL2 in neuroinflammatory diseases. J Neuroimmunol.

Conti, L., Pollard, S.M., Gorba, T., Reitano, E., Toselli, M., Biella, G., Sun, Y., Sanzone, S., Ying, Q.L., Cattaneo, E., *et al.* (2005). Niche-independent symmetrical self-renewal of a mammalian tissue stem cell. PLoS Biol *3*, e283.

Cox, T.M. (2001). Gaucher disease: understanding the molecular pathogenesis of sphingolipidoses. J Inherit Metab Dis *24 Suppl 2*, 106-121; discussion 187-108.

Cox, T.M. (2005). Substrate reduction therapy for lysosomal storage diseases. Acta Paediatr Suppl *94*, 69-75; discussion 57.

Curtis, M.A., Connor, B., and Faull, R.L. (2003a). Neurogenesis in the diseased adult human brain--new therapeutic strategies for neurodegenerative diseases. Cell Cycle *2*, 428-430.

Curtis, M.A., Kam, M., Nannmark, U., Anderson, M.F., Axell, M.Z., Wikkelso, C., Holtas, S., van Roon-Mom, W.M., Bjork-Eriksson, T., Nordborg, C., *et al.* (2007). Human neuroblasts migrate to the olfactory bulb via a lateral ventricular extension. Science *315*, 1243-1249.

Curtis, M.A., Penney, E.B., Pearson, A.G., van Roon-Mom, W.M., Butterworth, N.J., Dragunow, M., Connor, B., and Faull, R.L. (2003b). Increased cell proliferation and neurogenesis in the adult human Huntington's disease brain. Proc Natl Acad Sci U S A *100*, 9023-9027.

Cuvillier, O., Pirianov, G., Kleuser, B., Vanek, P.G., Coso, O.A., Gutkind, S., and Spiegel, S. (1996). Suppression of ceramide-mediated programmed cell death by sphingosine-1-phosphate. Nature *381*, 800-803.

Das, S., and Basu, A. (2008). Inflammation: a new candidate in modulating adult neurogenesis. J Neurosci Res *86*, 1199-1208.

de Duve, C. (1964). From cytases to lysosomes. Federation proceedings *23*, 1045.

de Duve, C. (2005). [The lysosome turns fifty.]. Med Sci (Paris) *21*, 12-15.

Desnick, R.J. (2004). Enzyme replacement and enhancement therapies for lysosomal diseases. J Inherit Metab Dis *27*, 385-410.

Di Domenico, C., Villani, G.R., Di Napoli, D., Nusco, E., Cali, G., Nitsch, L., and Di Natale, P. (2009). Intracranial gene delivery of LV-NAGLU vector corrects neuropathology in murine MPS IIIB. Am J Med Genet A *149A*, 1209-1218.

Doetsch, F., and Alvarez-Buylla, A. (1996). Network of tangential pathways for neuronal migration in adult mammalian brain. Proc Natl Acad Sci U S A *93*, 14895-14900.

Doetsch, F., Caille, I., Lim, D.A., Garcia-Verdugo, J.M., and Alvarez-Buylla, A. (1999a). Subventricular zone astrocytes are neural stem cells in the adult mammalian brain. Cell *97*, 703-716.

Doetsch, F., Garcia-Verdugo, J.M., and Alvarez-Buylla, A. (1997). Cellular composition and three-dimensional organization of the subventricular germinal zone in the adult mammalian brain. J Neurosci *17*, 5046-5061.

Doetsch, F., Garcia-Verdugo, J.M., and Alvarez-Buylla, A. (1999b). Regeneration of a germinal layer in the adult mammalian brain. Proc Natl Acad Sci U S A *96*, 11619-11624.

Doetsch, F., Petreanu, L., Caille, I., Garcia-Verdugo, J.M., and Alvarez-Buylla, A. (2002). EGF converts transit-amplifying neurogenic precursors in the adult brain into multipotent stem cells. Neuron *36*, 1021-1034.

Domercq, M., and Matute, C. (2004). Neuroprotection by tetracyclines. Trends Pharmacol Sci *25*, 609-612.

Ebadi, M., and Sharma, S.K. (2003). Peroxynitrite and mitochondrial dysfunction in the pathogenesis of Parkinson's disease. Antioxid Redox Signal *5*, 319-335.

Einstein, O., Karussis, D., Grigoriadis, N., Mizrachi-Kol, R., Reinhartz, E., Abramsky, O., and Ben-Hur, T. (2003). Intraventricular transplantation of neural precursor cell spheres attenuates acute experimental allergic encephalomyelitis. Mol Cell Neurosci *24*, 1074-1082.

Ekdahl, C.T., Claasen, J.H., Bonde, S., Kokaia, Z., and Lindvall, O. (2003). Inflammation is detrimental for neurogenesis in adult brain. Proc Natl Acad Sci U S A *100*, 13632-13637.

Elliot-Smith, E., Speak, A.O., Lloyd-Evans, E., Smith, D.A., van der Spoel, A.C., Jeyakumar, M., Butters, T.D., Dwek, R.A., d'Azzo, A., and Platt, F.M. (2008). Beneficial effects of substrate reduction therapy in a mouse model of GM1 gangliosidosis. Mol Genet Metab *94*, 204-211.

Eng, L.F., and Ghirnikar, R.S. (1994). GFAP and astrogliosis. Brain Pathol *4*, 229-237.

Escolar ML, P.M., Provenzale JM, Richards KC, Allison J, Wenger DA, Pietryga D, Wall D, Champagne M, Morse R, Krivit W, Kurtzberg J (2005). Transplantation of umbilical-cord blood in babies with infantile Krabbe's disease. N Engl J Med *May 19,*

352, 2069-2081.

Escolar, M.L., Poe, M.D., Smith, J.K., Gilmore, J.H., Kurtzberg, J., Lin, W., and Styner, M. (2009). Diffusion tensor imaging detects abnormalities in the corticospinal tracts of neonates with infantile Krabbe disease. AJNR Am J Neuroradiol *30*, 1017-1021.

Ezoe, T., Vanier, M.T., Oya, Y., Popko, B., Tohyama, J., Matsuda, J., Suzuki, K., and Suzuki, K. (2000). Biochemistry and neuropathology of mice doubly deficient in synthesis and degradation of galactosylceramide. J Neurosci Res *59*, 170-178.

Fan, J.Q., and Ishii, S. (2007). Active-site-specific chaperone therapy for Fabry disease. Yin and Yang of enzyme inhibitors. Febs J *274*, 4962-4971.

Farina, L., Bizzi, A., Finocchiaro, G., Pareyson, D., Sghirlanzoni, A., Bertagnolio, B., Savoiardo, M., Naidu, S., Singhal, B.S., and Wenger, D.A. (2000). MR imaging and proton MR spectroscopy in adult Krabbe disease. AJNR Am J Neuroradiol *21*, 1478-1482.

Farley, T.J., Ketonen, L.M., Bodensteiner, J.B., and Wang, D.D. (1992). Serial MRI and CT findings in infantile Krabbe disease. Pediatr Neurol *8*, 455-458.

Fasolo, A., Peretto, P., and Bonfanti, L. (2002). Cell migration in the rostral migratory stream. Chem Senses *27*, 581-582.

Fleming, D.R., Henslee-Downey, P.J., Ciocci, G., Romond, E.H., Marciniak, E., Munn, R.K., and Thompson, J.S. (1998). The use of partially HLA-mismatched donors for allogeneic transplantation in patients with mucopolysaccharidosis-I. Pediatr Transplant *2*, 299-304.

Formichi, P., Radi, E., Battisti, C., Pasqui, A., Pompella, G., Lazzerini, P.E., Laghi-Pasini, F., Leonini, A., Di Stefano, A., and Federico, A. (2007). Psychosine-induced apoptosis and cytokine activation in immune peripheral cells of Krabbe patients. J Cell Physiol *212*, 737-743.

Forrest, M., Sun, S.Y., Hajdu, R., Bergstrom, J., Card, D., Doherty, G., Hale, J., Keohane, C., Meyers, C., Milligan, J., *et al.* (2004). Immune cell regulation and cardiovascular effects of sphingosine 1-phosphate receptor agonists in rodents are mediated via distinct receptor subtypes. J Pharmacol Exp Ther *309*, 758-768.

Fratantoni, J.C., Hall, C.W., and Neufeld, E.F. (1968). Hurler and Hunter syndromes: mutual correction of the defect in cultured fibroblasts. Science *162*, 570-572.

Frustaci, A., Chimenti, C., Ricci, R., Natale, L., Russo, M.A., Pieroni, M., Eng, C.M., and Desnick, R.J. (2001). Improvement in cardiac function in the cardiac variant of Fabry's disease with galactose-infusion therapy. N Engl J Med *345*, 25-32.

Fukuda, T., Ewan, L., Bauer, M., Mattaliano, R.J., Zaal, K., Ralston, E., Plotz, P.H., and Raben, N. (2006). Dysfunction of endocytic and autophagic pathways in a lysosomal storage disease. Ann Neurol *59*, 700-708.

Futerman, A.H., and van Meer, G. (2004). The cell biology of lysosomal storage disorders. Nat Rev Mol Cell Biol *5*, 554-565.

Gage, F.H. (2000). Mammalian neural stem cells. Science *287*, 1433-1438.

Galbiati, F., Givogri, M.I., Cantuti, L., Rosas, A.L., Cao, H., van Breemen, R., and Bongarzone, E.R. (2009). Combined hematopoietic and lentiviral gene-transfer therapies in newborn Twitcher mice reveal contemporaneous neurodegeneration and demyelination in Krabbe disease. J Neurosci Res *87*, 1748-1759.

Galli, R., Fiocco, R., De Filippis, L., Muzio, L., Gritti, A., Mercurio, S., Broccoli, V., Pellegrini, M., Mallamaci, A., and Vescovi, A.L. (2002). Emx2 regulates the proliferation of stem cells of the adult mammalian central nervous system. Development *129*, 1633-1644.

Gama Sosa, M.A., de Gasperi, R., Undevia, S., Yeretsian, J., Rouse, S.C., 2nd, Lyerla, T.A., and Kolodny, E.H. (1996). Correction of the galactocerebrosidase deficiency in globoid cell leukodystrophy-cultured cells by SL3-3 retroviral-mediated gene transfer. Biochem Biophys Res Commun *218*, 766-771.

Gentner, B., Visigalli, I., Hiramatsu, H., Lechman, E., Ungari, S., Giustacchini, A., Schira, G., Amendola, M., Quattrini, A., Martino, S., *et al.* (2010). Identification of hematopoietic stem cell-specific miRNAs enables gene therapy of globoid cell leukodystrophy. Sci Transl Med *2*, 58ra84.

Giaume, C., and Venance, L. (1998). Intercellular calcium signaling and gap junctional communication in astrocytes. Glia *24*, 50-64.

Giri, S., Khan, M., Nath, N., Singh, I., and Singh, A.K. (2008). The role of AMPK in psychosine mediated effects on oligodendrocytes and astrocytes: implication for Krabbe disease. J Neurochem *105*, 1820-1833.

Giri, S., Khan, M., Rattan, R., Singh, I., and Singh, A.K. (2006). Krabbe disease: psychosine-mediated activation of phospholipase A2 in oligodendrocyte cell death. J Lipid Res *47*, 1478-1492.

Goings, G.E., Kozlowski, D.A., and Szele, F.G. (2006). Differential activation of microglia in neurogenic versus non-neurogenic regions of the forebrain. Glia *54*, 329-342.

Gonzalez-Perez, O., and Alvarez-Buylla, A. (2011). Oligodendrogenesis in the subventricular zone and the role of epidermal growth factor. Brain Res Rev.

Gonzalez-Perez, O., Romero-Rodriguez, R., Soriano-Navarro, M., Garcia-Verdugo, J.M., and Alvarez-Buylla, A. (2009). Epidermal growth factor induces the progeny of subventricular zone type B cells to migrate and differentiate into oligodendrocytes. Stem Cells *27*, 2032-2043.

Gotz, M., and Huttner, W.B. (2005). The cell biology of neurogenesis. Nat Rev Mol Cell Biol *6*, 777-788.

Gould, E., and Tanapat, P. (1997). Lesion-induced proliferation of neuronal progenitors in the dentate gyrus of the adult rat. Neuroscience *80*, 427-436.

Grabowski, G.A., Leslie, N., and Wenstrup, R. (1998). Enzyme therapy for Gaucher disease: the first 5 years. Blood Rev *12*, 115-133.

Gritti, A., and Bonfanti, L. (2007). Neuronal-glial interactions in central nervous system neurogenesis: the neural stem cell perspective. Neuron Glia Biol *3*, 309-323.

Gritti, A., Dal Molin, M., Foroni, C., and Bonfanti, L. (2009). Effects of developmental age, brain region, and time in culture on long-term proliferation and multipotency of neural stem cell populations. J Comp Neurol *517*, 333-349.

Gritti, A., Frolichsthal-Schoeller, P., Galli, R., Parati, E.A., Cova, L., Pagano, S.F., Bjornson, C.R., and Vescovi, A.L. (1999). Epidermal and fibroblast growth factors behave as mitogenic regulators for a single multipotent stem cell-like population from the subventricular region of the adult mouse forebrain. J Neurosci *19*, 3287-3297.

Gritti, A., Vescovi, A.L., and Galli, R. (2002). Adult neural stem cells: plasticity and developmental potential. J Physiol Paris *96*, 81-90.

Hagberg, B., Kollberg, H., Sourander, P., and Akesson, H.O. (1969). Infantile globoid cell leucodystrophy (Krabbe's disease). A clinical and genetic study of 32 Swedish cases 1953--1967. Neuropadiatrie *1*, 74-88.

Han, Y.G., Spassky, N., Romaguera-Ros, M., Garcia-Verdugo, J.M., Aguilar, A., Schneider-Maunoury, S., and Alvarez-Buylla, A. (2008). Hedgehog signaling and primary cilia are required for the formation of adult neural stem cells. Nat Neurosci *11*, 277-284.

Hannun, Y.A., and Obeid, L.M. (2008). Principles of bioactive lipid signalling: lessons from sphingolipids. Nat Rev Mol Cell Biol *9*, 139-150.

Haq, E., Contreras, M.A., Giri, S., Singh, I., and Singh, A.K. (2006). Dysfunction of peroxisomes in twitcher mice brain: a possible mechanism of psychosine-induced disease. Biochem Biophys Res Commun *343*, 229-238.

Haq, E., Giri, S., Singh, I., and Singh, A.K. (2003). Molecular mechanism of psychosine-induced cell death in human oligodendrocyte cell line. J Neurochem *86*, 1428-1440.

Harel, R., and Futerman, A.H. (1993). Inhibition of sphingolipid synthesis affects axonal outgrowth in cultured hippocampal neurons. J Biol Chem *268*, 14476-14481.

Harzer, K., Hiraiwa, M., and Paton, B.C. (2001). Saposins (sap) A and C activate the degradation of galactosylsphingosine. FEBS Lett *508*, 107-110.

Hasilik, A., Klein, U., Waheed, A., Strecker, G., and von Figura, K. (1980). Phosphorylated oligosaccharides in lysosomal enzymes: identification of alpha-N-acetylglucosamine(1)phospho(6)mannose diester groups. Proc Natl Acad Sci U S A *77*, 7074-7078.

Heinrich, M., Wickel, M., Schneider-Brachert, W., Sandberg, C., Gahr, J., Schwandner, R., Weber, T., Saftig, P., Peters, C., Brunner, J., *et al.* (1999). Cathepsin D targeted by acid sphingomyelinase-derived ceramide. Embo J *18*, 5252-5263.

Herken, R., Gotz, W., and Wattjes, K.H. (1989). Initial development of capillaries in the neuroepithelium of the mouse. J Anat *164*, 85-92.

Hickey, W.F. (1999). Leukocyte traffic in the central nervous system: the participants and their roles. Semin Immunol *11*, 125-137.

Hoehn, B.D., Palmer, T.D., and Steinberg, G.K. (2005). Neurogenesis in rats after focal cerebral ischemia is enhanced by indomethacin. Stroke *36*, 2718-2724.

Hoogerbrugge, P.M., Brouwer, O.F., Bordigoni, P., Ringden, O., Kapaun, P., Ortega, J.J., O'Meara, A., Cornu, G., Souillet, G., Frappaz, D., *et al.* (1995). Allogeneic bone marrow

transplantation for lysosomal storage diseases. The European Group for Bone Marrow Transplantation. Lancet *345*, 1398-1402.

Husain, A.M., Altuwaijri, M., and Aldosari, M. (2004). Krabbe disease: neurophysiologic studies and MRI correlations. Neurology *63*, 617-620.

Huwiler, A., Xin, C., Brust, A.K., Briner, V.A., and Pfeilschifter, J. (2004). Differential binding of ceramide to MEKK1 in glomerular endothelial and mesangial cells. Biochim Biophys Acta *1636*, 159-168.

Ibanez, C.F. (2004). Lipid rafts as organizing platforms for cell chemotaxis and axon guidance. Neuron *42*, 3-5.

Ichioka, T., Kishimoto, Y., Brennan, S., Santos, G.W., and Yeager, A.M. (1987). Hematopoietic cell transplantation in murine globoid cell leukodystrophy (the twitcher mouse): effects on levels of galactosylceramidase, psychosine, and galactocerebrosides. Proc Natl Acad Sci U S A *84*, 4259-4263.

Ida, H., Rennert, O.M., Watabe, K., Eto, Y., and Maekawa, K. (1994). Pathological and biochemical studies of fetal Krabbe disease. Brain Dev *16*, 480-484.

Im, D.S., Heise, C.E., Nguyen, T., O'Dowd, B.F., and Lynch, K.R. (2001). Identification of a molecular target of psychosine and its role in globoid cell formation. J Cell Biol *153*, 429-434.

Inokuchi, J., Mizutani, A., Jimbo, M., Usuki, S., Yamagishi, K., Mochizuki, H., Muramoto, K., Kobayashi, K., Kuroda, Y., Iwasaki, K., *et al.* (1997). Up-regulation of ganglioside biosynthesis, functional synapse formation, and memory retention by a synthetic ceramide analog (L-PDMP). Biochem Biophys Res Commun *237*, 595-600.

Ishibashi, T., Dakin, K.A., Stevens, B., Lee, P.R., Kozlov, S.V., Stewart, C.L., and Fields, R.D. (2006). Astrocytes promote myelination in response to electrical impulses. Neuron *49*, 823-832.

Itoh, M., Hayashi, M., Fujioka, Y., Nagashima, K., Morimatsu, Y., and Matsuyama, H. (2002). Immunohistological study of globoid cell leukodystrophy. Brain Dev *24*, 284-290.

Jaderstad, J., Jaderstad, L.M., Li, J., Chintawar, S., Salto, C., Pandolfo, M., Ourednik, V., Teng, Y.D., Sidman, R.L., Arenas, E., *et al.* (2010). Communication via gap junctions underlies early functional and beneficial interactions between grafted neural stem cells and the host. Proc Natl Acad Sci U S A *107*, 5184-5189.

Jaillard, C., Harrison, S., Stankoff, B., Aigrot, M.S., Calver, A.R., Duddy, G., Walsh, F.S., Pangalos, M.N., Arimura, N., Kaibuchi, K., *et al.* (2005). Edg8/S1P5: an oligodendroglial receptor with dual function on process retraction and cell survival. J Neurosci *25*, 1459-1469.

Jakubs, K., Bonde, S., Iosif, R.E., Ekdahl, C.T., Kokaia, Z., Kokaia, M., and Lindvall, O. (2008). Inflammation regulates functional integration of neurons born in adult brain. J Neurosci *28*, 12477-12488.

Jardim, L.B., Giugliani, R., Pires, R.F., Haussen, S., Burin, M.G., Rafi, M.A., and Wenger, D.A. (1999). Protracted course of Krabbe disease in an adult patient bearing a novel mutation. Arch Neurol *56*, 1014-1017.

Jatana, M., Giri, S., and Singh, A.K. (2002). Apoptotic positive cells in Krabbe brain and induction of apoptosis in rat C6 glial cells by psychosine. Neurosci Lett *330*, 183-187.

Jaworski, D.M., and Fager, N. (2000). Regulation of tissue inhibitor of metalloproteinase-3 (Timp-3) mRNA expression during rat CNS development. J Neurosci Res *61*, 396-408.

Jeyakumar, M., Butters, T.D., Cortina-Borja, M., Hunnam, V., Proia, R.L., Perry, V.H., Dwek, R.A., and Platt, F.M. (1999). Delayed symptom onset and increased life expectancy in Sandhoff disease mice treated with N-butyldeoxynojirimycin. Proc Natl Acad Sci U S A *96*, 6388-6393.

Jeyakumar, M., Dwek, R.A., Butters, T.D., and Platt, F.M. (2005). Storage solutions: treating lysosomal disorders of the brain. Nat Rev Neurosci *6*, 713-725.

Jeyakumar, M., Lee, J.P., Sibson, N.R., Lowe, J.P., Stuckey, D.J., Tester, K., Fu, G., Newlin, R., Smith, D.A., Snyder, E.Y., *et al.* (2009). Neural stem cell transplantation benefits a monogenic neurometabolic disorder during the symptomatic phase of disease. Stem Cells *27*, 2362-2370.

Jeyakumar, M., Norflus, F., Tifft, C.J., Cortina-Borja, M., Butters, T.D., Proia, R.L., Perry, V.H., Dwek, R.A., and Platt, F.M. (2001). Enhanced survival in Sandhoff disease mice receiving a combination of substrate deprivation therapy and bone marrow transplantation. Blood *97*, 327-329.

Jeyakumar, M., Smith, D.A., Williams, I.M., Borja, M.C., Neville, D.C., Butters, T.D., Dwek, R.A., and Platt, F.M. (2004). NSAIDs increase survival in the Sandhoff disease mouse: synergy with N-butyldeoxynojirimycin. Ann Neurol *56*, 642-649.

Jin, K., Galvan, V., Xie, L., Mao, X.O., Gorostiza, O.F., Bredesen, D.E., and Greenberg, D.A. (2004). Enhanced neurogenesis in Alzheimer's disease transgenic (PDGF-APPSw,Ind) mice. Proc Natl Acad Sci U S A *101*, 13363-13367.

Jin, K., Mao, X.O., Sun, Y., Xie, L., and Greenberg, D.A. (2002). Stem cell factor stimulates neurogenesis in vitro and in vivo. J Clin Invest *110*, 311-319.

Jolly, P.S., Bektas, M., Olivera, A., Gonzalez-Espinosa, C., Proia, R.L., Rivera, J., Milstien, S., and Spiegel, S. (2004). Transactivation of sphingosine-1-phosphate receptors by FcepsilonRI

triggering is required for normal mast cell degranulation and chemotaxis. J Exp Med *199*, 959-970.

Kajimoto, T., Shirai, Y., Sakai, N., Yamamoto, T., Matsuzaki, H., Kikkawa, U., and Saito, N. (2004). Ceramide-induced apoptosis by translocation, phosphorylation, and activation of protein kinase Cdelta in the Golgi complex. J Biol Chem *279*, 12668-12676.

Kam, M., Curtis, M.A., McGlashan, S.R., Connor, B., Nannmark, U., and Faull, R.L. (2009). The cellular composition and morphological organization of the rostral migratory stream in the adult human brain. J Chem Neuroanat *37*, 196-205.

Kamate, M., and Hattiholi, V. (2010). Predominant corticospinal tract involvement in early-onset Krabbe disease. Pediatr Neurol *44*, 155-156.

Kanazawa, T., Nakamura, S., Momoi, M., Yamaji, T., Takematsu, H., Yano, H., Sabe, H., Yamamoto, A., Kawasaki, T., and Kozutsumi, Y. (2000). Inhibition of cytokinesis by a lipid metabolite, psychosine. J Cell Biol *149*, 943-950.

Kazanis, I., Belhadi, A., Faissner, A., and Ffrench-Constant, C. (2007). The adult mouse subependymal zone regenerates efficiently in the absence of tenascin-C. J Neurosci *27*, 13991-13996.

Kemper, A.R., Knapp, A.A., Green, N.S., Comeau, A.M., Metterville, D.R., and Perrin, J.M. (2010). Weighing the evidence for newborn screening for early-infantile Krabbe disease. Genet Med *12*, 539-543.

Kim, S.J., Lee, B.H., Lee, Y.S., and Kang, K.S. (2007). Defective cholesterol traffic and neuronal differentiation in neural stem cells of Niemann-Pick type C disease improved by valproic acid, a histone deacetylase inhibitor. Biochem Biophys Res Commun *360*, 593-599.

Kim, S.J., Lim, M.S., Kang, S.K., Lee, Y.S., and Kang, K.S. (2008). Impaired functions of neural stem cells by abnormal nitric oxide-mediated signaling in an in vitro model of Niemann-Pick type C disease. Cell Res *18*, 686-694.

Kobayashi, T., Shinnoh, N., Goto, I., and Kuroiwa, Y. (1985). Hydrolysis of galactosylceramide is catalyzed by two genetically distinct acid beta-galactosidases. J Biol Chem *260*, 14982-14987.

Kobayashi, T., Yamanaka, T., Jacobs, J.M., Teixeira, F., and Suzuki, K. (1980). The Twitcher mouse: an enzymatically authentic model of human globoid cell leukodystrophy (Krabbe disease). Brain Res *202*, 479-483.

Koeberl, D.D., and Kishnani, P.S. (2009). Immunomodulatory gene therapy in lysosomal storage disorders. Curr Gene Ther *9*, 503-510.

Kohama, T., Olivera, A., Edsall, L., Nagiec, M.M., Dickson, R., and Spiegel, S. (1998). Molecular cloning and functional characterization of murine sphingosine kinase. J Biol Chem *273*, 23722-23728.

Kokaia, Z., and Lindvall, O. (2003). Neurogenesis after ischaemic brain insults. Curr Opin Neurobiol *13*, 127-132.

Kolesnick, R.N., Goni, F.M., and Alonso, A. (2000). Compartmentalization of ceramide signaling: physical foundations and biological effects. J Cell Physiol *184*, 285-300.

Kolodny, E.H., Raghavan, S., and Krivit, W. (1991). Late-onset Krabbe disease (globoid cell leukodystrophy): clinical and biochemical features of 15 cases. Dev Neurosci *13*, 232-239.

Kono, M., Belyantseva, I.A., Skoura, A., Frolenkov, G.I., Starost, M.F., Dreier, J.L., Lidington, D., Bolz, S.S., Friedman, T.B., Hla, T., *et al.* (2007). Deafness and stria vascularis defects in S1P2 receptor-null mice. J Biol Chem *282*, 10690-10696.

Korkotian, E., Schwarz, A., Pelled, D., Schwarzmann, G., Segal, M., and Futerman, A.H. (1999). Elevation of intracellular glucosylceramide levels results in an increase in endoplasmic reticulum density and in functional calcium stores in cultured neurons. J Biol Chem *274*, 21673-21678.

Krabbe (1916). A new familial, infantile form of diffuse brain. Brain *39*, 74-114.

Kramer, E.M., Klein, C., Koch, T., Boytinck, M., and Trotter, J. (1999). Compartmentation of Fyn kinase with glycosylphosphatidylinositol-anchored molecules in oligodendrocytes facilitates kinase activation during myelination. J Biol Chem *274*, 29042-29049.

Krivit, W., Aubourg, P., Shapiro, E., and Peters, C. (1999a). Bone marrow transplantation for globoid cell leukodystrophy, adrenoleukodystrophy, metachromatic leukodystrophy, and Hurler syndrome. Curr Opin Hematol *6*, 377-382.

Krivit, W., Peters, C., and Shapiro, E.G. (1999b). Bone marrow transplantation as effective treatment of central nervous system disease in globoid cell leukodystrophy, metachromatic leukodystrophy, adrenoleukodystrophy, mannosidosis, fucosidosis, aspartylglucosaminuria, Hurler, Maroteaux-Lamy, and Sly syndromes, and Gaucher disease type III. Curr Opin Neurol *12*, 167-176.

Krivit, W., Shapiro, E.G., Peters, C., Wagner, J.E., Cornu, G., Kurtzberg, J., Wenger, D.A., Kolodny, E.H., Vanier, M.T., Loes, D.J., *et al.* (1998). Hematopoietic stem-cell transplantation in globoid-cell leukodystrophy. N Engl J Med *338*, 1119-1126.

Krivit, W., Sung, J.H., Shapiro, E.G., and Lockman, L.A. (1995). Microglia: the effector cell for reconstitution of the central nervous system following bone marrow transplantation for lysosomal and peroxisomal storage diseases. Cell Transplant *4*, 385-392.

Kurtz, H.J., and Fletcher, T.F. (1970). The peripheral neuropathy of canine globoid-cell leukodystrophy (krabbe-type). Acta Neuropathol *16*, 226-232.

Lachmann, R.H., Grant, I.R., Halsall, D., and Cox, T.M. (2004). Twin pairs showing discordance of phenotype in adult Gaucher's disease. Qjm *97*, 199-204.

Lattanzi, A., Neri, M., Maderna, C., di Girolamo, I., Martino, S., Orlacchio, A., Amendola, M., Naldini, L., and Gritti, A. (2010). Widespread Enzymatic Correction of Cns Tissues by a Single Intracerebral Injection of Therapeutic Lentiviral Vector in Leukodystrophy Mouse Models. Hum Mol Genet.

Lee, J.P., Jeyakumar, M., Gonzalez, R., Takahashi, H., Lee, P.J., Baek, R.C., Clark, D., Rose, H., Fu, G., Clarke, J., *et al.* (2007a). Stem cells act through multiple mechanisms to benefit mice with neurodegenerative metabolic disease. Nat Med *13*, 439-447.

Lee, J.P., McKercher, S., Muller, F.J., and Snyder, E.Y. (2008). Neural stem cell transplantation in mouse brain. Curr Protoc Neurosci *Chapter 3*, Unit 3 10.

Lee, W.C., Courtenay, A., Troendle, F.J., Stallings-Mann, M.L., Dickey, C.A., DeLucia, M.W., Dickson, D.W., and Eckman, C.B. (2005). Enzyme replacement therapy results in substantial improvements in early clinical phenotype in a mouse model of globoid cell leukodystrophy. Faseb J *19*, 1549-1551.

Lee, W.C., Kang, D., Causevic, E., Herdt, A.R., Eckman, E.A., and Eckman, C.B. (2010). Molecular characterization of mutations that cause globoid cell leukodystrophy and pharmacological rescue using small molecule chemical chaperones. J Neurosci *30*, 5489-5497.

Lee, W.C., Tsoi, Y.K., Dickey, C.A., Delucia, M.W., Dickson, D.W., and Eckman, C.B. (2006). Suppression of galactosylceramidase (GALC) expression in the twitcher mouse model of globoid cell leukodystrophy (GLD) is caused by nonsense-mediated mRNA decay (NMD). Neurobiol Dis *23*, 273-280.

Lee, W.C., Tsoi, Y.K., Troendle, F.J., DeLucia, M.W., Ahmed, Z., Dicky, C.A., Dickson, D.W., and Eckman, C.B. (2007b). Single-dose intracerebroventricular administration of galactocerebrosidase improves survival in a mouse model of globoid cell leukodystrophy. Faseb J *21*, 2520-2527.

Lepley, D., Paik, J.H., Hla, T., and Ferrer, F. (2005). The G protein-coupled receptor S1P2 regulates Rho/Rho kinase pathway to inhibit tumor cell migration. Cancer Res *65*, 3788-3795.

Lie, D.C., Colamarino, S.A., Song, H.J., Desire, L., Mira, H., Consiglio, A., Lein, E.S., Jessberger, S., Lansford, H., Dearie, A.R., *et al.* (2005). Wnt signalling regulates adult hippocampal neurogenesis. Nature *437*, 1370-1375.

Lim, Z.Y., Ho, A.Y., Abrahams, S., Fensom, A., Aldouri, M., Pagliuca, A., Shaw, C., and Mufti, G.J. (2008). Sustained neurological improvement following reduced-intensity conditioning allogeneic haematopoietic stem cell transplantation for late-onset Krabbe disease. Bone Marrow Transplant *41*, 831-832.

Lin, D., Donsante, A., Macauley, S., Levy, B., Vogler, C., and Sands, M.S. (2007). Central nervous system-directed AAV2/5-mediated gene therapy synergizes with bone marrow transplantation in the murine model of globoid-cell leukodystrophy. Mol Ther *15*, 44-52.

Lin, D., Fantz, C.R., Levy, B., Rafi, M.A., Vogler, C., Wenger, D.A., and Sands, M.S. (2005). AAV2/5 vector expressing galactocerebrosidase ameliorates CNS disease in the murine model of globoid-cell leukodystrophy more efficiently than AAV2. Mol Ther *12*, 422-430.

Lindvall, O., and Kokaia, Z. (2006). Stem cells for the treatment of neurological disorders. Nature *441*, 1094-1096.

Liu, H., Sugiura, M., Nava, V.E., Edsall, L.C., Kono, K., Poulton, S., Milstien, S., Kohama, T., and Spiegel, S. (2000a). Molecular cloning and functional characterization of a novel mammalian sphingosine kinase type 2 isoform. J Biol Chem *275*, 19513-19520.

Liu, H., Toman, R.E., Goparaju, S.K., Maceyka, M., Nava, V.E., Sankala, H., Payne, S.G., Bektas, M., Ishii, I., Chun, J., *et al.* (2003). Sphingosine kinase type 2 is a putative BH3-only protein that induces apoptosis. J Biol Chem *278*, 40330-40336.

Liu, J., Solway, K., Messing, R.O., and Sharp, F.R. (1998). Increased neurogenesis in the dentate gyrus after transient global ischemia in gerbils. J Neurosci *18*, 7768-7778.

Liu, Y., Wada, R., Yamashita, T., Mi, Y., Deng, C.X., Hobson, J.P., Rosenfeldt, H.M., Nava, V.E., Chae, S.S., Lee, M.J., *et al.* (2000b). Edg-1, the G protein-coupled receptor for sphingosine-1-phosphate, is essential for vascular maturation. J Clin Invest *106*, 951-961.

Liu, Y.P., Lin, H.I., and Tzeng, S.F. (2005). Tumor necrosis factor-alpha and interleukin-18 modulate neuronal cell fate in embryonic neural progenitor culture. Brain Res *1054*, 152-158.

Loes, D.J., Peters, C., and Krivit, W. (1999). Globoid cell leukodystrophy: distinguishing early-onset from late-onset disease using a brain MR imaging scoring method. AJNR Am J Neuroradiol *20*, 316-323.

Lois, C., and Alvarez-Buylla, A. (1994). Long-distance neuronal migration in the adult mammalian brain. Science *264*, 1145-1148.

Loonen, M.C., Van Diggelen, O.P., Janse, H.C., Kleijer, W.J., and Arts, W.F. (1985). Late-onset globoid cell leucodystrophy (Krabbe's disease). Clinical and genetic delineation of two forms and their relation to the early-infantile form. Neuropediatrics *16*, 137-142.

Louis, S.A., Rietze, R.L., Deleyrolle, L., Wagey, R.E., Thomas, T.E., Eaves, A.C., and Reynolds, B.A. (2008). Enumeration of neural stem and progenitor cells in the neural colony-forming cell assay. Stem Cells *26*, 988-996.

Luddi, A., Volterrani, M., Strazza, M., Smorlesi, A., Rafi, M.A., Datto, J., Wenger, D.A., and Costantino-Ceccarini, E. (2001). Retrovirus-mediated gene transfer and galactocerebrosidase uptake into twitcher glial cells results in appropriate localization and phenotype correction. Neurobiol Dis *8*, 600-610.

Luzi, P., Abraham, R.M., Rafi, M.A., Curtis, M., Hooper, D.C., and Wenger, D.A. (2009). Effects of treatments on inflammatory and apoptotic markers in the CNS of mice with globoid cell leukodystrophy. Brain Res *1300*, 146-158.

Luzi, P., Rafi, M.A., and Wenger, D.A. (1995). Structure and organization of the human galactocerebrosidase (GALC) gene. Genomics *26*, 407-409.

Luzi, P., Rafi, M.A., Zaka, M., Curtis, M., Vanier, M.T., and Wenger, D.A. (2001). Generation of a mouse with low galactocerebrosidase activity by gene targeting: a new model of globoid cell leukodystrophy (Krabbe disease). Mol Genet Metab *73*, 211-223.

Luzi, P., Victoria, T., Rafi, M.A., and Wenger, D.A. (1997). Analysis of the 5' flanking region of the human galactocerebrosidase (GALC) gene. Biochem Mol Med *62*, 159-164.

Maceyka, M., Milstien, S., and Spiegel, S. (2007). Measurement of mammalian sphingosine-1-phosphate phosphohydrolase activity in vitro and in vivo. Methods Enzymol *434*, 243-256.

Maceyka, M., Milstien, S., and Spiegel, S. (2009). Sphingosine-1-phosphate: the Swiss army knife of sphingolipid signaling. J Lipid Res *50 Suppl*, S272-276.

Marcus, J., and Popko, B. (2002). Galactolipids are molecular determinants of myelin development and axo-glial organization. Biochim Biophys Acta *1573*, 406-413.

Marshall, J., McEachern, K.A., Kyros, J.A., Nietupski, J.B., Budzinski, T., Ziegler, R.J., Yew, N.S., Sullivan, J., Scaria, A., van Rooijen, N., *et al.* (2002). Demonstration of feasibility of in vivo gene therapy for Gaucher disease using a chemically induced mouse model. Mol Ther *6*, 179-189.

Martinez-Cerdeno, V., Noctor, S.C., and Kriegstein, A.R. (2006). The role of intermediate progenitor cells in the evolutionary expansion of the cerebral cortex. Cereb Cortex *16 Suppl 1*, i152-161.

Martino, G., and Pluchino, S. (2006). The therapeutic potential of neural stem cells. Nat Rev Neurosci *7*, 395-406.

Mathieu, P., Battista, D., Depino, A., Roca, V., Graciarena, M., and Pitossi, F. (2010). The more you have, the less you get: the functional role of inflammation on neuronal differentiation of endogenous and transplanted neural stem cells in the adult brain. J Neurochem *112*, 1368-1385.

Matloubian, M., Lo, C.G., Cinamon, G., Lesneski, M.J., Xu, Y., Brinkmann, V., Allende, M.L., Proia, R.L., and Cyster, J.G. (2004). Lymphocyte egress from thymus and peripheral lymphoid organs is dependent on S1P receptor 1. Nature *427*, 355-360.

Matsuda, J., Suzuki, O., Oshima, A., Yamamoto, Y., Noguchi, A., Takimoto, K., Itoh, M., Matsuzaki, Y., Yasuda, Y., Ogawa, S., *et al.* (2003). Chemical chaperone therapy for brain pathology in G(M1)-gangliosidosis. Proc Natl Acad Sci U S A *100*, 15912-15917.

Matsuda, J., Vanier, M.T., Saito, Y., Tohyama, J., Suzuki, K., and Suzuki, K. (2001). A mutation in the saposin A domain of the sphingolipid activator protein (prosaposin) gene results in a late-onset, chronic form of globoid cell leukodystrophy in the mouse. Hum Mol Genet *10*, 1191-1199.

Matzner, U., Herbst, E., Hedayati, K.K., Lullmann-Rauch, R., Wessig, C., Schroder, S., Eistrup, C., Moller, C., Fogh, J., and Gieselmann, V. (2005). Enzyme replacement improves nervous system pathology and function in a mouse model for metachromatic leukodystrophy. Hum Mol Genet *14*, 1139-1152.

McVerry, B.J., and Garcia, J.G. (2005). In vitro and in vivo modulation of vascular barrier integrity by sphingosine 1-phosphate: mechanistic insights. Cell Signal *17*, 131-139.

Meng, X.L., Shen, J.S., Ohashi, T., Maeda, H., Kim, S.U., and Eto, Y. (2003). Brain transplantation of genetically engineered human neural stem cells globally corrects brain lesions in the mucopolysaccharidosis type VII mouse. J Neurosci Res *74*, 266-277.

Mercier, F., Kitasako, J.T., and Hatton, G.I. (2002). Anatomy of the brain neurogenic zones revisited: fractones and the fibroblast/macrophage network. J Comp Neurol *451*, 170-188.

Merkle, F.T., Mirzadeh, Z., and Alvarez-Buylla, A. (2007). Mosaic organization of neural stem cells in the adult brain. Science *317*, 381-384.

Meyer, G., Perez-Garcia, C.G., and Gleeson, J.G. (2002). Selective expression of doublecortin and LIS1 in developing human cortex suggests unique modes of neuronal movement. Cereb Cortex *12*, 1225-1236.

Mirzadeh, Z., Doetsch, F., Sawamoto, K., Wichterle, H., and Alvarez-Buylla, A. (2010). The subventricular zone en-face: wholemount staining and ependymal flow. J Vis Exp.

Mirzadeh, Z., Merkle, F.T., Soriano-Navarro, M., Garcia-Verdugo, J.M., and Alvarez-Buylla, A. (2008). Neural stem cells confer unique pinwheel architecture to the ventricular surface in neurogenic regions of the adult brain. Cell Stem Cell *3*, 265-278.

Mitra, P., Oskeritzian, C.A., Payne, S.G., Beaven, M.A., Milstien, S., and Spiegel, S. (2006). Role of ABCC1 in export of sphingosine-1-phosphate from mast cells. Proc Natl Acad Sci U S A *103*, 16394-16399.

Miyagi, T., Wada, T., Yamaguchi, K., and Hata, K. (2004). Sialidase and malignancy: a minireview. Glycoconj J *20*, 189-198.

Miyatake, T., and Suzuki, K. (1972). Globoid cell leukodystrophy: additional deficiency of psychosine galactosidase. Biochem Biophys Res Commun *48*, 539-543.

Mizugishi, K., Yamashita, T., Olivera, A., Miller, G.F., Spiegel, S., and Proia, R.L. (2005). Essential role for sphingosine kinases in neural and vascular development. Mol Cell Biol *25*, 11113-11121.

Monje, M.L., and Palmer, T. (2003). Radiation injury and neurogenesis. Curr Opin Neurol *16*, 129-134.

Monje, M.L., Toda, H., and Palmer, T.D. (2003). Inflammatory blockade restores adult hippocampal neurogenesis. Science *302*, 1760-1765.

Morrison, S.J., and Kimble, J. (2006). Asymmetric and symmetric stem-cell divisions in development and cancer. Nature *441*, 1068-1074.

Morrison, S.J., and Spradling, A.C. (2008). Stem cells and niches: mechanisms that promote stem cell maintenance throughout life. Cell *132*, 598-611.

Muller, M., Carter, S., Hofer, M.J., and Campbell, I.L. (2010). Review: The chemokine receptor CXCR3 and its ligands CXCL9, CXCL10 and CXCL11 in neuroimmunity--a tale of conflict and conundrum. Neuropathol Appl Neurobiol *36*, 368-387.

Nagano, S., Yamada, T., Shinnoh, N., Furuya, H., Taniwaki, T., and Kira, J. (1998). Expression and processing of recombinant human galactosylceramidase. Clin Chim Acta *276*, 53-61.

Namba, T., Mochizuki, H., Onodera, M., Mizuno, Y., Namiki, H., and Seki, T. (2005). The fate of neural progenitor cells expressing astrocytic and radial glial markers in the postnatal rat dentate gyrus. Eur J Neurosci *22*, 1928-1941.

Ngamukote, S., Yanagisawa, M., Ariga, T., Ando, S., and Yu, R.K. (2007). Developmental changes of glycosphingolipids and expression of glycogenes in mouse brains. J Neurochem *103*, 2327-2341.

Niethammer, P., Delling, M., Sytnyk, V., Dityatev, A., Fukami, K., and Schachner, M. (2002). Cosignaling of NCAM via lipid rafts and the FGF receptor is required for neuritogenesis. J Cell Biol *157*, 521-532.

Nishizuka, Y. (1992). Intracellular signaling by hydrolysis of phospholipids and activation of protein kinase C. Science *258*, 607-614.

Norton, W.T. (1984). Some thoughts on the neurobiology of the leukodystrophies. Neuropediatrics *15 Suppl*, 28-31.

Nowakowski, R.S., Lewin, S.B., and Miller, M.W. (1989). Bromodeoxyuridine immunohistochemical determination of the lengths of the cell cycle and the DNA-synthetic phase for an anatomically defined population. J Neurocytol *18*, 311-318.

Ogretmen, B., and Hannun, Y.A. (2004). Biologically active sphingolipids in cancer pathogenesis and treatment. Nat Rev Cancer *4*, 604-616.

Okada, T., Ding, G., Sonoda, H., Kajimoto, T., Haga, Y., Khosrowbeygi, A., Gao, S., Miwa, N., Jahangeer, S., and Nakamura, S. (2005). Involvement of N-terminal-extended form of sphingosine kinase 2 in serum-dependent regulation of cell proliferation and apoptosis. J Biol Chem *280*, 36318-36325.

Olmstead, C.E. (1987). Neurological and neurobehavioral development of the mutant 'twitcher' mouse. Behav Brain Res *25*, 143-153.

Orchard, P.J., Blazar, B.R., Wagner, J., Charnas, L., Krivit, W., and Tolar, J. (2007). Hematopoietic cell therapy for metabolic disease. J Pediatr *151*, 340-346.

Orchard, P.J., and Tolar, J. (2010). Transplant outcomes in leukodystrophies. Semin Hematol *47*, 70-78.

Palmer, T.D., Willhoite, A.R., and Gage, F.H. (2000). Vascular niche for adult hippocampal neurogenesis. J Comp Neurol *425*, 479-494.

Pannu, R., Singh, A.K., and Singh, I. (2005). A novel role of lactosylceramide in the regulation of tumor necrosis factor alpha-mediated proliferation of rat primary astrocytes. Implications for astrogliosis following neurotrauma. J Biol Chem *280*, 13742-13751.

Pannu, R., Won, J.S., Khan, M., Singh, A.K., and Singh, I. (2004). A novel role of lactosylceramide in the regulation of lipopolysaccharide/interferon-gamma-mediated inducible nitric oxide synthase gene expression: implications for neuroinflammatory diseases. J Neurosci *24*, 5942-5954.

Parent, J.M. (2003). Injury-induced neurogenesis in the adult mammalian brain. Neuroscientist *9*, 261-272.

Parent, J.M., Yu, T.W., Leibowitz, R.T., Geschwind, D.H., Sloviter, R.S., and Lowenstein, D.H. (1997). Dentate granule cell neurogenesis is increased by seizures and contributes to aberrant network reorganization in the adult rat hippocampus. J Neurosci *17*, 3727-3738.

Park, K.I., Teng, Y.D., and Snyder, E.Y. (2002). The injured brain interacts reciprocally with neural stem cells supported by scaffolds to reconstitute lost tissue. Nat Biotechnol *20*, 1111-1117.

Pasqui, A.L., Di Renzo, M., Auteri, A., Federico, G., and Puccetti, L. (2007). Increased TNF-alpha production by peripheral blood mononuclear cells in patients with Krabbe's disease: effect of psychosine. Eur J Clin Invest *37*, 742-745.

Passini, M.A., Macauley, S.L., Huff, M.R., Taksir, T.V., Bu, J., Wu, I.H., Piepenhagen, P.A., Dodge, J.C., Shihabuddin, L.S., O'Riordan, C.R., *et al.* (2005). AAV vector-mediated correction of brain pathology in a mouse model of Niemann-Pick A disease. Mol Ther *11*, 754-762.

Pastores, G.M., Barnett, N.L., and Kolodny, E.H. (2005). An open-label, noncomparative study of miglustat in type I Gaucher disease: efficacy and tolerability over 24 months of treatment. Clin Ther *27*, 1215-1227.

Patterson, M.C., Vecchio, D., Prady, H., Abel, L., and Wraith, J.E. (2007). Miglustat for treatment of Niemann-Pick C disease: a randomised controlled study. Lancet Neurol *6*, 765-772.

Pellegatta, S., Tunici, P., Poliani, P.L., Dolcetta, D., Cajola, L., Colombelli, C., Ciusani, E., Di Donato, S., and Finocchiaro, G. (2006). The therapeutic potential of neural stem/progenitor cells in murine globoid cell leukodystrophy is conditioned by macrophage/microglia activation. Neurobiol Dis *21*, 314-323.

Pencea, V., Bingaman, K.D., Freedman, L.J., and Luskin, M.B. (2001). Neurogenesis in the subventricular zone and rostral migratory stream of the neonatal and adult primate forebrain. Exp Neurol *172*, 1-16.

Peretto, P., Dati, C., De Marchis, S., Kim, H.H., Ukhanova, M., Fasolo, A., and Margolis, F.L. (2004). Expression of the secreted factors noggin and bone morphogenetic proteins in the subependymal layer and olfactory bulb of the adult mouse brain. Neuroscience *128*, 685-696.

Peretto, P., Giachino, C., Aimar, P., Fasolo, A., and Bonfanti, L. (2005). Chain formation and glial tube assembly in the shift from neonatal to adult subventricular zone of the rodent forebrain. J Comp Neurol *487*, 407-427.

Peters, C., and Steward, C.G. (2003). Hematopoietic cell transplantation for inherited metabolic diseases: an overview of outcomes and practice guidelines. Bone Marrow Transplant *31*, 229-239.

Pettus, B.J., Chalfant, C.E., and Hannun, Y.A. (2002). Ceramide in apoptosis: an overview and current perspectives. Biochim Biophys Acta *1585*, 114-125.

Pfeiffer, S.E., Warrington, A.E., and Bansal, R. (1993). The oligodendrocyte and its many cellular processes. Trends Cell Biol *3*, 191-197.

Piccinini, M., Scandroglio, F., Prioni, S., Buccinna, B., Loberto, N., Aureli, M., Chigorno, V., Lupino, E., DeMarco, G., Lomartire, A., *et al.* (2010). Deregulated sphingolipid metabolism and membrane organization in neurodegenerative disorders. Mol Neurobiol *41*, 314-340.

Pinto, L., and Gotz, M. (2007). Radial glial cell heterogeneity--the source of diverse progeny in the CNS. Prog Neurobiol *83*, 2-23.

Platt, F.M., and Jeyakumar, M. (2008). Substrate reduction therapy. Acta Paediatr Suppl *97*, 88-93.

Pluchino, S., and Martino, G. (2008a). Neural stem cell-mediated immunomodulation: repairing the haemorrhagic brain. Brain *131*, 604-605.

Pluchino, S., and Martino, G. (2008b). The therapeutic plasticity of neural stem/precursor cells in multiple sclerosis. J Neurol Sci *265*, 105-110.

Pluchino, S., Muzio, L., Imitola, J., Deleidi, M., Alfaro-Cervello, C., Salani, G., Porcheri, C., Brambilla, E., Cavasinni, F., Bergamaschi, A., *et al.* (2008). Persistent inflammation alters the function of the endogenous brain stem cell compartment. Brain.

Pluchino, S., Quattrini, A., Brambilla, E., Gritti, A., Salani, G., Dina, G., Galli, R., Del Carro, U., Amadio, S., Bergami, A., *et al.* (2003). Injection of adult neurospheres induces recovery in a chronic model of multiple sclerosis. Nature *422*, 688-694.

Pluchino, S., Zanotti, L., Deleidi, M., and Martino, G. (2005). Neural stem cells and their use as therapeutic tool in neurological disorders. Brain Res Brain Res Rev *48*, 211-219.

Pollard, S.M., Conti, L., Sun, Y., Goffredo, D., and Smith, A. (2006). Adherent neural stem (NS) cells from fetal and adult forebrain. Cereb Cortex *16 Suppl 1*, i112-120.

Potten, C.S., and Loeffler, M. (1990). Stem cells: attributes, cycles, spirals, pitfalls and uncertainties. Lessons for and from the crypt. Development *110*, 1001-1020.

Puri, V., Watanabe, R., Dominguez, M., Sun, X., Wheatley, C.L., Marks, D.L., and Pagano, R.E. (1999). Cholesterol modulates membrane traffic along the endocytic pathway in sphingolipid-storage diseases. Nat Cell Biol *1*, 386-388.

Quinones-Hinojosa, A., Sanai, N., Soriano-Navarro, M., Gonzalez-Perez, O., Mirzadeh, Z., Gil-Perotin, S., Romero-Rodriguez, R., Berger, M.S., Garcia-Verdugo, J.M., and Alvarez-Buylla, A. (2006). Cellular composition and cytoarchitecture of the adult human subventricular zone: a niche of neural stem cells. J Comp Neurol *494*, 415-434.

Radin, N.S. (1996). Treatment of Gaucher disease with an enzyme inhibitor. Glycoconj J *13*, 153-157.

Rafi, M.A., Fugaro, J., Amini, S., Luzi, P., de Gala, G., Victoria, T., Dubell, C., Shahinfar, M., and Wenger, D.A. (1996). Retroviral vector-mediated transfer of the galactocerebrosidase (GALC) cDNA leads to overexpression and transfer of GALC activity to neighboring cells. Biochem Mol Med *58*, 142-150.

Rafi, M.A., Zhi Rao, H., Passini, M.A., Curtis, M., Vanier, M.T., Zaka, M., Luzi, P., Wolfe, J.H., and Wenger, D.A. (2005). AAV-mediated expression of galactocerebrosidase in brain results in attenuated symptoms and extended life span in murine models of globoid cell leukodystrophy. Mol Ther *11*, 734-744.

Rajesh, M., Kolmakova, A., and Chatterjee, S. (2005). Novel role of lactosylceramide in vascular endothelial growth factor-mediated angiogenesis in human endothelial cells. Circ Res *97*, 796-804.

Rakic, P. (2003). Developmental and evolutionary adaptations of cortical radial glia. Cereb Cortex *13*, 541-549.

Ramirez-Castillejo, C., Sanchez-Sanchez, F., Andreu-Agullo, C., Ferron, S.R., Aroca-Aguilar, J.D., Sanchez, P., Mira, H., Escribano, J., and Farinas, I. (2006). Pigment epithelium-derived factor is a niche signal for neural stem cell renewal. Nat Neurosci *9*, 331-339.

Reynolds, B.A., and Rietze, R.L. (2005). Neural stem cells and neurospheres--re-evaluating the relationship. Nat Methods *2*, 333-336.

Reynolds, B.A., and Weiss, S. (1992). Generation of neurons and astrocytes from isolated cells of the adult mammalian central nervous system. Science *255*, 1707-1710.

Reynolds, B.A., and Weiss, S. (1996). Clonal and population analyses demonstrate that an EGF-responsive mammalian embryonic CNS precursor is a stem cell. Dev Biol *175*, 1-13.

Rodriguez, M., Alvarez-Erviti, L., Blesa, F.J., Rodriguez-Oroz, M.C., Arina, A., Melero, I., Ramos, L.I., and Obeso, J.A. (2007). Bone-marrow-derived cell differentiation into microglia: a study in a progressive mouse model of Parkinson's disease. Neurobiol Dis *28*, 316-325.

Rodriguez-Perez, L.M., Perez-Martin, M., Jimenez, A.J., and Fernandez-Llebrez, P. (2003). Immunocytochemical characterisation of the wall of the bovine lateral ventricle. Cell Tissue Res *314*, 325-335.

Rohatgi, R., Milenkovic, L., and Scott, M.P. (2007). Patched1 regulates hedgehog signaling at the primary cilium. Science *317*, 372-376.

Rohrbach, M., and Clarke, J.T. (2007). Treatment of lysosomal storage disorders : progress with enzyme replacement therapy. Drugs *67*, 2697-2716.

Rolls, A., Shechter, R., London, A., Ziv, Y., Ronen, A., Levy, R., and Schwartz, M. (2007). Toll-like receptors modulate adult hippocampal neurogenesis. Nat Cell Biol *9*, 1081-1088.

Russo, I., Barlati, S., and Bosetti, F. (2011). Effects of neuroinflammation on the regenerative capacity of brain stem cells. J Neurochem *116*, 947-956.

Saba, J.D., and Hla, T. (2004). Point-counterpoint of sphingosine 1-phosphate metabolism. Circ Res *94*, 724-734.

Sabatelli, M., Quaranta, L., Madia, F., Lippi, G., Conte, A., Lo Monaco, M., Di Trapani, G., Rafi, M.A., Wenger, D.A., Vaccaro, A.M., *et al.* (2002). Peripheral neuropathy with hypomyelinating features in adult-onset Krabbe's disease. Neuromuscul Disord *12*, 386-391.

Sabatini, D.a.A., MB (2001). The biogenesis of membranes and organelles, Vol The Metabolic and Molecular Bases of Inherited Disease, 8th edn. (New York, McGraw-Hill).

Sakai, N., Fukushima, H., Inui, K., Fu, L., Nishigaki, T., Yanagihara, I., Tatsumi, N., Ozono, K., and Okada, S. (1998). Human galactocerebrosidase gene: promoter analysis of the 5'-flanking region and structural organization. Biochim Biophys Acta *1395*, 62-67.

Sakai, N., Inui, K., Tatsumi, N., Fukushima, H., Nishigaki, T., Taniike, M., Nishimoto, J., Tsukamoto, H., Yanagihara, I., Ozono, K., *et al.* (1996). Molecular cloning and expression of cDNA for murine galactocerebrosidase and mutation analysis of the twitcher mouse, a model of Krabbe's disease. J Neurochem *66*, 1118-1124.

Salegio, E.A., Kells, A.P., Richardson, R.M., Hadaczek, P., Forsayeth, J., Bringas, J., Sardi, S.P., Passini, M.A., Shihabuddin, L.S., Cheng, S.H., *et al.* (2010). Magnetic resonance imaging-guided delivery of adeno-associated virus type 2 to the primate brain for the treatment of lysosomal storage disorders. Hum Gene Ther *21*, 1093-1103.

Sanai, N., Tramontin, A.D., Quinones-Hinojosa, A., Barbaro, N.M., Gupta, N., Kunwar, S., Lawton, M.T., McDermott, M.W., Parsa, A.T., Manuel-Garcia Verdugo, J., *et al.* (2004). Unique astrocyte ribbon in adult human brain contains neural stem cells but lacks chain migration. Nature *427*, 740-744.

Sanchez, T., Skoura, A., Wu, M.T., Casserly, B., Harrington, E.O., and Hla, T. (2007). Induction of vascular permeability by the sphingosine-1-phosphate receptor-2 (S1P2R) and its downstream effectors ROCK and PTEN. Arterioscler Thromb Vasc Biol *27*, 1312-1318.

Satoh, J.I., Tokumoto, H., Kurohara, K., Yukitake, M., Matsui, M., Kuroda, Y., Yamamoto, T., Furuya, H., Shinnoh, N., Kobayashi, T., *et al.* (1997). Adult-onset Krabbe disease with

homozygous T1853C mutation in the galactocerebrosidase gene. Unusual MRI findings of corticospinal tract demyelination. Neurology *49*, 1392-1399.

Sawamoto, K., Wichterle, H., Gonzalez-Perez, O., Cholfin, J.A., Yamada, M., Spassky, N., Murcia, N.S., Garcia-Verdugo, J.M., Marin, O., Rubenstein, J.L., *et al.* (2006). New neurons follow the flow of cerebrospinal fluid in the adult brain. Science *311*, 629-632.

Schiffmann, R. (2010). Therapeutic approaches for neuronopathic lysosomal storage disorders. J Inherit Metab Dis *33*, 373-379.

Schiffmann, R., Fitzgibbon, E.J., Harris, C., DeVile, C., Davies, E.H., Abel, L., van Schaik, I.N., Benko, W., Timmons, M., Ries, M., *et al.* (2008). Randomized, controlled trial of miglustat in Gaucher's disease type 3. Ann Neurol *64*, 514-522.

Schwartz, P.H., and Brick, D.J. (2008). Stem cell therapies for the lysosomal storage diseases - the quintessential neurodegenerative diseases. Curr Stem Cell Res Ther *3*, 88-98.

Schwarz, A., Rapaport, E., Hirschberg, K., and Futerman, A.H. (1995). A regulatory role for sphingolipids in neuronal growth. Inhibition of sphingolipid synthesis and degradation have opposite effects on axonal branching. J Biol Chem *270*, 10990-10998.

Seri, B., Garcia-Verdugo, J.M., Collado-Morente, L., McEwen, B.S., and Alvarez-Buylla, A. (2004). Cell types, lineage, and architecture of the germinal zone in the adult dentate gyrus. J Comp Neurol *478*, 359-378.

Settembre, C., Fraldi, A., Jahreiss, L., Spampanato, C., Venturi, C., Medina, D., de Pablo, R., Tacchetti, C., Rubinsztein, D.C., and Ballabio, A. (2008). A block of autophagy in lysosomal storage disorders. Hum Mol Genet *17*, 119-129.

Shan, X., Chi, L., Bishop, M., Luo, C., Lien, L., Zhang, Z., and Liu, R. (2006). Enhanced de novo neurogenesis and dopaminergic neurogenesis in the substantia nigra of 1-methyl-4-phenyl-1,2,3,6-tetrahydropyridine-induced Parkinson's disease-like mice. Stem Cells *24*, 1280-1287.

Shen, J.S., Watabe, K., Ohashi, T., and Eto, Y. (2001). Intraventricular administration of recombinant adenovirus to neonatal twitcher mouse leads to clinicopathological improvements. Gene Ther *8*, 1081-1087.

Shen, Q., Goderie, S.K., Jin, L., Karanth, N., Sun, Y., Abramova, N., Vincent, P., Pumiglia, K., and Temple, S. (2004). Endothelial cells stimulate self-renewal and expand neurogenesis of neural stem cells. Science *304*, 1338-1340.

Shihabuddin, L.S., and Aubert, I. (2010). Stem cell transplantation for neurometabolic and neurodegenerative diseases. Neuropharmacology *58*, 845-854.

Shihabuddin, L.S., Numan, S., Huff, M.R., Dodge, J.C., Clarke, J., Macauley, S.L., Yang, W., Taksir, T.V., Parsons, G., Passini, M.A., *et al.* (2004). Intracerebral transplantation of adult mouse neural progenitor cells into the Niemann-Pick-A mouse leads to a marked decrease in lysosomal storage pathology. J Neurosci *24*, 10642-10651.

Shimogori, T., Banuchi, V., Ng, H.Y., Strauss, J.B., and Grove, E.A. (2004). Embryonic signaling centers expressing BMP, WNT and FGF proteins interact to pattern the cerebral cortex. Development *131*, 5639-5647.

Simard, A.R., Soulet, D., Gowing, G., Julien, J.P., and Rivest, S. (2006). Bone marrow-derived microglia play a critical role in restricting senile plaque formation in Alzheimer's disease. Neuron *49*, 489-502.

Singla, V., and Reiter, J.F. (2006). The primary cilium as the cell's antenna: signaling at a sensory organelle. Science *313*, 629-633.

Snyder, E.Y., and Wolfe, J.H. (1996). Central nervous system cell transplantation: a novel therapy for storage diseases? Curr Opin Neurol *9*, 126-136.

Song, H., Stevens, C.F., and Gage, F.H. (2002). Astroglia induce neurogenesis from adult neural stem cells. Nature *417*, 39-44.

Spiegel, S., and Milstien, S. (2003). Sphingosine-1-phosphate: an enigmatic signalling lipid. Nat Rev Mol Cell Biol *4*, 397-407.

Spiliotopoulos, D., Goffredo, D., Conti, L., Di Febo, F., Biella, G., Toselli, M., and Cattaneo, E. (2009). An optimized experimental strategy for efficient conversion of embryonic stem (ES)-derived mouse neural stem (NS) cells into a nearly homogeneous mature neuronal population. Neurobiol Dis *34*, 320-331.

Staretz-Chacham, O., Lang, T.C., LaMarca, M.E., Krasnewich, D., and Sidransky, E. (2009). Lysosomal storage disorders in the newborn. Pediatrics *123*, 1191-1207.

Steele, A.D., Emsley, J.G., Ozdinler, P.H., Lindquist, S., and Macklis, J.D. (2006). Prion protein (PrPc) positively regulates neural precursor proliferation during developmental and adult mammalian neurogenesis. Proc Natl Acad Sci U S A *103*, 3416-3421.

Steiner, B., Klempin, F., Wang, L., Kott, M., Kettenmann, H., and Kempermann, G. (2006). Type-2 cells as link between glial and neuronal lineage in adult hippocampal neurogenesis. Glia *54*, 805-814.

Strub, G.M., Maceyka, M., Hait, N.C., Milstien, S., and Spiegel, S. (2010). Extracellular and intracellular actions of sphingosine-1-phosphate. Adv Exp Med Biol *688*, 141-155.

Suh, H., Consiglio, A., Ray, J., Sawai, T., D'Amour, K.A., and Gage, F.H. (2007). In vivo fate analysis reveals the multipotent and self-renewal capacities of Sox2+ neural stem cells in the adult hippocampus. Cell Stem Cell *1*, 515-528.

Suzuki, K. (1998). Twenty five years of the "psychosine hypothesis": a personal perspective of its history and present status. Neurochem Res *23*, 251-259.

Suzuki, K. (2003). Globoid cell leukodystrophy (Krabbe's disease): update. J Child Neurol *18*, 595-603.

Svennerholm, L., Bostrom, K., Fredman, P., Mansson, J.E., Rosengren, B., and Rynmark, B.M. (1989). Human brain gangliosides: developmental changes from early fetal stage to advanced age. Biochim Biophys Acta *1005*, 109-117.

Svennerholm, L., Rynmark, B.M., Vilbergsson, G., Fredman, P., Gottfries, J., Mansson, J.E., and Percy, A. (1991). Gangliosides in human fetal brain. J Neurochem *56*, 1763-1768.

Takahashi, T., Nowakowski, R.S., and Caviness, V.S., Jr. (1992). BUdR as an S-phase marker for quantitative studies of cytokinetic behaviour in the murine cerebral ventricular zone. J Neurocytol *21*, 185-197.

Tamaki, S.J., Jacobs, Y., Dohse, M., Capela, A., Cooper, J.D., Reitsma, M., He, D., Tushinski, R., Belichenko, P.V., Salehi, A., *et al.* (2009). Neuroprotection of host cells by human central nervous system stem cells in a mouse model of infantile neuronal ceroid lipofuscinosis. Cell Stem Cell *5*, 310-319.

Tanaka, K., Nagara, H., Kobayashi, T., and Goto, I. (1989). The twitcher mouse: accumulation of galactosylsphingosine and pathology of the central nervous system. Brain Res *482*, 347-350.

Tapasi, S., Padma, P., and Setty, O.H. (1998). Effect of psychosine on mitochondrial function. Indian J Biochem Biophys *35*, 161-165.

Taupin, P. (2006). The therapeutic potential of adult neural stem cells. Curr Opin Mol Ther *8*, 225-231.

Taupin, P. (2008). Adult neurogenesis, neuroinflammation and therapeutic potential of adult neural stem cells. Int J Med Sci *5*, 127-132.

Tavazoie, M., Van der Veken, L., Silva-Vargas, V., Louissaint, M., Colonna, L., Zaidi, B., Garcia-Verdugo, J.M., and Doetsch, F. (2008). A specialized vascular niche for adult neural stem cells. Cell Stem Cell *3*, 279-288.

Taylor, R.M., Lee, J.P., Palacino, J.J., Bower, K.A., Li, J., Vanier, M.T., Wenger, D.A., Sidman, R.L., and Snyder, E.Y. (2006). Intrinsic resistance of neural stem cells to toxic metabolites may

make them well suited for cell non-autonomous disorders: evidence from a mouse model of Krabbe leukodystrophy. J Neurochem *97*, 1585-1599.

Tessitore, A., del, P.M.M., Sano, R., Ma, Y., Mann, L., Ingrassia, A., Laywell, E.D., Steindler, D.A., Hendershot, L.M., and d'Azzo, A. (2004). GM1-ganglioside-mediated activation of the unfolded protein response causes neuronal death in a neurodegenerative gangliosidosis. Mol Cell *15*, 753-766.

Tramontin, A.D., Garcia-Verdugo, J.M., Lim, D.A., and Alvarez-Buylla, A. (2003). Postnatal development of radial glia and the ventricular zone (VZ): a continuum of the neural stem cell compartment. Cereb Cortex *13*, 580-587.

Tran, P.B., Banisadr, G., Ren, D., Chenn, A., and Miller, R.J. (2007). Chemokine receptor expression by neural progenitor cells in neurogenic regions of mouse brain. J Comp Neurol *500*, 1007-1033.

Tran, P.B., Ren, D., Veldhouse, T.J., and Miller, R.J. (2004). Chemokine receptors are expressed widely by embryonic and adult neural progenitor cells. J Neurosci Res *76*, 20-34.

Van Brocklyn, J.R., Graler, M.H., Bernhardt, G., Hobson, J.P., Lipp, M., and Spiegel, S. (2000). Sphingosine-1-phosphate is a ligand for the G protein-coupled receptor EDG-6. Blood *95*, 2624-2629.

Victoria, T., Rafi, M.A., and Wenger, D.A. (1996). Cloning of the canine GALC cDNA and identification of the mutation causing globoid cell leukodystrophy in West Highland White and Cairn terriers. Genomics *33*, 457-462.

Visigalli, I., Ungari, S., Martino, S., Park, H., Cesani, M., Gentner, B., Sergi Sergi, L., Orlacchio, A., Naldini, L., and Biffi, A. (2010). The galactocerebrosidase enzyme contributes to the maintenance of a functional hematopoietic stem cell niche. Blood.

Vite, C.H., McGowan, J.C., Niogi, S.N., Passini, M.A., Drobatz, K.J., Haskins, M.E., and Wolfe, J.H. (2005). Effective gene therapy for an inherited CNS disease in a large animal model. Ann Neurol *57*, 355-364.

Wenger (2000). Krabbe Disease (University of Washington, Seattle).

Wenger, D.A., Rafi, M.A., and Luzi, P. (1997). Molecular genetics of Krabbe disease (globoid cell leukodystrophy): diagnostic and clinical implications. Hum Mutat *10*, 268-279.

Wenger, D.A., Rafi, M.A., Luzi, P., Datto, J., and Costantino-Ceccarini, E. (2000). Krabbe disease: genetic aspects and progress toward therapy. Mol Genet Metab *70*, 1-9.

Wenk, J., Hille, A., and von Figura, K. (1991). Quantitation of Mr 46000 and Mr 300000 mannose 6-phosphate receptors in human cells and tissues. Biochem Int *23*, 723-731.

Whetton, A.D., and Graham, G.J. (1999). Homing and mobilization in the stem cell niche. Trends Cell Biol *9*, 233-238.

White, A.B., Givogri, M.I., Lopez-Rosas, A., Cao, H., van Breemen, R., Thinakaran, G., and Bongarzone, E.R. (2009). Psychosine accumulates in membrane microdomains in the brain of krabbe patients, disrupting the raft architecture. J Neurosci *29*, 6068-6077.

Winchester, B., Vellodi, A., and Young, E. (2000). The molecular basis of lysosomal storage diseases and their treatment. Biochem Soc Trans *28*, 150-154.

Windrem, M.S., Nunes, M.C., Rashbaum, W.K., Schwartz, T.H., Goodman, R.A., McKhann, G., 2nd, Roy, N.S., and Goldman, S.A. (2004). Fetal and adult human oligodendrocyte progenitor cell isolates myelinate the congenitally dysmyelinated brain. Nat Med *10*, 93-97.

Won, J.S., Singh, A.K., and Singh, I. (2007). Lactosylceramide: a lipid second messenger in neuroinflammatory disease. J Neurochem *103 Suppl 1*, 180-191.

Wu, Y.P., Mizugishi, K., Bektas, M., Sandhoff, R., and Proia, R.L. (2008). Sphingosine kinase 1/S1P receptor signaling axis controls glial proliferation in mice with Sandhoff disease. Hum Mol Genet *17*, 2257-2264.

Wu, Y.P., and Proia, R.L. (2004). Deletion of macrophage-inflammatory protein 1 alpha retards neurodegeneration in Sandhoff disease mice. Proc Natl Acad Sci U S A *101*, 8425-8430.

Yamada, H., Martin, P., and Suzuki, K. (1996). Impairment of protein kinase C activity in twitcher Schwann cells in vitro. Brain Res *718*, 138-144.

Yamashita, T., Wada, R., Sasaki, T., Deng, C., Bierfreund, U., Sandhoff, K., and Proia, R.L. (1999). A vital role for glycosphingolipid synthesis during development and differentiation. Proc Natl Acad Sci U S A *96*, 9142-9147.

Yang, S.R., Kim, S.J., Byun, K.H., Hutchinson, B., Lee, B.H., Michikawa, M., Lee, Y.S., and Kang, K.S. (2006). NPC1 gene deficiency leads to lack of neural stem cell self-renewal and abnormal differentiation through activation of p38 mitogen-activated protein kinase signaling. Stem Cells *24*, 292-298.

Yang, Z., Covey, M.V., Bitel, C.L., Ni, L., Jonakait, G.M., and Levison, S.W. (2007). Sustained neocortical neurogenesis after neonatal hypoxic/ischemic injury. Ann Neurol *61*, 199-208.

Yin, T., and Li, L. (2006). The stem cell niches in bone. J Clin Invest *116*, 1195-1201.

Yu, R.K., Nakatani, Y., and Yanagisawa, M. (2009). The role of glycosphingolipid metabolism in the developing brain. J Lipid Res *50 Suppl*, S440-445.

Zahs, K.R. (1998). Heterotypic coupling between glial cells of the mammalian central nervous system. Glia *24*, 85-96.

Zaka, M., Rafi, M.A., Rao, H.Z., Luzi, P., and Wenger, D.A. (2005). Insulin-like growth factor-1 provides protection against psychosine-induced apoptosis in cultured mouse oligodendrocyte progenitor cells using primarily the PI3K/Akt pathway. Mol Cell Neurosci *30*, 398-407.

Zaka, M., and Wenger, D.A. (2004). Psychosine-induced apoptosis in a mouse oligodendrocyte progenitor cell line is mediated by caspase activation. Neurosci Lett *358*, 205-209.

Zervas, M., Somers, K.L., Thrall, M.A., and Walkley, S.U. (2001). Critical role for glycosphingolipids in Niemann-Pick disease type C. Curr Biol *11*, 1283-1287.

Zhao, G., McCarthy, N.F., Sheehy, P.A., and Taylor, R.M. (2007). Comparison of the behavior of neural stem cells in the brain of normal and twitcher mice after neonatal transplantation. Stem Cells Dev *16*, 429-438.

Zheng, W., Kollmeyer, J., Symolon, H., Momin, A., Munter, E., Wang, E., Kelly, S., Allegood, J.C., Liu, Y., Peng, Q., *et al.* (2006). Ceramides and other bioactive sphingolipid backbones in health and disease: lipidomic analysis, metabolism and roles in membrane structure, dynamics, signaling and autophagy. Biochim Biophys Acta *1758*, 1864-1884.

Ziv, Y., Ron, N., Butovsky, O., Landa, G., Sudai, E., Greenberg, N., Cohen, H., Kipnis, J., and Schwartz, M. (2006). Immune cells contribute to the maintenance of neurogenesis and spatial learning abilities in adulthood. Nat Neurosci *9*, 268-275.

Sara Santamaria